Vision Research

Optical phase nullification partially restores visual and stereo acuity lost to simulated blur from higher-order wavefront aberrations of keratoconic eyes

--Manuscript Draft--

Manuscript Number:	VR-24-175R2
Article Type:	Full Length Article
Keywords:	Contrast; Correspondence matching; Ghosting; Higher-order aberrations; Retinal image quality

Corresponding Author:	Shrikant R Bharadwaj, BSopt., PhD L V Prasad Eye Institute, Hyderabad, IN Hyderabad, Andhra Pradesh INDIA
First Author:	Bhagya Lakshmi Marella
Order of Authors:	Bhagya Lakshmi Marella
	Miriam Conway
	Pravin K. Vaddavalli
	Catherine Suttle
	Shrikant R Bharadwaj, BSopt., PhD

Abstract:	Contrast demodulation and phase distortions are exaggerated in retinal images blurred by the higher-order wavefront aberrations of keratoconic eyes. While the performance loss from the former parameter is well understood, little is known about the impact of the latter on visual functions in this disease condition. The present study investigated the impact of phase distortions on the monocular logMAR visual acuity, letter discriminability and random-dot stereoacuity of seventeen visually healthy adults using images that were computationally blurred by four different higher-order wavefront aberration profiles of keratoconic eyes that showed significant distortions in the phase spectrum. Participants viewed these images through 2mm artificial pupils to negate their native ocular wavefront aberrations. The results showed progressive losses in visual acuity and stereoacuity with increasing blur, a third of which could be recovered following phase nullification. Letter discriminability also improved following phase nullification, more so for smaller than larger optotypes. Stereoacuity loss and, consequently, its recovery following phase nullification was more prominent for profiles simulating unilateral asymmetric keratoconus than for profiles simulating bilateral symmetric keratoconus. These results agree with previous reports obtained from blur induced with lower-order aberrations and indicate that a similar trend may be observed for more complex patterns of blur like keratoconus. Overall, both contrast demodulation and misalignment of the local features of the blurred image may contribute to losses of spatial and depth vision in keratoconus. Phase nullification may partially mitigate these losses, thereby allowing the processing of finer spatial details and veridical disparity estimations for improved depth perception.

Suggested Reviewers:	Scott Stevenson SBStevenson@UH.edu
	Pablo Artal pablo@um.es
	David Atchison d.atchison@qut.edu.au
	Hema Radhakrishnan hema.radhakrishnan@manchester.ac.uk

Cover Letter

4th September 2024

Dear Prof. McGraw:

We would like to submit the second revision of our manuscript entitled ***"Optical phase nullification partially restores visual and stereo acuity lost to simulated blur from higher-order wavefront aberrations of keratoconic eyes"*** for peer review to Vision Research.

We thank you and the editor for the in-principle acceptance of our article for publication in Vision Research. We are very excited by this news. As recommended by the editor, we have modified the abstract in the revised submission. We hope that you are satisfied by the amendments and will accept the article for final publication in Vision Research.

Thanking you
Sincerely

Bhagya Lakshmi Marella
Miriam Conway
Pravin K. Vaddavalli
Catherine Suttle
Shrikant R. Bharadwaj

Response to reviewers

Comments from Action Editor

I have now received the Referees' comments for your manuscript "Optical phase nullification partially restores visual and stereo acuity lost to simulated blur from higher-order wavefront aberrations of keratoconic eyes." I am pleased to report that your revisions have satisfactorily addressed the scientific concerns. However, in the pre-production check of the manuscript, one or more issues have been noted that require your attention. Please make the necessary changes and then resubmit the revised manuscript for editorial review.

Response: *Thank you very much!*

The following issues need to be addressed:

Please remove the statistical results from the abstract and ensure it is no more than 250 words. ***Response:*** *Statistical results have been removed from the abstract. The abstract has also been shortened to 250 words in the revised manuscript.*

Figure 1

Click here to access/download;Figure;Figure 1.tif

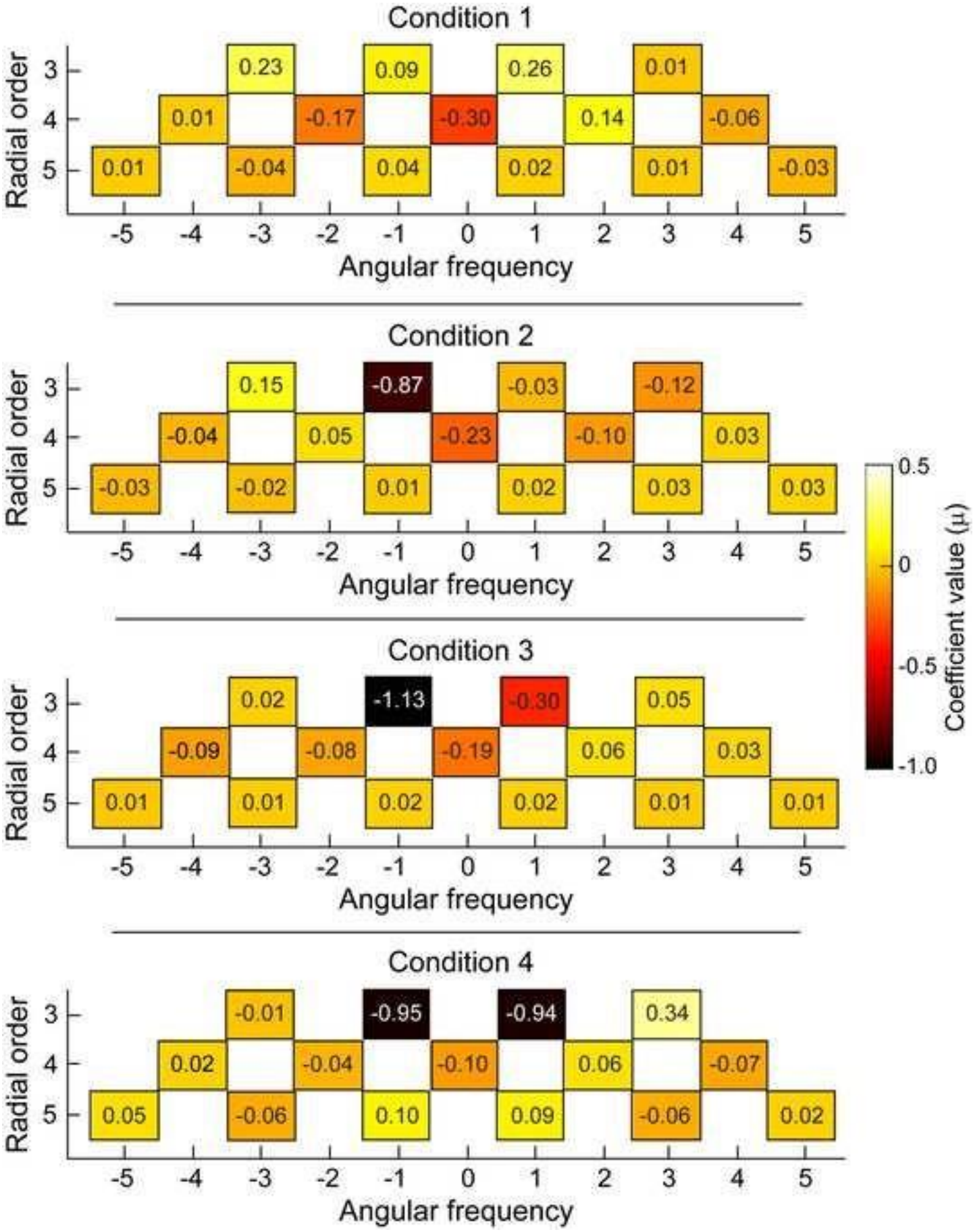

Figure 2

Click here to access/download;Figure;Figure 2.tif

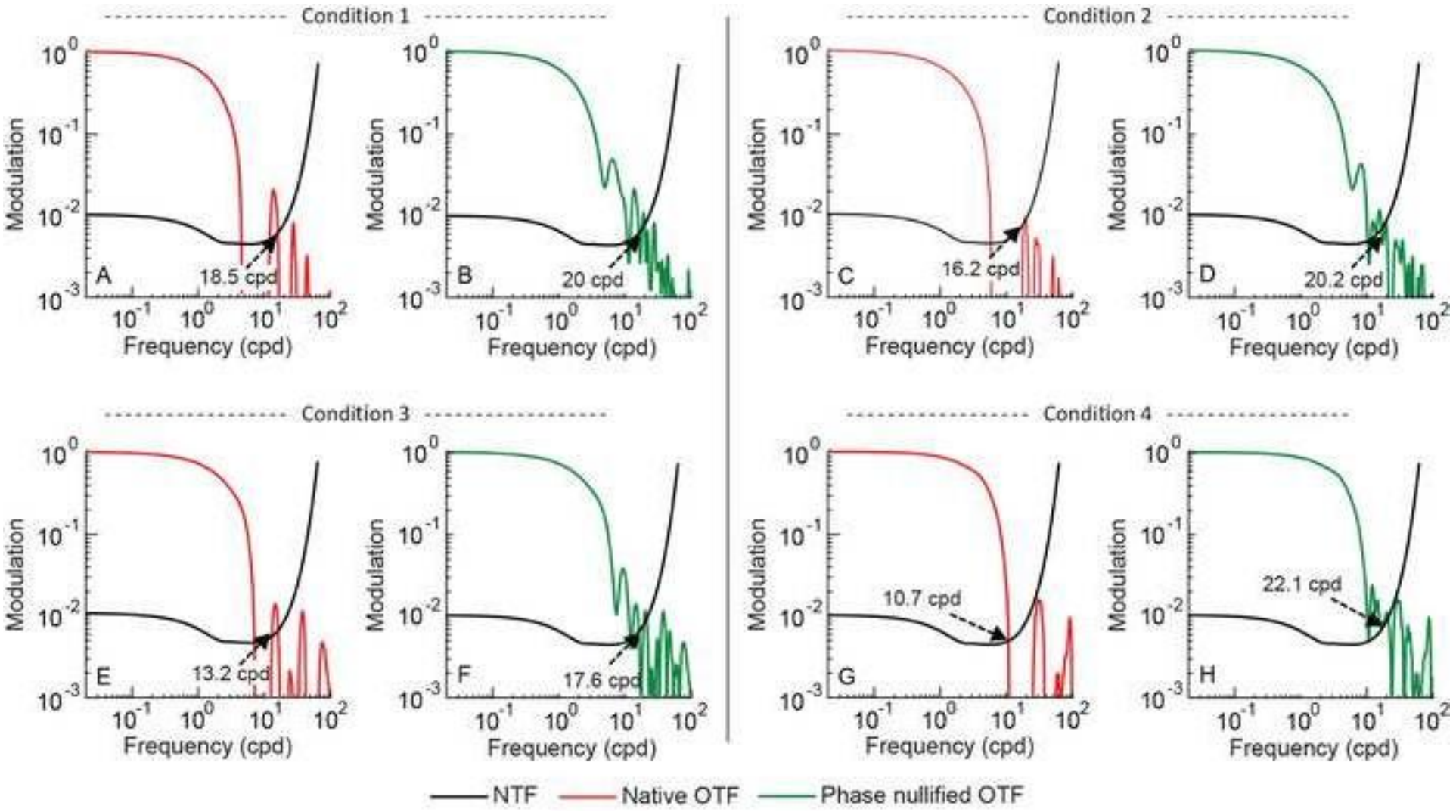

Figure 3

Click here to access/download;Figure;Figure 3.tif

A. Unblurred stereogram

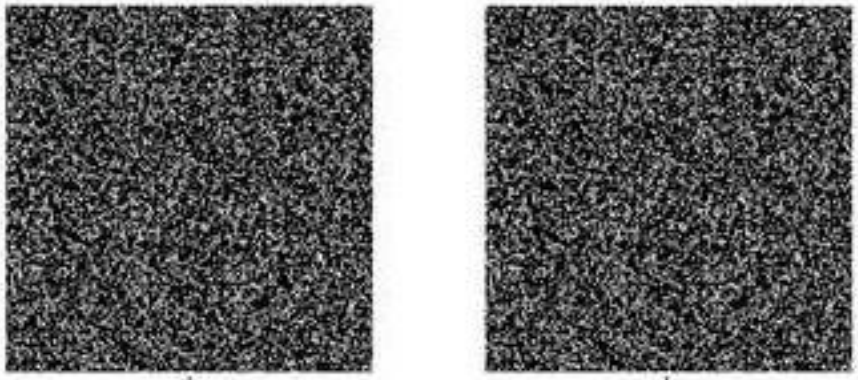

B. Bilaterally blurred stereogram with native phase

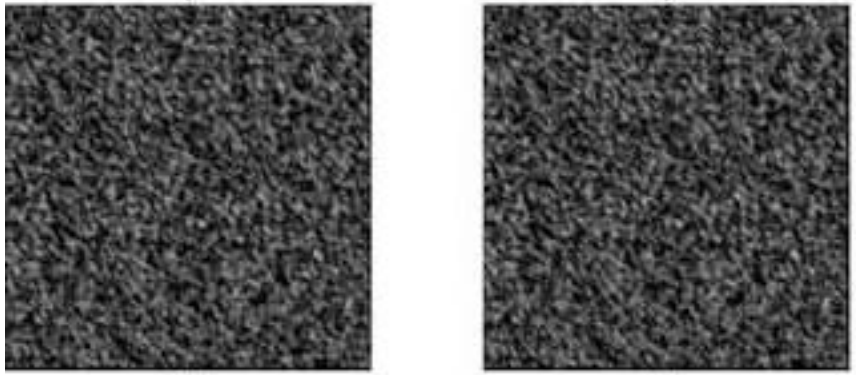

C. Bilaterally blurred stereogram with nullified phase

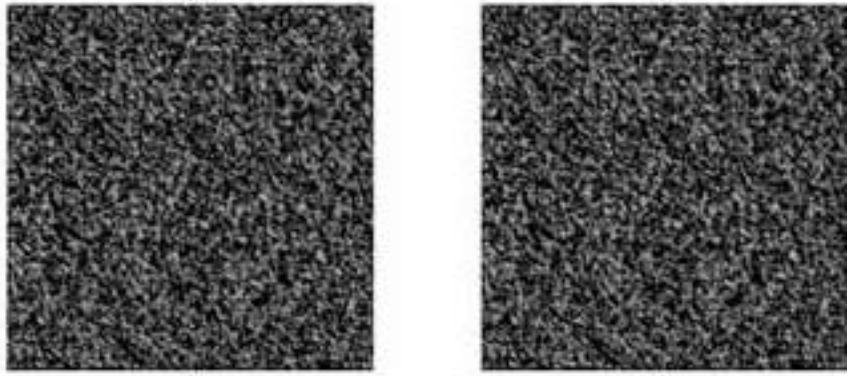

D. Unilaterally blurred stereogram with native phase

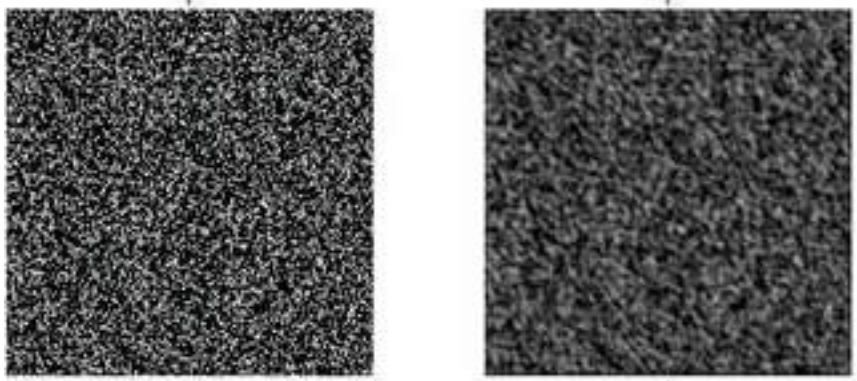

E. Unilaterally blurred stereogram with nullified phase

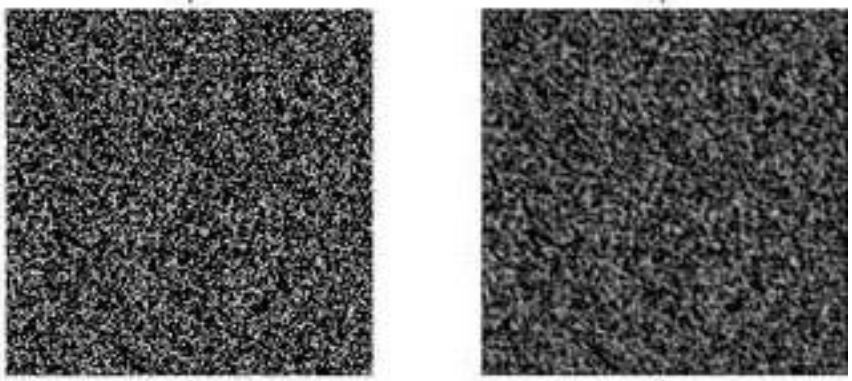

Figure 4

Click here to access/download;Figure;Figure 4.tif

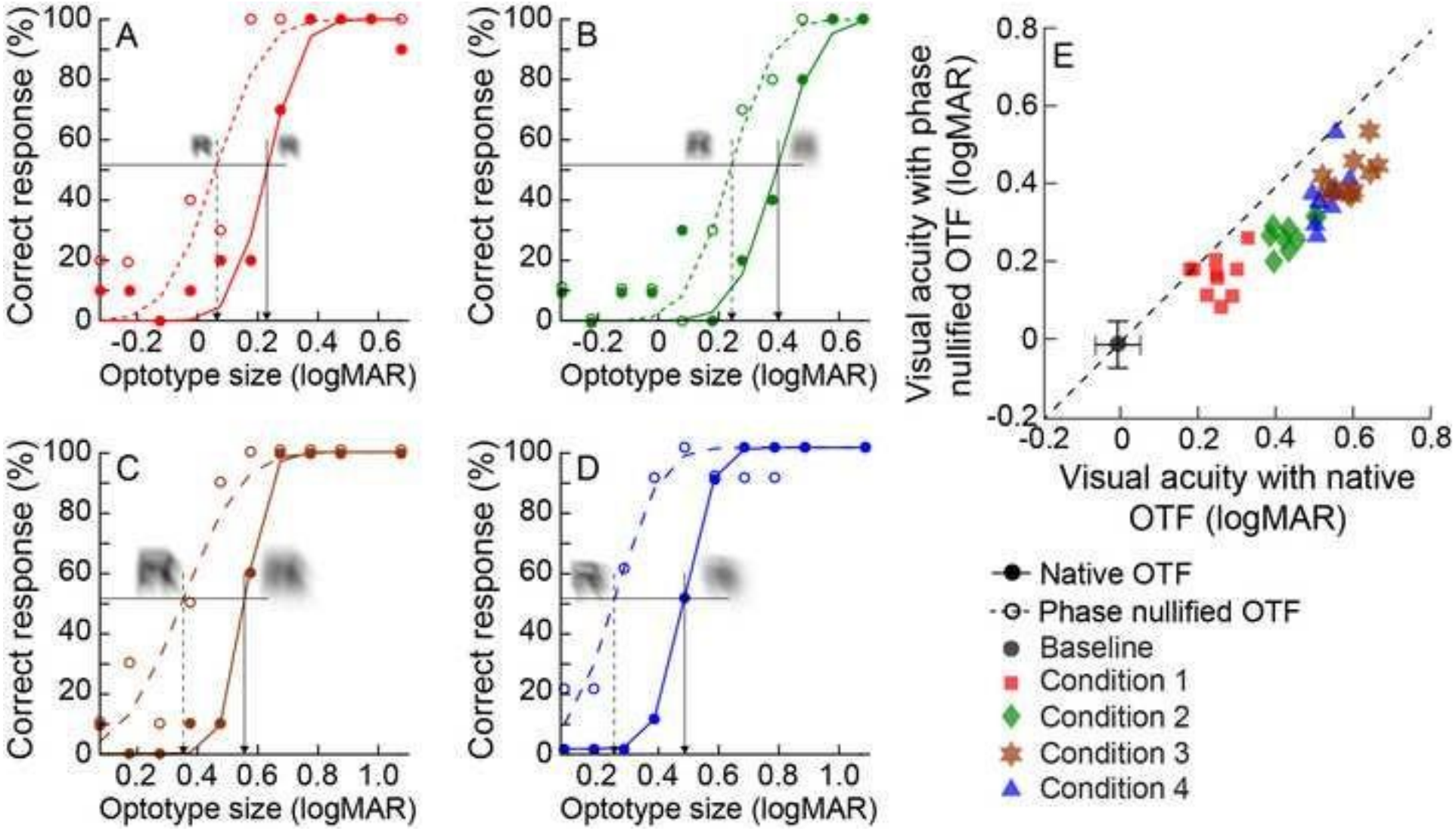

Figure 5

Click here to access/download;Figure;Figure 5.tif

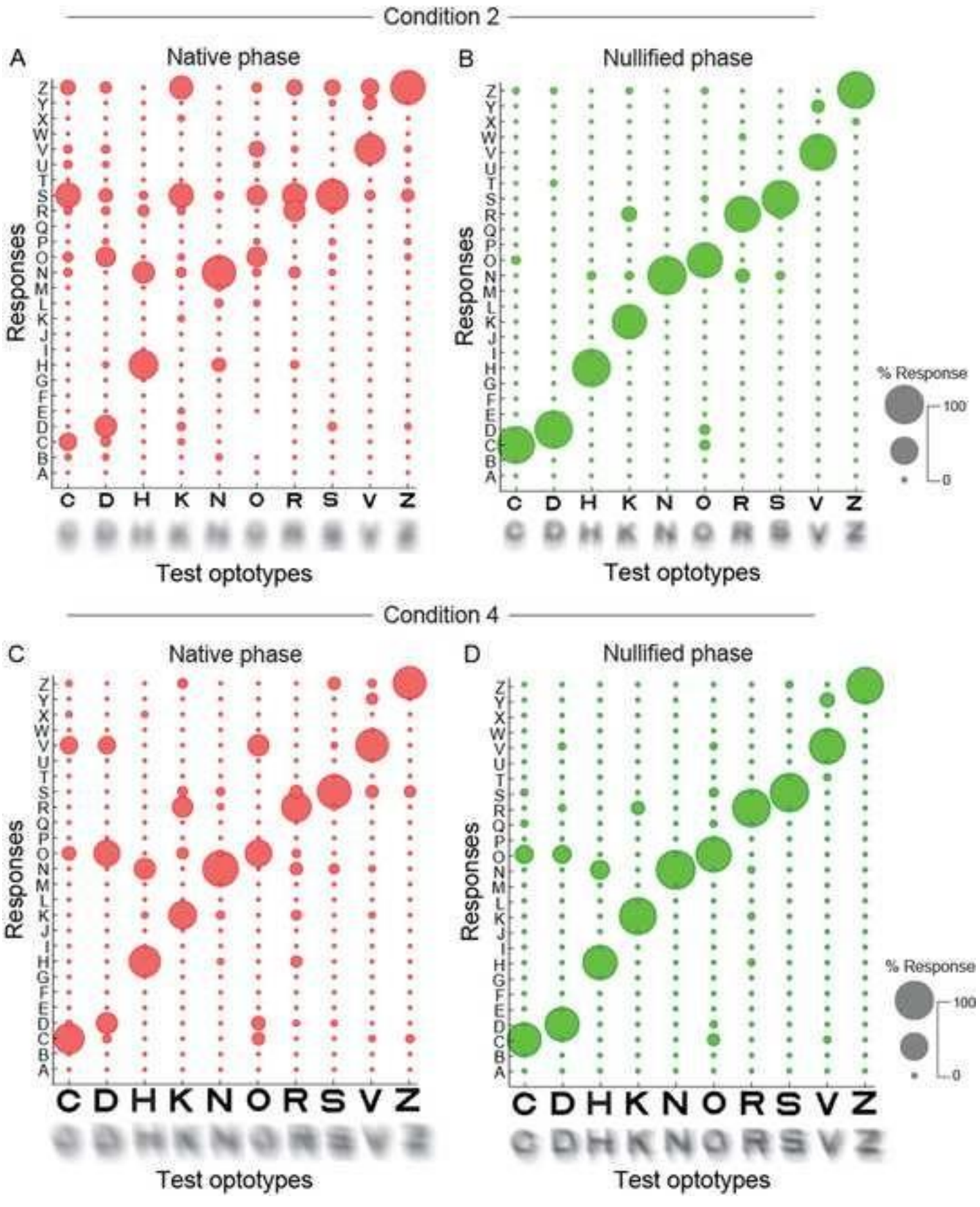

Figure 6

Click here to access/download;Figure;Figure 6.tif

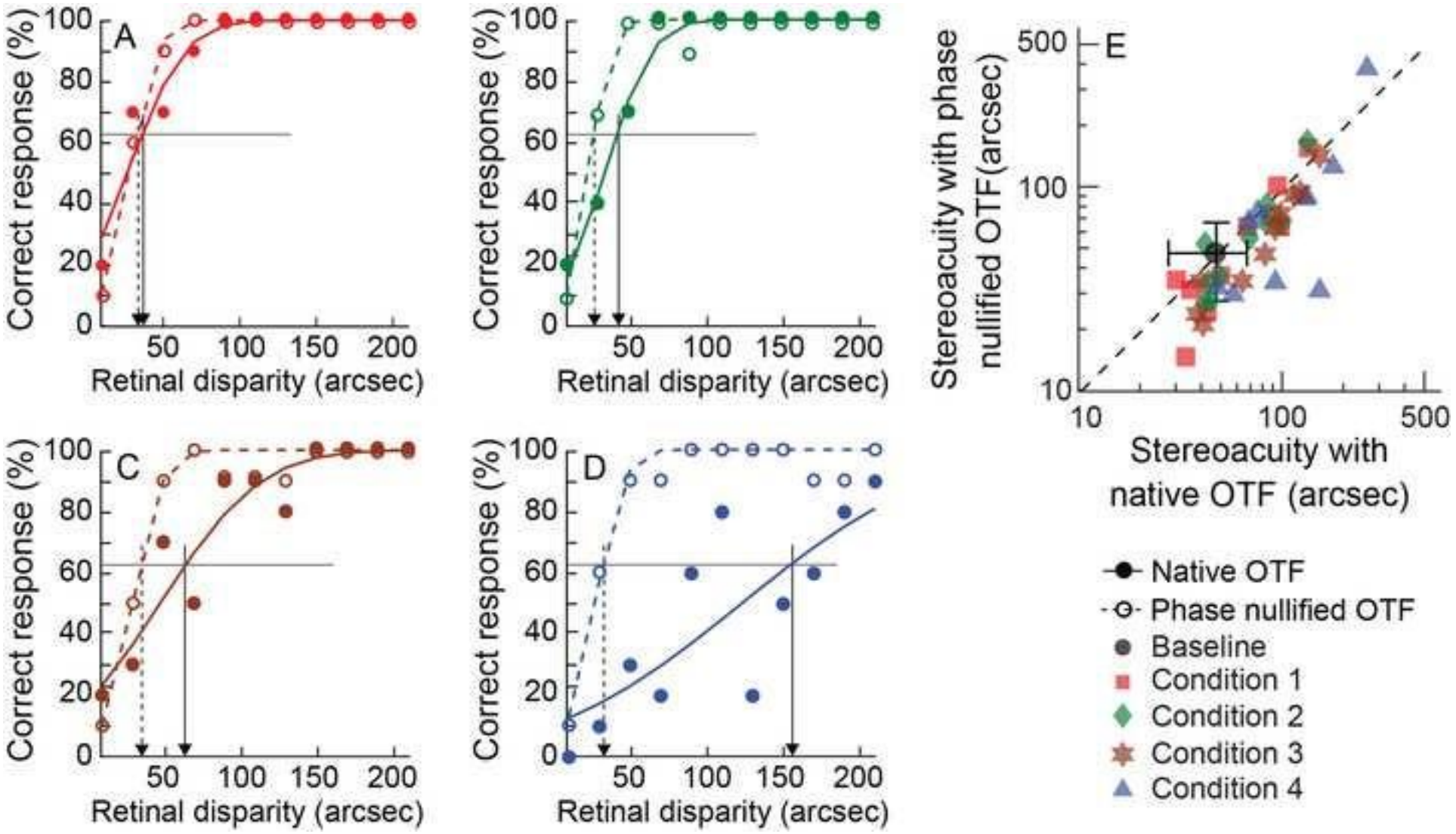

Figure 7

Click here to access/download;Figure;Figure 7.tif

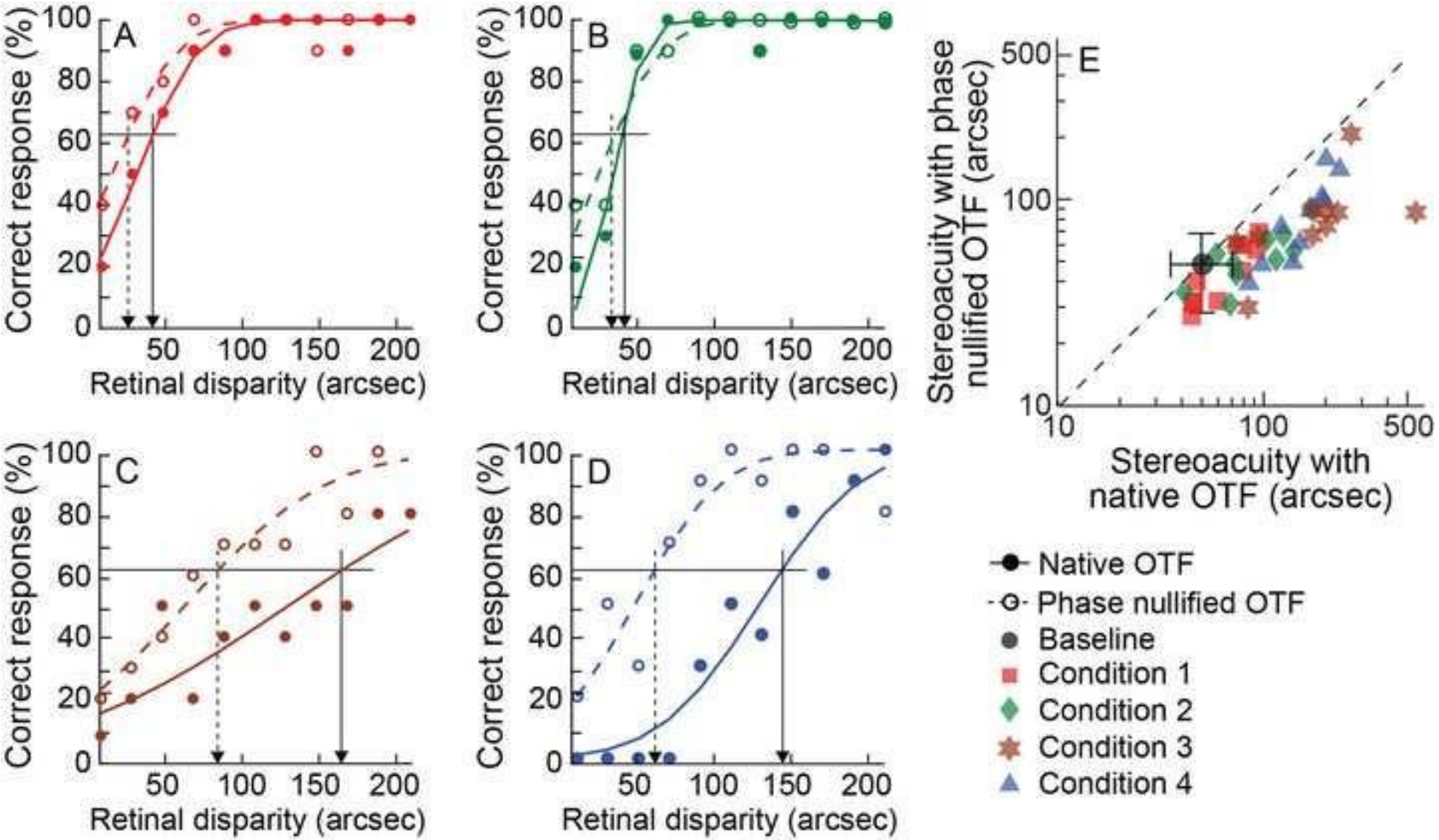

Figure A1

Click here to access/download;Figure;Figure A1.tif

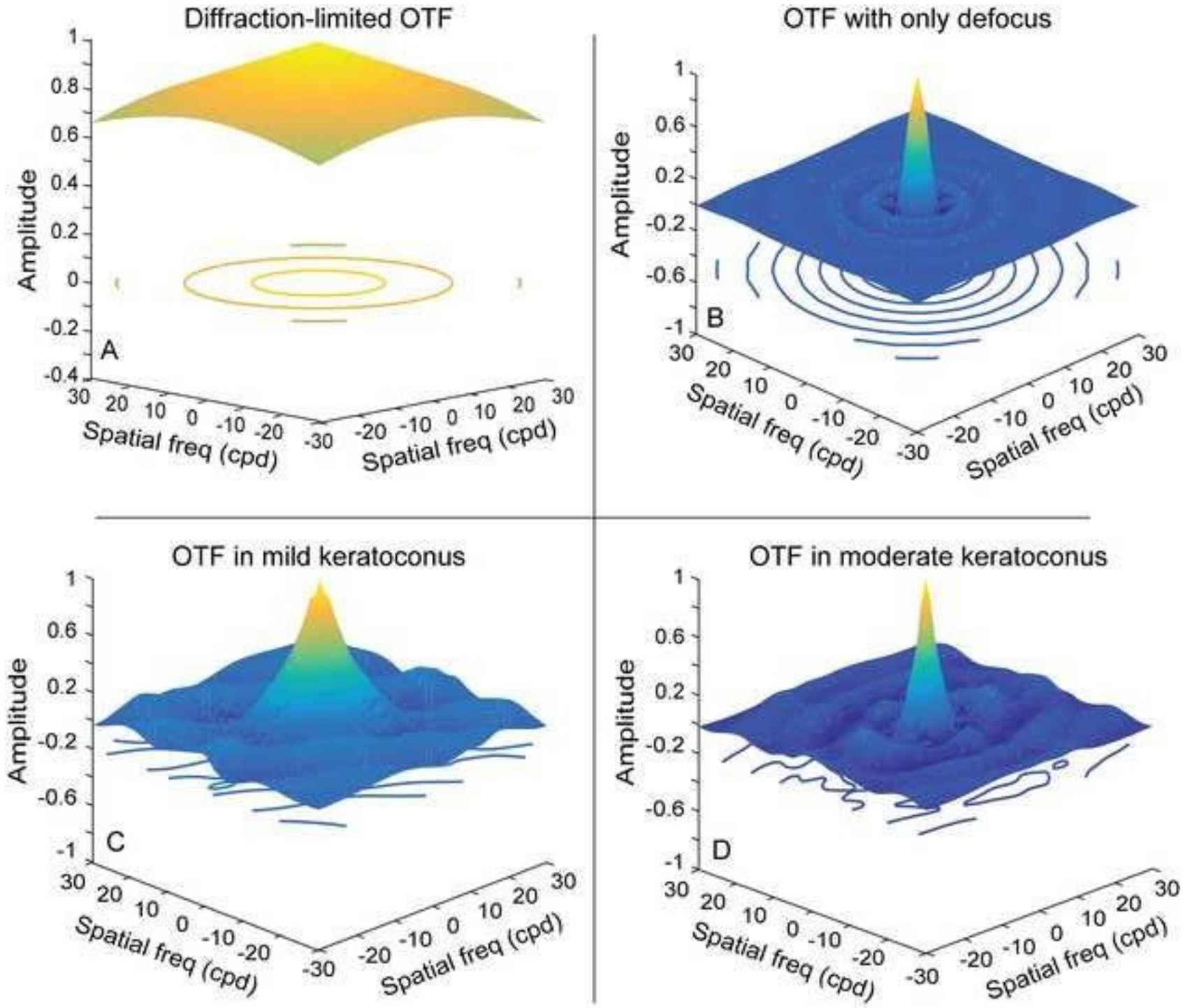
Diffraction-limited OTF
OTF with only defocus
OTF in mild keratoconus
OTF in moderate keratoconus
Amplitude
Spatial freq (cpd)
A
B
C
D

Figure A2

Click here to access/download;Figure;Figure A2.tif

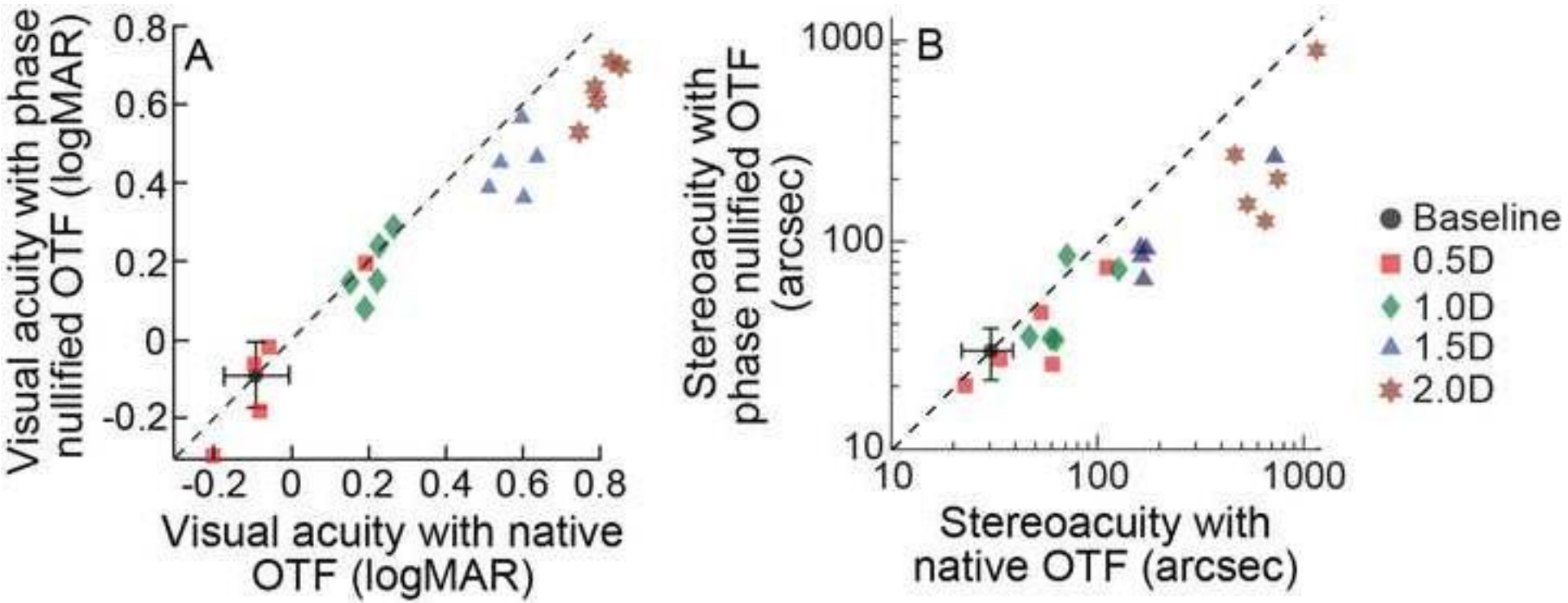

Optical phase nullification partially restores visual and stereo acuity lost to simulated blur from higher-order wavefront aberrations of keratoconic eyes

Bhagya Lakshmi Marella[1,2,3], Miriam Conway[3], Pravin K. Vaddavalli[4], Catherine Suttle[3], and Shrikant R. Bharadwaj[1,2]

[1]Brien Holden Institute of Optometry and Vision Sciences, L V Prasad Eye Institute, Road 2 Banjara Hills, Hyderabad – 500034 Telangana, India.

[2]Prof. Brien Holden Eye Research Centre, L V Prasad Eye Institute, Road 2 Banjara Hills, Hyderabad – 500034 Telangana, India.

[3]Centre for Applied Vision Research, City, University of London, Northampton Square, London EC1V 0HB, United Kingdom.

[4]Shantilal Sanghvi Cornea Institute, L V Prasad Eye Institute, Road no. 2, Banjara Hills, Hyderabad – 500034, Telangana, India.

Corresponding author: Shrikant R. Bharadwaj

Brien Holden Institute of Optometry and Vision Sciences, L V Prasad Eye Institute, Road no. 2, Banjara Hills, Hyderabad – 500034 Telangana, India.

bharadwaj@lvpei.org

Running title: Vision improvement with phase nullification in keratoconus

Number of figures in manuscript: 7

Number of figures in appendix: 2

Number of tables in manuscript: 1

Word count in abstract: 284

Word count in revised abstract: 250

Word count in original manuscript: 5435

Word count in revised manuscript: 6273

Highlights

- Keratoconic blur is characterized by exaggerated contrast demodulation and phase distortions.
- Phase nullification partially recovers the visual acuity and stereoacuity lost to this optical blurring.
- Stereoacuity improvement with phase nullification is more prominent for unilateral than bilateral blur.
- Discriminability of letters also improves following phase nullification of the blurred image.
- Alignment of local image features following phase nullification contributes to vision improvement in keratoconus.

Abstract

Contrast demodulation and phase distortions are exaggerated in retinal images blurred by the higher-order wavefront aberrations of keratoconic eyes. While the performance loss from the former parameter is well understood, little is known about the impact of the latter on visual functions in this disease condition. The present study investigated the impact of phase distortions on the monocular logMAR visual acuity, letter discriminability and random-dot stereoacuity of seventeen visually healthy adults using images that were computationally blurred by four different higher-order wavefront aberration profiles of keratoconic eyes that showed significant distortions in the phase spectrum. Participants viewed these images through 2mm artificial pupils to negate their native ocular wavefront aberrations. The results showed progressive losses in visual acuity and stereoacuity with increasing blur, a third of which could be recovered following phase nullification. Letter discriminability also improved following phase nullification, more so for smaller than larger optotypes. Stereoacuity loss and, consequently, its recovery following phase nullification was more prominent for profiles simulating unilateral asymmetric keratoconus than for profiles simulating bilateral symmetric keratoconus. These results agree with previous reports obtained from blur induced with lower-order aberrations and indicate that a similar trend may be observed for more complex patterns of blur like keratoconus. Overall, both contrast demodulation and misalignment of the local features of the blurred image may contribute to losses of spatial and depth vision in keratoconus. Phase nullification may partially mitigate these losses, thereby allowing the processing of finer spatial details and veridical disparity estimations for improved depth perception.

Keywords: Contrast; Correspondence matching; Ghosting; Higher-order aberrations; Retinal image quality, phase correction.

Keratoconus is an ectatic disorder of the cornea causing significant impairment in vision and vision-related quality of life (Fan, Kandel & Watson, 2024, Gothwal, Gujar, Sharma, Begum & Pesudovs, 2022, Pinto, Abe, Gomes, Barbisan, Martini, de Almeida Borges, Fernandes, Arieta & Alves, 2021, Santodomingo-Rubido, Carracedo, Suzaki, Villa-Collar, Vincent & Wolffsohn, 2022). This disease leads to elevated levels of wavefront error, which, when described by the Zernike polynomial, shows elevated levels of vertical coma (z_3^{-1}), horizontal coma (z_3^{1}), vertical trefoil (z_3^{-3}), spherical aberration (z_4^{0}), and secondary astigmatism (z_4^{2}) in the keratoconic eye, compared to a typical population (Devi, Kumar, Marella & Bharadwaj, 2022, Nilagiri, Metlapally, Schor & Bharadwaj, 2020, Pantanelli, MacRae, Jeong & Yoon, 2007). These Zernike components may all interact in complex ways to degrade the retinal image quality in keratoconus (Applegate, Sarver & Khemsara, 2002, Devi et al., 2022). This degraded retinal image, like any other defocused image, is characterized by significant contrast demodulation and phase alterations of the individual spatial frequency components (Artal, Santamaria & Bescos, 1988, Smith, 1982, Walsh & Charman, 1989, Yellott & Yellott, 2007). While the combined impact of contrast demodulation and phase alterations or the isolated impact of the former factor on the spatial and depth vision in keratoconus has been investigated earlier (Bell, Hastings, Nguyen, Applegate & Marsack, 2023, Marella, Conway, Suttle & Bharadwaj, 2021, Marella, Vaddavalli, Reddy, Conway, Suttle & Bharadwaj, 2023, Metlapally, Bharadwaj, Roorda, Nilagiri, Yu & Schor, 2019, Nilagiri, Metlapally, Kalaiselvan, Schor & Bharadwaj, 2018, Rozema, Hastings, Marsack, Koppen & Applegate, 2021), the latter's impact on visual functions is less well-understood. That the phase alterations may have a strong impact on vision in keratoconus is indicated by the "ghosting" / "doubling" of images often reported by patients during a routine eye examination. These effects qualitatively reduce with rigid contact lens wear that improve the eye's optical quality by replacing the distorted cornea with a uniform refracting surface (Devi, Kumar & Bharadwaj, 2023). However, the underlying optical/psychophysical basis for such perceptual experiences have not been systematically investigated in keratoconus thus far.

Given that the amplitude spectra of natural images often share a common 1/f distribution (Tadmor & Tolhurst, 1993), the global structure of an image is best described by its unique phase structure (Piotrowski & Campbell, 1982, Sarver & Applegate, 2004). Phase disruptions and the accompanying altered structure of an image created by optical aberrations certainly contribute to reduced visual acuity in humans (Akutsu, Bedell & Patel, 2000, Artal et al., 1988, Cheng, Bradley & Thibos, 2004, Ravikumar, Bradley & Thibos, 2010,

Yellott & Yellott, 2007). For instance, Ravikumar et al (2010) demonstrated the impact of phase alteration and its nullification by computationally blurring targets with specific combinations of monochromatic wavefront aberration terms and measuring visual acuity with the native and a nullified phase spectrum. Their results showed that the alignment of the local image features following phase nullification improved the edge contrast of the letter targets, partially restoring the visual acuity loss encountered with the native phase. Phase nullification also qualitatively decreased the ghosting/doubling of the targets (as evident from their simulations), even while these effects were not quantified in their study (Ravikumar et al., 2010). It remains unknown if these observations can be directly extrapolated to the visual experience of targets blurred using the pattern of retinal image blur generated in keratoconus.

When phase disruptions are dissimilar in the right and left eyes, the binocular perception of object location is affected and stereoacuity is impaired (Ding, Klein & Levi, 2013a, Ding, Klein & Levi, 2013b). These effects were demonstrated computationally for keratoconic blur by Metlapally et al (2019) who showed that retinal images blurred by dissimilar keratoconic point spread functions (PSFs) impaired the overall strength of the retinal disparity signal in the fused cyclopean image. Phase nullifying these PSF's decreased the false correspondence matches and produced a commensurate improvement in the strength of the retinal disparity signal (Metlapally et al., 2019). This improvement correlated with the participant's stereoacuity, even while the phase nullified stereoacuities were not directly tested in their study.

The present study addressed these gaps in the literature by investigating the impact of the phase distortions and their nullification on spatial and depth vision in keratoconus. Two specific hypotheses were tested. First, phase nullification of the keratoconic PSF will improve visual acuity and optotype discriminability through better alignment of the local image features, all relative to the native phase condition. Second, phase nullification of the keratoconic PSFs will enhance detection of the disparate monocular images of a random dot stereogram pair, resulting in improved stereoacuity, again relative to the native phase condition. The stereoacuity improvement will be greater for conditions simulating bilaterally asymmetric keratoconus than for conditions simulating bilaterally symmetric disease. This may be so, because, unlike the bilaterally symmetric disease conditions, monocular phase distortions will result in dissimilar contrast and dissimilar alterations in the local image structure of the two eyes. The former may be more deleterious to stereoacuity, as expected from the contrast paradox phenomenon of

stereopsis (Cormack, Stevenson & Landers, 1997, Stevenson & Cormack, 2000), while the latter may impact stereo processing by inducing mismatches in retinal correspondence (Ding et al., 2013a, Ding et al., 2013b, Metlapally et al., 2019). Nullifying the phase in the blurred eye may reduce the impact of both factors, resulting in greater improvement of stereoacuity, relative to the bilateral blur conditions. These hypotheses were tested by comparing the visual acuity, optotype discriminability, and random dot stereoacuity of otherwise visually healthy individuals who viewed images that were blurred by the native and phase nullified PSFs derived from the higher-order wavefront aberrations of keratoconic eyes.

2. Methods

2.1. Participants

Seventeen adults (23 to 31 years of age; 7 males), familiar with psychophysical measurement protocols but naïve to the present study aims, were recruited from the staff and student pool of L V Prasad Eye Institute (LVPEI), Hyderabad, India. The study protocol adhered to the tenets of the declaration of Helsinki and was approved by the Institutional Review Board of LVPEI and City, University London, London, UK. All participants were visually healthy, had best-corrected visual acuity better than 20/25 in both eyes and best-corrected stereoacuity of at least 40 arcsec, as estimated using routine clinical protocols. Ten individuals each participated in the visual acuity and stereoacuity experiments. Three individuals were common to both experiments. The participant's right eye was chosen for visual acuity testing (left eye remained occluded throughout). The participant's head was stabilized using a chin and forehead rest.

2.2. The wavefront aberration profiles for blurring the targets

Blurred targets were generated using the wavefront aberration profiles measured earlier in our laboratory in four patients with unilateral keratoconus through a mesopic pupil diameter of >5.0 mm for 555 nm light using the irx3™ wavefront aberrometer (Imagine Eyes®, Orsay, France) (Nilagiri et al., 2020). The wavefronts were then scaled down to a constant 5 mm pupil diameter using the technique described by Campbell (2003). Zernike coefficients of the three lower-order terms of defocus, and astigmatism ($z_2^2, z_2^0 \& z_2^{-2}$) were set to zero to determine the impact of only higher-order aberrations on visual functions before and after phase nullification. The coefficients of the 3rd to 5th order terms that were used for blurring the targets in this study were retained as is (Figure 1). The higher-order root mean squared (HORMS) deviation of these wavefront aberration profile were 0.52 µm, 0.93 µm, 1.21 µm and 1.39 µm

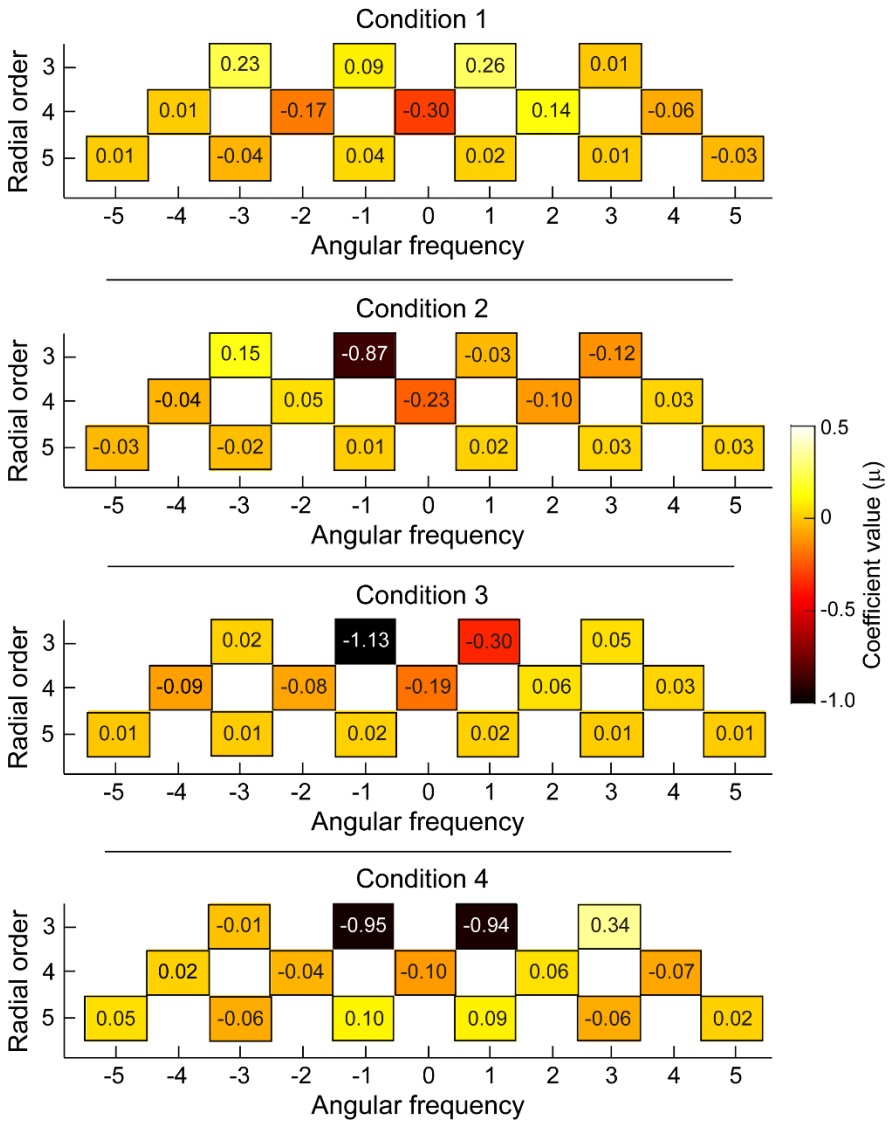

Figure 1: *Heatmaps of the coefficient values of the individual Zernike polynomial terms from the 3rd to the 5th radial order used in this study. Panels A – D show these values for Conditions 1 – 4, respectively. Zernike coefficients of the two lower-order terms of defocus, and astigmatism were set to zero to mimic an eye fully-corrected for its sphero-cylindrical refractive error.*

for Conditions 1 – 4, respectively. Two of the patients whose wavefront profiles were chosen had mild disease severity (Maximum keratometry value: 48.9 D and 48.7 D; henceforth referred to as Conditions 1 and 2, respectively) and the remaining two had moderate disease severity (Maximum keratometry value: 51.3 D and 52.9 D; henceforth referred to as Conditions 3 and 4, respectively). These profiles were specifically chosen as they showed significant phase reversals in the optical transfer function (OTF) [Figures 2A, C, E and G; see Appendix I for 3D representations of the OTF) and that there was enough contrast in the phase reversed portions of these functions to improve visual performance [see, portions of the phase

nullified OTFs – essentially the modulation transfer function (MTF) – crossing the neural transfer function in Figures 2B, D, F and H, relative to the OTFs with native phase]. In general, phase nullification had greater impact in increasing the spatial frequency range for eyes with moderate keratoconus (i.e., Conditions 3 and 4) than for eyes with mild keratoconus (i.e., Conditions 1 and 2) (Figure 2). The shift in the intersection of the highest spatial frequency of the radially-averaged MTFs and the NTF following phase nullification is indicated for each condition in Figure 2.

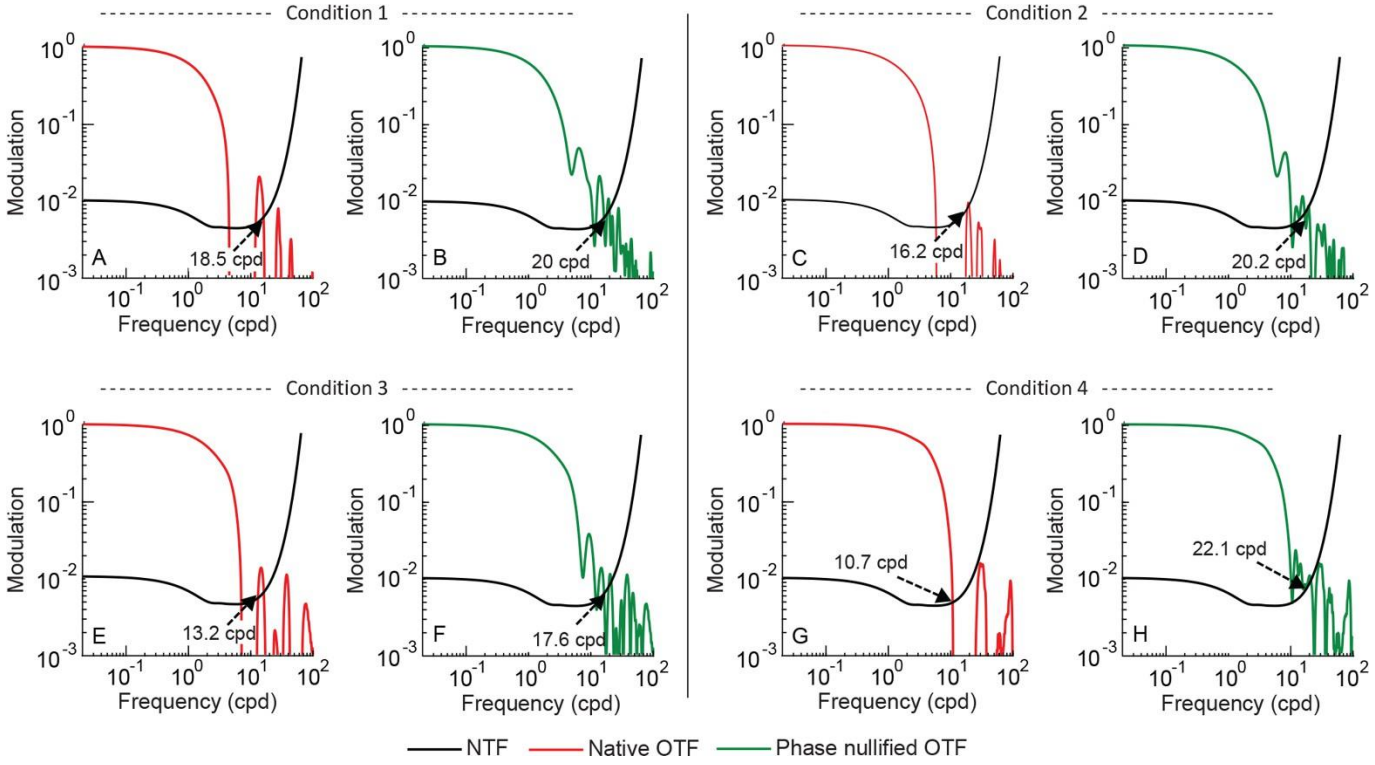

Figure 2: *The amplitude spectrum of the real part of the radially-averaged complex-valued optical transfer function (OTF) computed from the 3rd to 5th order monochromatic wavefront aberrations of the four keratoconic eyes chosen for this study (Conditions 1 – 4). Panels A, C, E and G show the OTF with native phase while panels B, D, F and H show the corresponding curves with phase nullification for Conditions 1 – 4. The portions of the OTF with contrast energy <10^{-3} indicate phase reversals for the corresponding spatial frequencies. The black trace in each panel shows the neural threshold function (NTF) obtained from Hastings et al (2020) for a 25-year-old human observer at 1100 Td of retinal illuminance. The spatial frequency cut-off at the point of last intersection between the OTF and NTF are indicated in each panel (Thibos, Hong, Bradley & Applegate, 2004).*

A separate control experiment was conducted to validate the present study protocol by replicating the main experiment of Ravikumar et al (2010) (see Appendix II for details). This experiment determined the impact of blur induced by a combination of myopic defocus and positive spherical aberration with native and nullified phase on visual acuity and stereoacuity. The blur levels induced in this experiment were equal

to those used by Ravikumar et al (2010) for estimating visual acuity. The visual acuity results of this control experiment were equivalent to the Ravikumar et al. study.

2.3. Generation of blurred optotypes and visual acuity assessment

The "source" method that allowed independent manipulation of the amplitude and phase spectrum of the image was employed in this study to generate the blurred optotypes (Chan, Smith & Jacobs, 1985, Smith, Jacobs & Chan, 1989). A database comprising of the grayscales images of all 10 Sloan optotypes between -0.50 logMAR unit (20/6.3 Snellen fraction) to +1.30 logMAR unit (20/399 Snellen fraction) was created in steps of 0.1 logMAR unit. All optotype sizes were calibrated for a 2-meter viewing distance and were 255 x 255 pixels in size, with a resolution of 92 dots per inch. These optotypes were blurred by convolving them with the PSFs derived from the wavefront aberrations profile described in the previous section using the techniques described by Thibos (2019) and implemented onto the Fourier Optics Calculator [presently called Indiana Retinal Image Simulator (IRIS); https://blogs.iu.edu/corl/iris/], an open-source software for retinal image simulations using standard Fourier optics techniques. The complex-valued OTF, obtained by Fourier transforming the keratoconic PSF, was then phase nullified by taking the absolute values of this OTF function using the syntax abs(OTF) in Matlab® (R2016b, MathWorks Inc, Natick, USA). This manipulation effectively returns the modulation transfer function (MTF) of the image, with phase information being set to zero. This absolute value of the OTF function with zero phase was inverse Fourier transformed to obtain the phase nullified PSF. These PSF's were then convolved with optotypes, as before, to get the phase nullified blurred images. This protocol was implemented using the Fourier Optics Calculator written in Matlab®.

Visual acuity was determined using a method of constant stimuli paradigm, custom-written in Matlab®. All measurements were obtained with each participant's sphero-cylindrical refractive correction placed in a trial lens frame at 10 mm vertex distance. Participants viewed the optotypes through a 2 mm diameter artificial aperture placed before the tested eye in the same trial frame to avoid any effect of inherent higher-order aberrations of the eye (Applegate, Donnelly, Marsack, Koenig & Pesudovs, 2007).[3] The

[3]Diffraction effects on the visual acuity could not controlled and it remained constant for both the native phase and phase nullified testing protocols.

psychometric function was constructed using 11 different-sized optotypes, presented 10 times each, resulting in a total of 110 presentations. For each presentation, the optotype and its size were randomly chosen from amongst the Sloan set (C, D, H, K, N, O, R, S, V and Z). The central value of the optotype was chosen based on pilot testing of the visual acuity for all four conditions tested in this study. Five sizes on either side of the central value with an interval of 0.1 logMAR unit was used for generating the psychometric function. The stimuli were presented from 2 meters on a gamma-corrected LCD monitor with 1680 x 1050-pixel resolution and 59Hz refresh rate using the Psychtoolbox-3 interface of Matlab (Brainard, 1997). A single optotype of the desired size with a bounding box was flashed for the duration of 300 msec to avoid eye movements from influencing the subjective response of the participant, as is the standard practice in psychophysical experiments of this nature (Pelli, Burns, Farell & Moore-Page, 2006). This duration is long-enough for the near-perfect identification of single optotypes in human adults (Bundesen & Harms 1999, Petersen & Andersen, 2012). Participants were asked to identify the letter from the English alphabet with a chance-level performance of 3.85%.[$] The resultant psychometric function was fit using a cumulative Gaussian distribution function, with the mean and standard deviation of the function optimized using the fminsearch function in Matlab, based on the maximum likelihood–based Nelder–Mead simplex algorithm. The logMAR value corresponding to 51.6% correct response was considered as the threshold visual acuity. The visual acuity was obtained nine times in each participant – baseline and once each for Conditions 1 – 4 with native and nullified phase spectra, all in random order.

2.4. The optotype discrimination task

A subset of five individuals that participated in the visual acuity experiment were recruited for the optotype discrimination task that involved identifying the 10 Sloan optotypes blurred using the PSF's from Condition 2 and 4 of the main experiment. Each blurred optotype was presented 10 times in random order, each for 300 msec duration, at the participant's visual acuity threshold value and two lines above this threshold value. The mean (± 1 SD) letter size at threshold value for the discrimination task was 0.45 ± 0.05 and 0.59 ± 0.05 logMAR units for Conditions 2 and 4, respectively, across participants. The examiner

[$]Some participants experienced in psychophysical assessment of visual acuity may tend to limit their choices to the 10 Sloan letters especially towards the end of the trials. This would change the chance-level performance to 10% from 3.85%. This small change in chance-level performance is unlikely to impact the threshold estimates obtained from the psychometric functions.

recorded the participant's response for each presentation and analysed the data using confusion matrices (Barhoom, Joshi & Schmidtmann, 2021, Candy, Mishoulam, Nosofsky & Dobson, 2011).

2.5. Generation of blurred stereograms and stereoacuity assessment

A database comprising of black and white random-dot stereogram pairs were generated using custom-written software in Matlab®. Each image of the stereogram pair was 500 x 500 pixels in size and subtended 17° × 17° at 50 cm viewing distance with 2 min of arc/pixel (Figure 3). The disparity stimulus in each stereogram pair was an isosceles triangle pattern with one of four possible apex orientations (right, left, up and down) (Figure 3). The stimuli were presented in crossed disparity ranging from 10 arcsec to 1000 arcsec in steps of 10 arcsec between 10 to 400 arcsec and in steps of 50 arcsec between 400 to 1000 arcsec. All disparities were generated for a constant interpupillary distance of 60 mm. Each image in the database had a different pattern of random dots to avoid participants using the spatial pattern of the stimulus to perform the psychophysical judgements. The convolution process used to generate the blurred stereograms with native and nullified phase was identical to that used for generating the blurred optotypes. Bilaterally symmetric keratoconus (i.e., similar severity of keratoconus in both eyes) was simulated by presenting the same pattern of blur to the individual images in a stereogram pair (Figures 3B and C). While optically normal individuals tend to show mirror symmetry of the wavefront aberrations in the two eyes (Castejon-Mochon, Lopez-Gil, Benito & Artal, 2002, Porter, Guirao, Cox & Williams, 2001, Thibos, Hong, Bradley & Cheng, 2002), such a pattern may not exist in keratoconic individuals owing to asymmetric disease progression in the two eyes. Hence, mirror symmetry in the Zernike coefficients of the two eyes was not introduced during the blurring of the stereogram image pairs in the bilateral blur conditions. Unilaterally asymmetric keratoconus (i.e., one eye was keratoconic while the fellow eye was normal) was simulated by presenting the blur pattern to the right eye while the left eye's pattern remained unmanipulated (Figures 3D and E). Bilaterally asymmetric keratoconus (i.e., both eyes with keratoconus but of different severities) were not tested due to the extensive nature of psychophysical testing involved.

Stereoacuity measurements were obtained from a viewing distance of 50 cm with the participant's sphero-cylindrical refractive correction placed in a trial lens frame at 10mm vertex distance. Subjects fused the stereogram pair through a stereoscope whose mirror angle could be adjusted to overcome the participant's horizontal heterophoria, if any. Participants viewed the stimuli through 2 mm diameter

artificial apertures that were mounted onto the back surface of the mirror stereoscope. The positions of the apertures and the mirror angle were carefully adjusted such that each image of the stereogram pair was dichoptically visible to the participant. Stereoacuity measurements started only after the subjects reported stable fusion. Stereoacuity was measured using a method of constant stimuli psychophysical procedure involving 11 different disparity values, each presented 10 times in random order. The experiment was carried out on the same LCD monitor used for acuity testing, with the stimuli displayed using the Psychtoolbox-3 interface of Matlab® (Brainard, 1997). The stimulus was flashed for a 300 msec

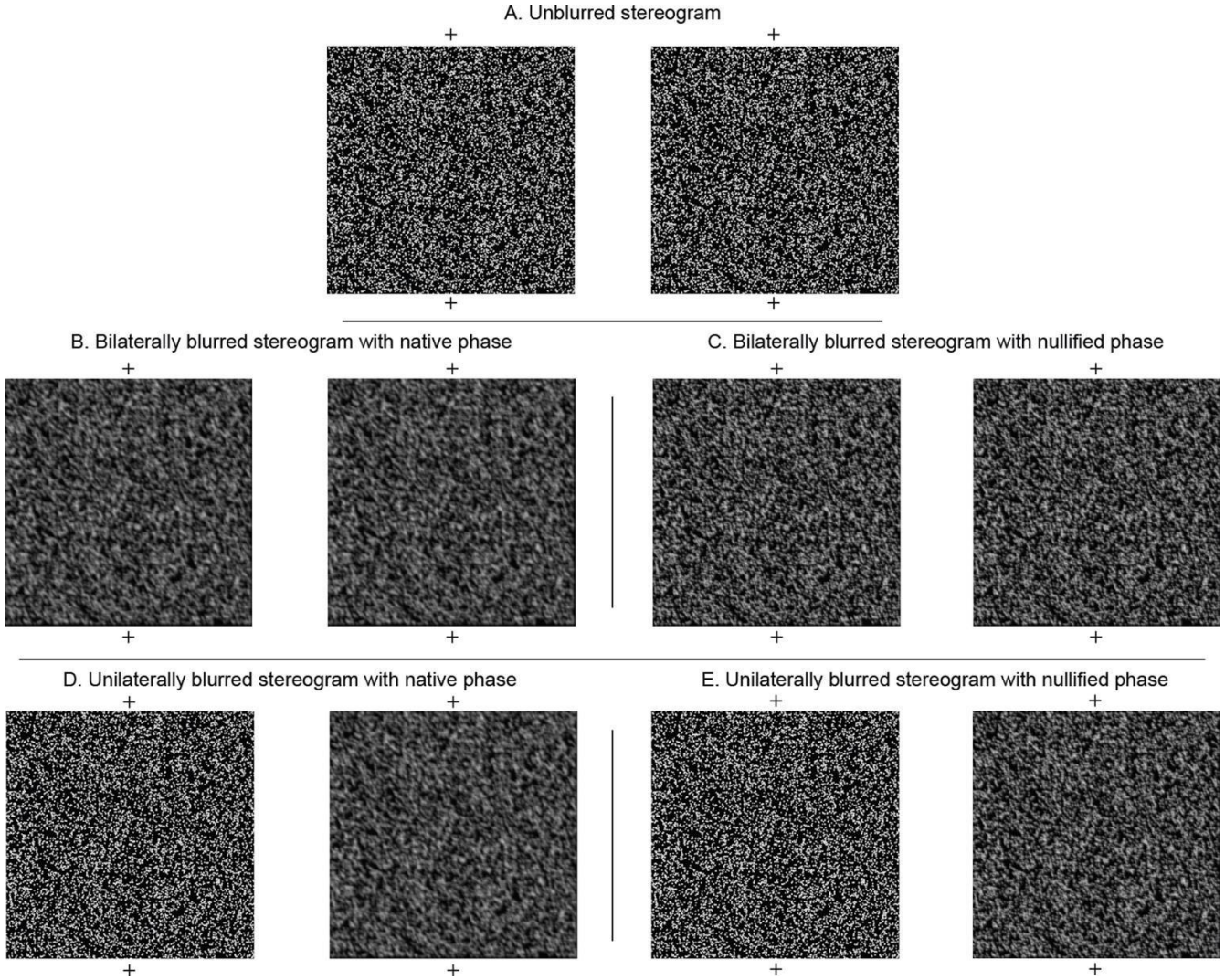

Figure 3: *Representative random-dot stereogram pairs used to estimate stereoacuity in this study. The unblurred stereogram pair shown in Panel A was blurred using the blur profile in Condition 3 (moderate keratoconus) of this study. Panels B and C show bilaterally blurred version of the stereogram pairs with native and nullified phase, respectively. Panels D and E show unilaterally blurred version of the same stereogram pairs. Each stereogram pair with 120 arcsec of crossed retinal disparity may be cross-fused to experience an isosceles triangle with its apex pointing downwards appearing in depth.*

duration and the participant made a four-alternate forced-choice judgement of the apex orientation of the triangle. The resultant psychometric function was fit using the same technique described for acuity judgments and the stereoacuity was estimated from the stimulus disparity value that produced a 62.5% correct response. Stereoacuities were obtained in 17 conditions in each participant – baseline and, four times each with native and nullified phase in the four bilateral- and four unilateral conditions.

It took several hours to complete the data collection across all 26 sessions (9 for visual acuity and 17 for stereoacuity) in a given participant. These sessions were grouped into several smaller blocks and executed on different days based on the participant's availability and fatigue. The visual acuity and stereoacuity measurements were obtained in no specific order on separate sessions in each participant.

2.6. Data analysis

Data were analysed using Microsoft Excel® (Microsoft Corporation, Redmond, USA), IBM SPSS statistics v20.0® (SPSS, Chicago, IL, USA) and Matlab R2016b. Kolmogorov-Smirnov test indicated that all data (except the stereoacuity at Condition 3) were normally distributed and, therefore, parametric tests were used for all statistical analyses. Separate two-factor repeated measures analysis of variances (RM-ANOVAs) were conducted to determine the impact of induced blur magnitude and phase nullification on visual acuity and the impact of bilaterally and unilaterally induced blur and phase nullification on stereoacuity. Separate one-factor RM-ANOVAs were conducted to determine the impact of blur magnitude and phase nullification on visual acuity and stereoacuity, from their respective baseline values (i.e., without any induced blur). The Mauchly's test of sphericity for equal variances among the differences between all possible pairs of blur magnitudes remained unviolated for visual acuity ($p = 0.11$) but was violated for the stereoacuity conditions ($\varepsilon \leq 0.45$, for both; $p = 0.001$). The within-subject effects of the RM-ANOVAs are therefore reported as for visual acuity and following the Greenhouse-Geisser correction for the stereoacuity measurements. Post-hoc Bonferroni test with adjustment for multiple comparisons was performed for all pairwise comparisons. $P < 0.05$ was considered statistically significant and the effect size was estimated using the partial η^2 values.

3. Results

3.1. Visual acuity with native and phase nullified blur

The mean (± 1SD) cohort level visual acuity at baseline was -0.02 ± 0.07 logMAR units. Figure 4 shows representative psychometric functions for visual acuity assessment from one participant across the four induced blur conditions tested in this study with native (solid curves) and nullified (dashed curves) phase. The psychometric functions expectedly shifted towards larger optotype sizes with an increase in induced blur magnitude (Figures 4A – D). Phase nullification resulted in a leftward shift in the psychometric function for all four wavefront aberration patterns, signalling a partial restoration in visual acuity relative to the native phase (Figures 4A – D). The two-factor RM-ANOVA showed significant main effects of blur magnitude [$F(3, 27) = 122.52$; $p < 0.001$; partial $\eta^2 = 0.98$] and phase profile [$F(1, 9) = 336.93$; $p < 0.001$; partial $\eta^2 = 0.97$] on visual acuity (Table 1, Figure 4E). Pairwise comparisons revealed the visual acuities differed significantly between all levels of induced blur ($p \leq 0.01$, for all). The interaction effect between the two main factors was also significant [$F(3, 27) = 4.60$; $p < 0.04$; partial $\eta^2 = 0.66$], indicating that the improvement in visual acuity with phase nullification was not uniform across all magnitudes of induced blur (Figure 4E). Condition 1, with the lowest magnitude of induced blur, resulted in the least visual acuity improvement with phase nullification (0.08 logMAR units) while the other three conditions, with increasing magnitudes of induced blur, resulted in larger but similar acuity improvements following phase nullification (Condition 2: 0.16 logMAR units; Condition 3: 0.15 logMAR units; Condition 4: 0.17 logMAR units). A separate one-way RM-ANOVA analysis with appropriate post hoc comparison revealed that the baseline visual acuity was significantly different from all the four levels of induced blur with native ($F = 267.69$; $p < 0.001$) and nullified phase profiles ($F = 94.56$; $p < 0.001$) (Figure 4E).

Table 1: *Mean (± 1SD) monocular visual and stereo acuity obtained across all four induced blur conditions with native and nullified phase. Stereoacuity obtained with bilaterally and unilaterally induced blur are shown in this table.*

	Visual acuity (logMAR)		Stereoacuity (arcsec)			
			Bilateral		Unilateral	
	Native	Nullified	Native	Nullified	Native	Nullified
Condition 1	0.25 (0.21 - 0.28)	0.17 (0.13 - 0.21)	68.30 (42.87 - 93.74)	60.58 (29.16 - 92.00)	63.76 (49.87 - 77.66)	45.2 (34.46 - 55.94)
Condition 2	0.44 (0.41 - 0.48)	0.29 (0.25 - 0.32)	69.78 (47.44 - 92.12)	62.67 (32.75 - 92.59)	93.27 (65.33 - 121.22)	53.89 (41.59 - 66.18)
Condition 3	0.53 (0.51 - 0.55)	0.38 (0.33 - 0.43)	120.71 (73.03 - 168.39)	98.32 (20.52 - 176.13)	152.97 (119.37 - 186.56)	86.54 (57.98 - 115.09)
Condition 4	0.59 (0.56 - 0.63)	0.42 (0.39 - 0.46)	85.52 (57.29 - 113.75)	63.43 (35.54 - 91.32)	197.81 (102.89 - 292.74)	85.25 (51.93 - 118.57)

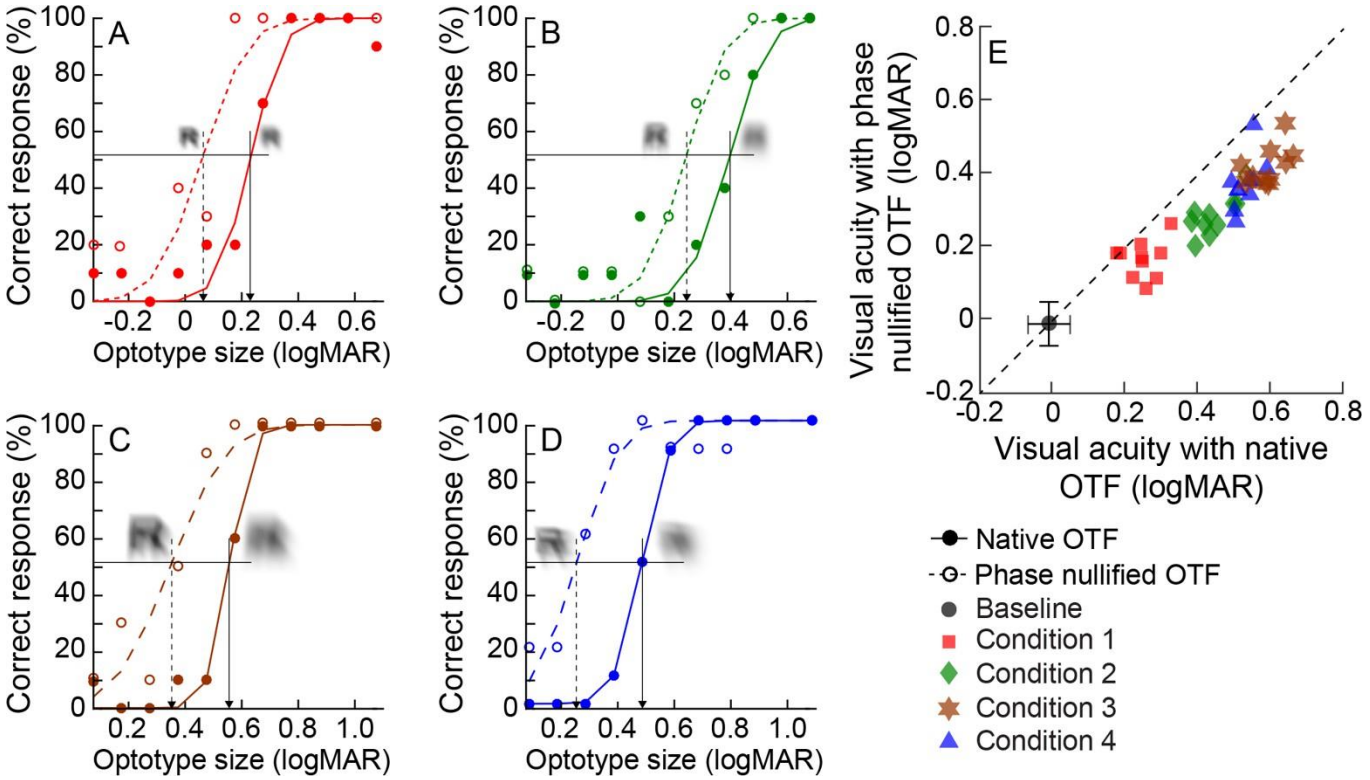

Figure 4: *Psychometric functions of visual acuity obtained from a representative participant for the four induced blur conditions tested in this study (Condition 1, Condition2, Condition 3 & Condition 4, respectively) (Panels A – D). The filled symbols and solid psychometric function show data obtained for the native phase condition while the open symbols and dashed psychometric function show data obtained for the phase nullified condition. Panel E shows the logMAR visual acuity obtained while viewing optotypes blurred using their native and nullified phase for the four keratoconus conditions tested in this study. Each symbol of a particular colour represents data from a single participant. The mean (±1SD) visual acuity obtained at baseline is also shown in this panel for comparison purposes.*

3.2. Optotype discrimination with native and phase nullified blur

Figure 5 shows bubble plots of the mean percentage correct identification of the presented optotype across the five subjects for targets blurred with the native and nullified phase of one mild (Condition 2; panels A and B) and one moderate (Condition 4; panels C and D) keratoconic eye used in this study. The mean percentage correct identification of the presented optotype across the five subjects that participated in this experiment is shown here. Three patterns were evident from the confusion matrices. First, the optotype discrimination for the native phase targets was far from ideal for both blurring conditions (Figure 5A and C). Some optotypes (e.g., C, D, O, R and V) were more prone to confusion than others (e.g., H, N, S and Z), with no uniform pattern of misjudgement across the confused optotypes. Second, phase nullification minimized this confusion for both blurring conditions, with the confusion matrix showing near 100% correct response for all 10 Sloan optotypes (compare red with green confusion matrices in Figure 5). Third, the

bubble plot obtained for native phase in Condition 4 with the larger optotypes obtained with showed relatively better discrimination that those in Condition 2 with the smaller optotypes. Consequently, the improvement in the confusion matrix following phase nullification was also smaller for Condition 4 than Condition 2 (Figures 5B and D). The visual impact of the two blurring conditions and the phase nullification on optotype discrimination may be observed from the simulated optotypes shown along the abscissa in each panel.

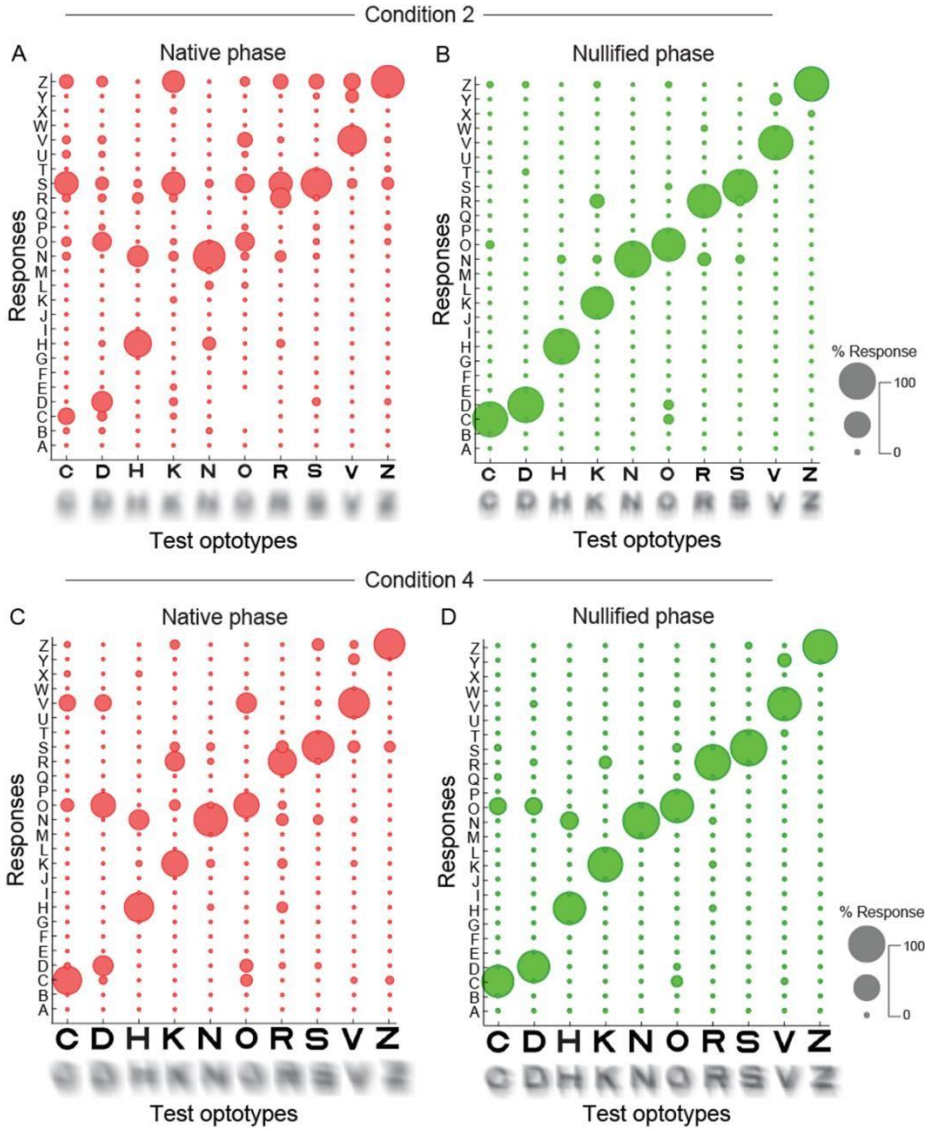

Figure 5: *Bubble plots showing the outcomes of the optotype discrimination task performed in this study using native and phase nullified blur of one mild (Condition 2; panels A and B) and one moderate (Condition 4; panels C and D) keratoconic eye. Bubble size represents the mean percentage of times the presented optotype (x-axis scale) was identified as a given English alphabet (y-axis scale). The scaling of bubble size to the percentage identification of the alphabet is shown in the figure inset. Optotypes simulated with the pattern of blur corresponding to the native and phase nullified viewing in Conditions 2 and 4 are shown along the abscissa in each panel.*

3.3. Stereoacuity with native and phase nullified blur

The mean (± 1SD) cohort level stereoacuity at baseline was 48.86 ± 20.13 arcsec. Table 1 and Figures 6 and 7 show representative psychometric functions for estimating stereoacuity and cohort level stereoacuity data for bilaterally-induced blur (Figure 6) and unilaterally-induced blur (Figure 7) with native and nullified phase in the four keratoconic conditions tested in this study. The impact of induced blur, and consequently, the phase nullification, on stereoacuity was smaller in the bilateral than unilateral induced-blur conditions (compare the partial η^2 values for the main effects of blur magnitude and phase nullification in the ANOVA analyses below). The representative psychometric functions showed a smaller and a non-uniform shift in the stereoacuity across the four bilaterally induced blur conditions (Figure 6A – D). The restoration of stereoacuity following phase nullification was also uniform across these conditions (Figure 6A – D). The two-factor RM-ANOVA showed no statistically significant main effect of blur magnitude [$F(1.28, 11.48) = 3.98$; $p = 0.063$; partial $\eta^2 = 0.31$], a marginal significance of phase nullification [$F(1, 9) = 5.17$; $p = 0.049$; partial $\eta^2 = 0.37$] and no significance of interaction between the two main effects [$F(1.19, 10.68) = 0.73$; $p = 0.44$; partial $\eta^2 = 0.08$] on stereoacuity with bilaterally induced blur (Table 1, Figure 6E).

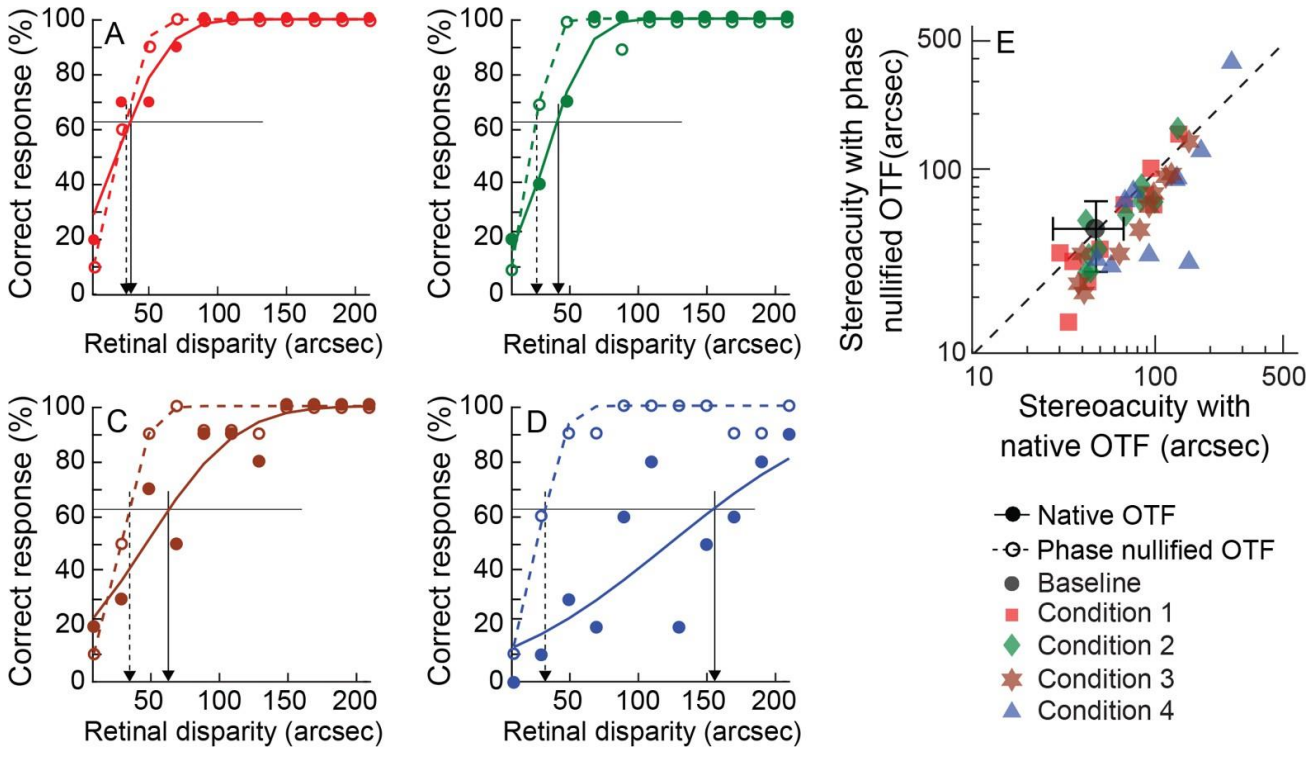

Figure 6: *Psychometric functions of stereoacuity obtained from a representative participant for the four bilaterally induced blur conditions tested in this study (Panels A – D). All other details are the same as Figure 4.*

In contrast, the psychometric functions for the unilaterally blurred conditions for the same participant in Figure 7A – D showed a progressive worsening of stereoacuity across Conditions 2, 3 and 4, while the stereoacuity in Conditions 1 and 2 were similar to each other. Phase nullification showed a larger restoration of stereoacuity for Conditions 3 and 4, relative to Conditions 1 and 2 (Figure 7A – D). The two-factor RM-ANOVA showed significant main effects of both blur magnitude [$F(1.34, 12.09) = 12.72$; $p = 0.002$; partial $\eta^2 = 0.59$] and phase nullification [$F(1,9) = 28.39$; $p < 0.001$; partial $\eta^2 = 0.76$] on stereoacuity with unilaterally induced blur (Table 1, Figure 7E). Pairwise comparisons indicated that the stereoacuity in each unilaterally induced blur condition was significantly different from the other three conditions ($p \leq 0.023$, for all) (Table 1). Although the interaction between the two main effects was not significant [$F(1.15, 10.3) = 4.20$; $p = 0.06$; partial $\eta^2 = 0.32$], the mean data showed a systematic increase in the improvement of stereoacuity following phase nullification, across blur magnitudes (Improvement in stereoacuity following phase nullification: 23.56 arcsec for Condition 1; 39.38 arcsec for Condition 2; 66.43 arcsec for Condition 3; 112.56 arcsec for Condition 4) (Table 1).

The results of the one-factor ANOVA analysis of the baseline stereoacuity to the stereoacuity with induced

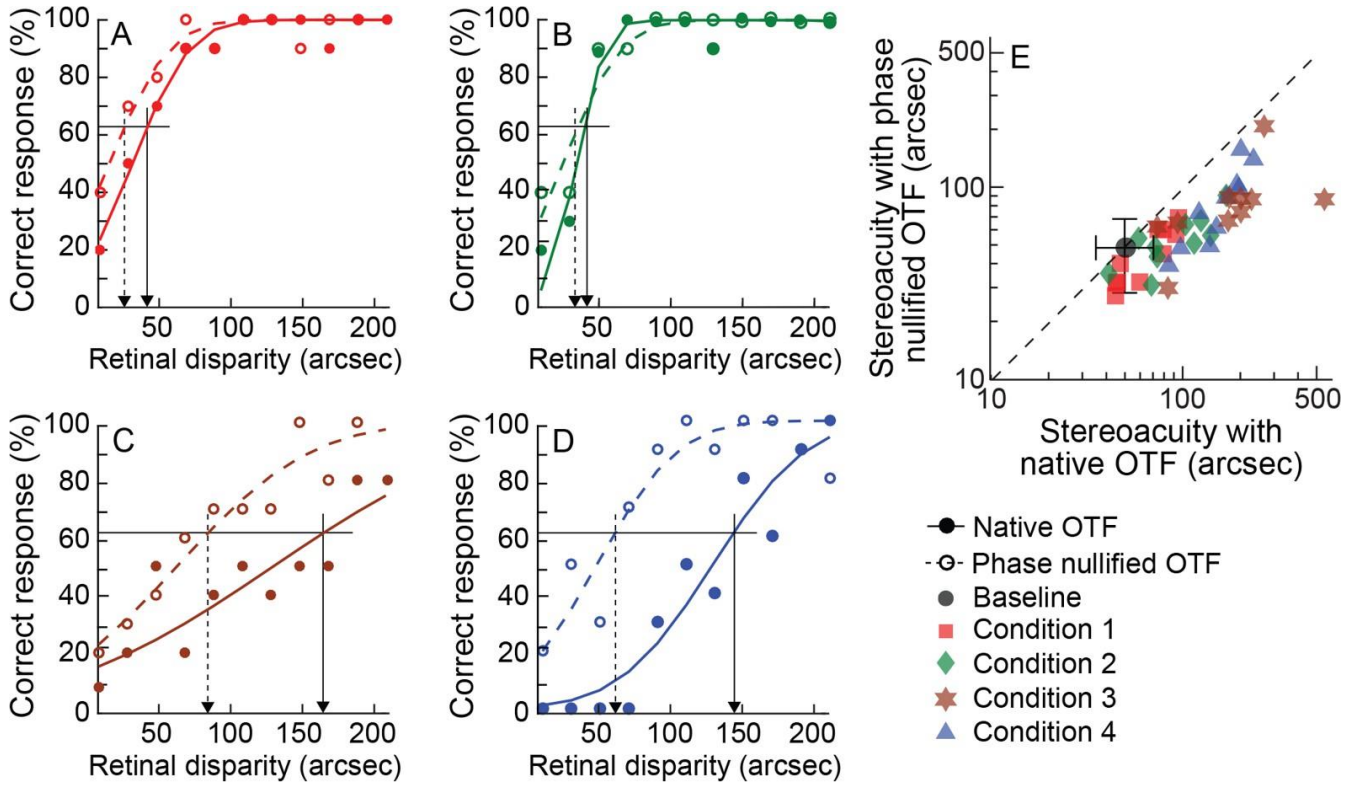

Figure 7: *Similar to Figure 6, but for the four unilaterally induced blur conditions.*

phase profiles and phase nullified conditions. A separate one-factor RM-ANOVA indicated that the baseline stereoacuity was significantly better than those with bilateral ($F = 4.18$; $P = 0.006$) and unilateral ($F = 8.87$; $p<0.001$) blur with native phase. Only the stereoacuity in Condition 3 of the bilateral blur was significantly worse than the baseline condition ($p = 0.004$) while Conditions 3 and 4 of unilateral blur were significantly worse than the baseline condition ($p \leq 0.01$, for both). Stereoacuity in the phase nullified conditions were not significantly different from the baseline level for bilateral and unilateral blur ($p \geq 0.09$).

4. Discussion

4.1. Summary of results and implications for vision loss in keratoconus

The present results confirm that visual and stereo acuity losses encountered for images blurred by keratoconic higher-order wavefront aberrations may be partially restored following phase nullification (Figures 3, 6 and 7). The impact of phase nullification on stereoacuity is more pronounced for targets simulating unilaterally asymmetric keratoconus with interocular differences in retinal image quality (Figure 7), relative to those simulating bilaterally symmetric disease (Figure 6). Phase nullification also improves character recognition, more so for those with smaller than larger angular subtense (Figure 5).

These results show that the combination of phase alterations and contrast demodulation of the component spatial frequencies arising in the blurred image contribute to spatial and depth vision losses in keratoconus. While contrast and phase are two independent characteristics of an image, alterations in the latter characteristic for local features in the image may influence the global contrast of complex images with broadband spatial frequency content, like the optotypes and random-dot patterns used in this study (Field & Brady, 1997, Haun & Peli, 2013, Peli, 1990). In fact, standard definitions of contrast, such as the Michaelson's contrast, may fail under such circumstances, as shown in the aforementioned literature. Phase nullification realigns the relative phases at which different spatial frequencies are combined, leading to improved edge contrast of the image feature (see the simulated optotypes before and after phase nullification in Figures 4 and 5), even while the overall contrast energy in the entire image may remain unchanged. The improved edge contrast may lead to an improved visual resolution and discrimination between optotypes, as seen in Figures 4 and 5, respectively, of this study. Perceptually, the phase realignment may also minimize the ghosting and doubling of targets (see simulated optotypes before and after phase nullification in Figures 4 and 5), improving object recognition and higher-level

functions like face perception (Ravikumar et al., 2010). All these factors combined may significantly improve the overall quality of vision and vision-related quality of life of the keratoconic patient (Fan et al., 2024, Gothwal et al., 2022, Pinto et al., 2021, Santodomingo-Rubido et al., 2022). Rigid contact lens designs that are routinely prescribed as a correction modality in keratoconus reduce both the contrast demodulation and the phase distortions simultaneously by virtue of their ability to replace the distorted cornea with a more uniform refracting surface (Devi et al., 2023, Kumar, Bandela & Bharadwaj, 2020). Similar outcomes are achieved under experimental conditions involving adaptive optics correction of the keratoconic eye's wavefront aberrations (Barbot, Park, Ng, Zhang, Huxlin, Tadin & Yoon, 2021, Sabesan, Ahmad & Yoon, 2007, Sabesan & Yoon, 2009). As a future possibility, the theoretical simulations of Yellott and Yellott (2007) propose phase nullifications as a means of restoring recognition of blurred images at near viewing distances in a presbyopic eye. The practical feasibility of this strategy, however, remains to be explored. Whether such corrections will directly benefit patients with chronic optical degradations like keratoconus also depends on how much of the patient's habitual visual experience is shaped by neural recalibration to prolonged blurred/distorted vision during the critical periods of visual development (Barbot et al., 2021, Ng, Sabesan, Barbot, Banks & Yoon, 2022, Sabesan, Barbot & Yoon, 2017, Sabesan & Yoon, 2009). All these issues need further investigation.

4.2. Changes in visual acuity before and after phase nullification

The present study extends the findings of Ravikumar et al (2010) to an optically complex situation like keratoconus wherein the retinal image quality is determined by complex interactions between several Zernike components in the higher-order wavefront aberration profile (Devi et al., 2023). The spatial frequency where the radially-averaged OTF intersected with the neural threshold function following phase nullification all increased to about 20 cpd in Conditions 1 – 4 tested in this study, even while these intersection points progressively declined with increasing magnitudes of blur with the native OTF (Figure 2). This translated into increases in the cut-off spatial frequency by 8.1% (18.5 cpd to 20 cpd = 8.1% increase), 24.7%, 33.3% and 106.5% following phase nullification in these four conditions (Figure 2). The empirical results, however, showed a uniform magnitude of improvement in visual acuity following phase nullification – 28.8% to 34% across Conditions 1 – 4 (Table 1, Figure 4E). This result may simply reflect how this study represents visual acuity changes in a logarithmic scale – the same percentage of improvement with phase nullification for a given blur condition may represent a larger quantum of change for

Conditions 3 and 4 with poorer logMAR acuities than for Conditions 1 and 2 with relative better logMAR acuities. Two alternate possibilities exist. First, the empirical measures of acuity loss restoration may not be veridically captured by the analysis involving the intersection of the radially-averaged OTF and the neural threshold function. After all, optotype recognition is a more complex task involving several cognitive processes and is only broadly correlated with acuity measures involving resolution of sinewave gratings (Mayer, Fulton & Rodier, 1984). Second, the Zernike coefficients present in a keratoconic wavefront aberration profile produce a radially asymmetric point spread function (Appendix I). Such radial asymmetries may significantly influence the recognition of Sloan optotypes used in this study, even while they were ignored by radially-averaging the OTF in the theoretical calculations described above (Figure 2). Perhaps, the intersection between the OTF and the neural threshold function should be computed for every orientation of the OTF, and the range of intersection values should be compared with the empirical estimates of acuity loss restoration obtained in this study. That this was not performed remains a limitation of the study.

4.3. Changes in stereoacuity before and after phase nullification

In the present study, the stereoacuity was determined as the smallest retinal disparity that allowed the participant to discern the orientation of an isosceles triangle from within a field of randomly distributed black and white dots (Figure 3). Optical blur challenges the computation of retinal disparity in two ways. First, the contrast loss associated with blur degrades stereoacuity, more so when the contrast attenuation is dissimilar in the two eyes compared to when they are bilaterally similar [the contrast paradox in stereopsis (Cormack et al., 1997, Cormack, Stevenson & Schor, 1991, Kumar, Campbell, Vaddavalli, Hull & Bharadwaj, 2023, Stevenson & Cormack, 2000)]. Second, the alterations in the spatial position of the local features in the monocular retinal image arising from dissimilar phase distortions in the two eyes impair correspondence matching, leading to false matches and non-veridical depth estimates (Ding et al., 2013a, Metlapally et al., 2019). Deterioration of stereo performance in the unilateral blur conditions is likely to arise from both the contrast paradox and non-veridical depth estimates from correspondence mismatches of the two differently blurred retinal images (Table 1, Figures 3, and 7). Phase nullification may minimize the positional mismatches between the two eyes in the unilateral-induced blur conditions, thus improving the strength of the retinal disparity signal available for stereo processing. Additionally, the reduction in positional mismatches following phase nullification decreases the interocular contrast

difference of the local image features, further supporting an improvement in stereoacuity. Stereoacuity losses with bilaterally symmetric blur may be attributed only to the overall attenuation of contrast arising from the blurred image in the two eyes (Table 1, Figures 3 and 6). The phase distortions may not impact stereoacuity in this condition as the positional shifts in the local features will be equal in both retinal images, thus leaving the correspondence matching process unimpaired. The modest improvement of stereoacuity in these conditions may be attributed only to the overall improvement of contrast of the locally realigned features following phase nullification. That the stereoacuity improvements following phase nullification were more pronounced for the unilateral- than bilateral-blur conditions indicate that the positional mismatches play a more dominant role in limiting stereo processing than the contrast attenuation of high spatial frequencies in keratoconus. This is not surprising considering that resolution of features in the stereo domain is mediated through low spatial frequencies, unlike the corresponding measures in the luminance domain – stereo spatial resolution is approximately a factor of ten lower than luminance spatial resolution (~30 cpd) (Banks, Gepshtein & Landy, 2004). Thus, the bulk of stereo processing may all happen in the region of the OTF that remains more or less unimpaired by the keratoconic blur (Figure 3). This may also explain why Vlaskamp et al. found no benefit to stereoacuity by correcting the higher-order monochromatic aberrations of individuals with otherwise normal optics (Vlaskamp, Yoon & Banks, 2011). The small magnitude of wavefront aberrations in normal eyes may not have induced significant phase distortions and, therefore, positional mismatches between the monocular images to impact stereoacuity to begin with; nullifying them may thus add no further benefit to stereo processing.

4.4. Study limitations

This study had three limitations from a clinical standpoint. First, the impact of phase nullification on spatial and depth vision have been demonstrated only for images blurred by the higher-order wavefront aberrations of the eye. In reality, even with the best-possible spherocylindrical correction, the keratoconic eye is seldom free of lower-order defocus and astigmatism. This is so because refining the sphero-cylindrical correction of the eye is a challenge in keratoconus owing to their large optical depth of focus (Nilagiri et al., 2020), poor repeatability of the objective and subjective refraction endpoints (Davis, Schechtman, Begley, Shin & Zadnik, 1998, Raasch, Schechtman, Davis, Zadnik & Study, 2001) and the possibility of the habitual correction of the patient not matching with the endpoint of subjective refraction

obtained through the earlier means. What this residual defocus and astigmatism for a keratoconic eye is and how this interaction will pan out is hard to predict (Applegate et al., 2002, Cheng, Bradley, Ravikumar & Thibos, 2010). Hence, the study took a more simplistic approach of removing all lower-order wavefront aberrations from the optical simulations and investigate only the impact of blur from higher-order aberrations on visual performance. A second limitation was the study's inability to test the stereoacuity impact of phase nullification on conditions that simulated bilateral asymmetric keratoconus. While testing these conditions was certainly considered during the study design, it was dropped for operational reasons of time spent in the experiment and the availability of participants for prolonged testing. Lack of this data does limit direct extrapolation of the results to the stereoscopic experience of patients with dissimilar severities of keratoconus in the two eyes. However, for the reasons described above, it may be hypothesized that phase nullification may improve stereoacuity in bilateral asymmetric keratoconus, perhaps, to a greater extent than what was observed here for the unilateral conditions (Figure 7). A third limitation of the study revolves around the extrapolation of the present results to the entire heterogeneity of keratoconus disease presentation (Santodomingo-Rubido et al., 2022). That only four wavefront aberration patterns were chosen in this study clearly indicates that such an extrapolation is superfluous, at best. Instead, the results should be viewed as a proof of concept for how phase nullification may augment vision in highly-aberrated and optically compromised eyes such as those with keratoconus.

5. Conclusions

Nullifying the phase disruptions caused by the monochromatic higher-order wavefront aberrations present in keratoconic eyes produces significant improvements in visual acuity, character recognition and stereoacuity. The effect is more pronounced for stereoacuity when the phase nullification is applied for unilateral than bilateral blur. These effects may be explained by the improved positional registry and the associated reduction in interocular contrast difference between the monocular image features aid veridical calculation of stereopsis. These results form the basis for the improvement in visual performance of keratoconic patients with optical interventions such as rigid contact lens or experimental adaptive optics corrections.

Acknowledgments

The authors thank the study participants, Dr L. S. Varadharajan for the visual acuity measurement software, Prof Larry Thibos and Prof. Arthur Bradley for assistance with the computational simulations described in this study, the terminology of "phase nullification" to faithfully represent the optical manipulation performed in the study and for a critical review of the manuscript. Financial support for the study came through intramural funds from the Hyderabad Eye Research Foundation, L V Prasad Eye Institute and a Fulbright-Nehru Academic and Professional Excellence Fellowship to SRB during the writing phase of the study.

References

Akutsu, H., Bedell, H.E., & Patel, S.S. (2000). Recognition thresholds for letters with simulated dioptric blur. Optom Vis Sci, 77 (10), 524-530.

Applegate, R.A., Donnelly, W.J., 3rd, Marsack, J.D., Koenig, D.E., & Pesudovs, K. (2007). Three-dimensional relationship between high-order root-mean-square wavefront error, pupil diameter, and aging. J Opt Soc Am A Opt Image Sci Vis, 24 (3), 578-587.

Applegate, R.A., Sarver, E.J., & Khemsara, V. (2002). Are all aberrations equal? J Refract Surg, 18 (5), S556-562.

Artal, P., Santamaria, J., & Bescos, J. (1988). Phase-transfer function of the human eye and its influence on point-spread function and wave aberration. J Opt Soc Am A, 5 (10), 1791-1795.

Banks, M.S., Gepshtein, S., & Landy, M.S. (2004). Why is spatial stereoresolution so low? J Neurosci, 24 (9), 2077-2089.

Barbot, A., Park, W.J., Ng, C.J., Zhang, R.Y., Huxlin, K.R., Tadin, D., & Yoon, G. (2021). Functional reallocation of sensory processing resources caused by long-term neural adaptation to altered optics. Elife, 10

Barhoom, H., Joshi, M.R., & Schmidtmann, G. (2021). The effect of response biases on resolution thresholds of Sloan letters in central and paracentral vision. Vision Res, 187, 110-119.

Bell, E.L.S., Hastings, G.D., Nguyen, L.C., Applegate, R.A., & Marsack, J.D. (2023). Utilising a visual image quality metric to optimise spectacle prescriptions for eyes with keratoconus. Ophthalmic Physiol Opt, 43 (5), 1007-1015.

Brainard, D.H. (1997). The Psychophysics Toolbox. Spat Vis, 10 (4), 433-436.

Bundesen, C., & Harms , L. (1999). Single-letter recognition as a function of exposure duration. Psychological Research, 62, 275–279.

Campbell, C.E. (2003). Matrix method to find a new set of Zernike coefficients from an original set when the aperture radius is changed. J Opt Soc Am A Opt Image Sci Vis, 20 (2), 209-217.

Candy, T.R., Mishoulam, S.R., Nosofsky, R.M., & Dobson, V. (2011). Adult discrimination performance for pediatric acuity test optotypes. Invest Ophthalmol Vis Sci, 52 (7), 4307-4313.

Castejon-Mochon, J.F., Lopez-Gil, N., Benito, A., & Artal, P. (2002). Ocular wave-front aberration statistics in a normal young population. Vision Res, 42 (13), 1611-1617.

Chan, C., Smith, G., & Jacobs, R.J. (1985). Simulating refractive errors: source and observer methods. Am J Optom Physiol Opt, 62 (3), 207-216.

Cheng, X., Bradley, A., Ravikumar, S., & Thibos, L.N. (2010). Visual impact of Zernike and Seidel forms of monochromatic aberrations. Optom Vis Sci, 87 (5), 300-312.

Cheng, X., Bradley, A., & Thibos, L.N. (2004). Predicting subjective judgment of best focus with objective image quality metrics. J Vis, 4 (4), 310-321.

Cormack, L.K., Stevenson, S.B., & Landers, D.D. (1997). Interactions of spatial frequency and unequal monocular contrasts in stereopsis. Perception, 26 (9), 1121-1136.

596 Cormack, L.K., Stevenson, S.B., & Schor, C.M. (1991). Interocular correlation, luminance contrast and cyclopean
597 processing. Vision Res, 31 (12), 2195-2207.
598 Davis, L.J., Schechtman, K.B., Begley, C.G., Shin, J.A., & Zadnik, K. (1998). Repeatability of refraction and corrected
599 visual acuity in keratoconus. The CLEK Study Group. Collaborative Longitudinal Evaluation of Keratoconus.
600 Optom Vis Sci, 75 (12), 887-896.
601 Devi, P., Kumar, P., & Bharadwaj, S.R. (2023). Computational analysis of retinal image quality with different contact
602 lens designs in keratoconus. Cont Lens Anterior Eye, 46 (2), 101794.
603 Devi, P., Kumar, P., Marella, B.L., & Bharadwaj, S.R. (2022). Impact of Degraded Optics on Monocular and Binocular
604 Vision: Lessons from Recent Advances in Highly-Aberrated Eyes. Semin Ophthalmol, 37 (7-8), 869-886.
605 Ding, J., Klein, S.A., & Levi, D.M. (2013a). Binocular combination in abnormal binocular vision. J Vis, 13 (2), 14.
606 Ding, J., Klein, S.A., & Levi, D.M. (2013b). Binocular combination of phase and contrast explained by a gain-control
607 and gain-enhancement model. J Vis, 13 (2), 13.
608 Fan, L., Kandel, H., & Watson, S.L. (2024). Impacts of keratoconus on quality of life: a qualitative study. Eye (Lond),
609 Field, D.J., & Brady, N. (1997). Visual sensitivity, blur and the sources of variability in the amplitude spectra of natural
610 scenes. Vision Res, 37 (23), 3367-3383.
611 Gothwal, V.K., Gujar, R., Sharma, S., Begum, N., & Pesudovs, K. (2022). Factors affecting quality of life in
612 keratoconus. Ophthalmic Physiol Opt, 42 (5), 986-997.
613 Hastings, G.D., Marsack, J.D., Thibos, L.N., & Applegate, R.A. (2020). Combining optical and neural components in
614 physiological visual image quality metrics as functions of luminance and age. J Vis, 20 (7), 20.
615 Haun, A.M., & Peli, E. (2013). Perceived contrast in complex images. J Vis, 13 (13), 3.
616 Kumar, P., Bandela, P.K., & Bharadwaj, S.R. (2020). Do visual performance and optical quality vary across different
617 contact lens correction modalities in keratoconus? Cont Lens Anterior Eye, 43 (6), 568-576.
618 Kumar, P., Campbell, P., Vaddavalli, P.K., Hull, C.C., & Bharadwaj, S.R. (2023). Structure-Function Relationship in
619 Keratoconus: Spatial and Depth Vision. Transl Vis Sci Technol, 12 (12), 21.
620 Marella, B.L., Conway, M.L., Suttle, C., & Bharadwaj, S.R. (2021). Contrast Rivalry Paradigm Reveals Suppression of
621 Monocular Input in Keratoconus. Invest Ophthalmol Vis Sci, 62 (2), 15.
622 Marella, B.L., Vaddavalli, P.K., Reddy, J.C., Conway, M.L., Suttle, C.M., & Bharadwaj, S.R. (2023). Interocular Contrast
623 Balancing Partially Improves Stereoacuity in Keratoconus. Optom Vis Sci, 100 (4), 239-247.
624 Mayer, D.L., Fulton, A.B., & Rodier, D. (1984). Grating and recognition acuities of pediatric patients. Ophthalmology,
625 91 (8), 947-953.
626 Metlapally, S., Bharadwaj, S.R., Roorda, A., Nilagiri, V.K., Yu, T.T., & Schor, C.M. (2019). Binocular cross-correlation
627 analyses of the effects of high-order aberrations on the stereoacuity of eyes with keratoconus. J Vis, 19 (6), 12.
628 Ng, C.J., Sabesan, R., Barbot, A., Banks, M.S., & Yoon, G. (2022). Suprathreshold Contrast Perception Is Altered by
629 Long-term Adaptation to Habitual Optical Blur. Invest Ophthalmol Vis Sci, 63 (11), 6.
630 Nilagiri, V.K., Metlapally, S., Kalaiselvan, P., Schor, C.M., & Bharadwaj, S.R. (2018). LogMAR and Stereoacuity in
631 Keratoconus Corrected with Spectacles and Rigid Gas-permeable Contact Lenses. Optom Vis Sci, 95 (4), 391-
632 398.
633 Nilagiri, V.K., Metlapally, S., Schor, C.M., & Bharadwaj, S.R. (2020). A computational analysis of retinal image quality
634 in eyes with keratoconus. Sci Rep, 10 (1), 1321.
635 Pantanelli, S., MacRae, S., Jeong, T.M., & Yoon, G. (2007). Characterizing the wave aberration in eyes with
636 keratoconus or penetrating keratoplasty using a high-dynamic range wavefront sensor. Ophthalmology, 114
637 (11), 2013-2021.
638 Peli, E. (1990). Contrast in complex images. J Opt Soc Am A, 7 (10), 2032-2040.
639 Pelli, D.G., Burns, C.W., Farell, B., & Moore-Page, D.C. (2006). Feature detection and letter identification. Vision Res,
640 46 (28), 4646-4674.
641 Petersen, A., & Andersen, T.S. (2012). The effect of exposure duration on visual character identification in single,
642 whole, and partial report. J Exp Psychol Hum Percept Perform, 38 (2), 498-514.

Pinto, R.D.P., Abe, R.Y., Gomes, F.C., Barbisan, P.R.T., Martini, A.F., de Almeida Borges, D., Fernandes, A.G., Arieta, C.E.L., & Alves, M. (2021). Quality of life in keratoconus: evaluation with Keratoconus Outcomes Research Questionnaire (KORQ). Sci Rep, 11 (1), 12970.

Piotrowski, L.N., & Campbell, F.W. (1982). A demonstration of the visual importance and flexibility of spatial-frequency amplitude and phase. Perception, 11 (3), 337-346.

Porter, J., Guirao, A., Cox, I.G., & Williams, D.R. (2001). Monochromatic aberrations of the human eye in a large population. J Opt Soc Am A Opt Image Sci Vis, 18 (8), 1793-1803.

Raasch, T.W., Schechtman, K.B., Davis, L.J., Zadnik, K., & Study, C.S.G.C.L.E.o.K. (2001). Repeatability of subjective refraction in myopic and keratoconic subjects: results of vector analysis. Ophthalmic Physiol Opt, 21 (5), 376-383.

Ravikumar, S., Bradley, A., & Thibos, L. (2010). Phase changes induced by optical aberrations degrade letter and face acuity. J Vis, 10 (14), 18.

Rozema, J.J., Hastings, G.D., Marsack, J., Koppen, C., & Applegate, R.A. (2021). Modeling refractive correction strategies in keratoconus. J Vis, 21 (10), 18.

Sabesan, R., Ahmad, K., & Yoon, G. (2007). Correcting highly aberrated eyes using large-stroke adaptive optics. J Refract Surg, 23 (9), 947-952.

Sabesan, R., Barbot, A., & Yoon, G. (2017). Enhanced neural function in highly aberrated eyes following perceptual learning with adaptive optics. Vision Res, 132, 78-84.

Sabesan, R., & Yoon, G. (2009). Visual performance after correcting higher order aberrations in keratoconic eyes. J Vis, 9 (5), 6 1-10.

Santodomingo-Rubido, J., Carracedo, G., Suzaki, A., Villa-Collar, C., Vincent, S.J., & Wolffsohn, J.S. (2022). Keratoconus: An updated review. Cont Lens Anterior Eye, 45 (3), 101559.

Sarver, E.J., & Applegate, R.A. (2004). The importance of the phase transfer function to visual function and visual quality metrics. J Refract Surg, 20 (5), S504-507.

Smith, G. (1982). Ocular defocus, spurious resolution and contrast reversal. Ophthalmic Physiol Opt, 2 (1), 5-23.

Smith, G., Jacobs, R.J., & Chan, C.D. (1989). Effect of defocus on visual acuity as measured by source and observer methods. Optom Vis Sci, 66 (7), 430-435.

Stevenson, S.B., & Cormack, L.K. (2000). A contrast paradox in stereopsis, motion detection, and vernier acuity. Vision Res, 40 (21), 2881-2884.

Tadmor, Y., & Tolhurst, D.J. (1993). Both the phase and the amplitude spectrum may determine the appearance of natural images. Vision Res, 33 (1), 141-145.

Thibos, L.N. (2019). Calculation of the geometrical point-spread function from wavefront aberrations. Ophthalmic Physiol Opt, 39 (4), 232-244.

Thibos, L.N., Hong, X., Bradley, A., & Applegate, R.A. (2004). Accuracy and precision of objective refraction from wavefront aberrations. J Vis, 4 (4), 329-351.

Thibos, L.N., Hong, X., Bradley, A., & Cheng, X. (2002). Statistical variation of aberration structure and image quality in a normal population of healthy eyes. J Opt Soc Am A Opt Image Sci Vis, 19 (12), 2329-2348.

Vlaskamp, B.N., Yoon, G., & Banks, M.S. (2011). Human stereopsis is not limited by the optics of the well-focused eye. J Neurosci, 31 (27), 9814-9818.

Walsh, G., & Charman, W.N. (1989). The effect of defocus on the contrast and phase of the retinal image of a sinusoidal grating. Ophthalmic Physiol Opt, 9 (4), 398-404.

Yellott, J.I., & Yellott, J.W. (2007). Correcting spurious resolution in defocused images. Proceedings of SPIE - The International Society for Optical Engineering, 6492.

Appendices

Appendix I: 3D representation of the optical transfer function

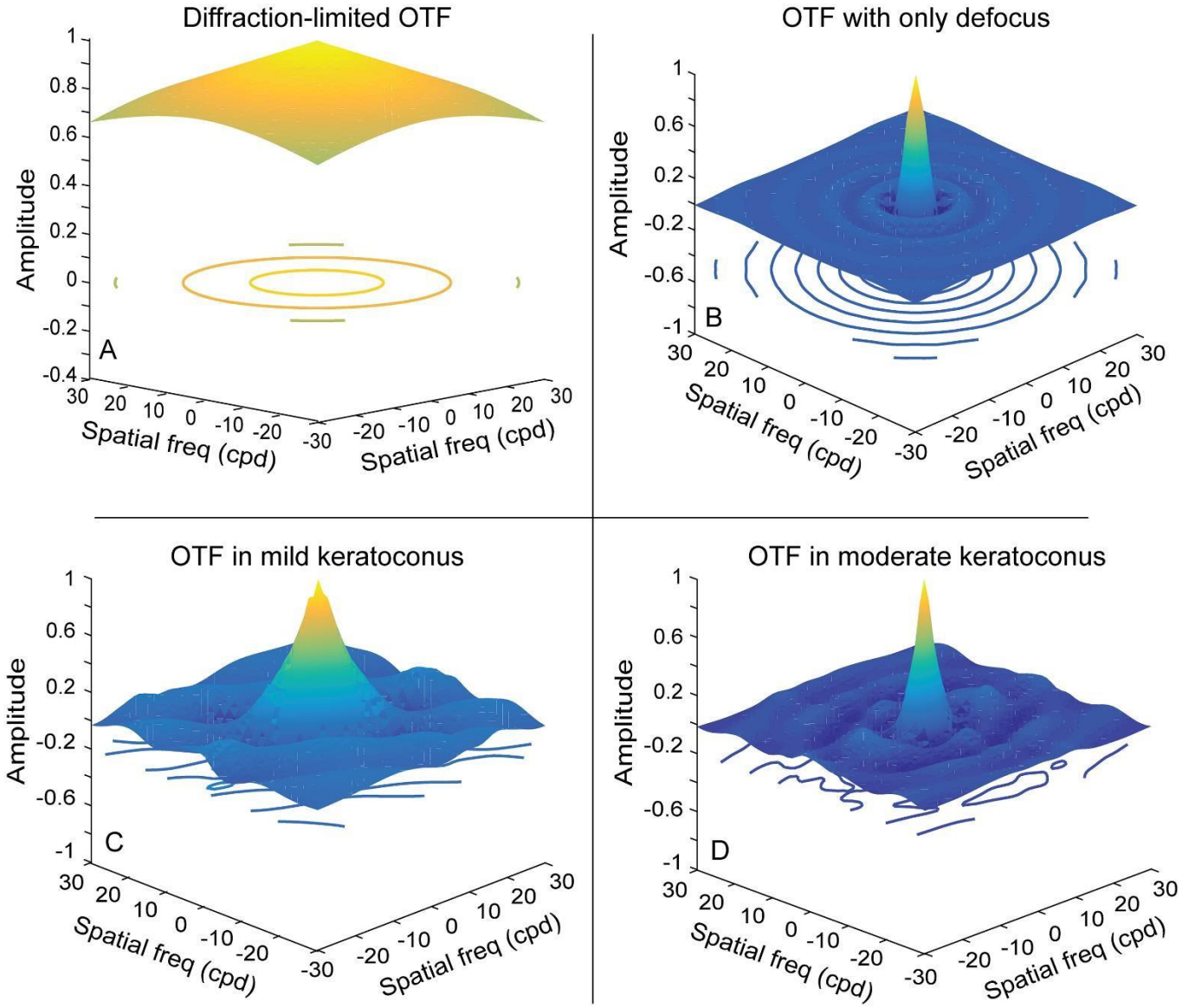

Figure A1: *3D surf plots of the real-part of the complex-valued optical transfer function (OTF) constructed from the monochromatic wavefront aberrations of a diffraction-limited eye (panel A), an eye with only 1D myopic defocus (panel B), an eye with mild keratoconus (panel C) and an eye with moderate keratoconus (D), all for 5 mm pupil diameter. The OTF's for the two keratoconic eyes are the same used for generating the blurred optotypes and stereograms. They are constructed using only their 3rd to 5th order wavefront aberrations. The ripples in the OTF are indicative of the phase reversals. In contrast to the OTF with only defocus, those from keratoconic eyes show also prominent differences in contrast demodulation across orientations, reflecting the impact of the radially-asymmetric Zernike polynomials in the keratoconic wavefront profiles. Prominent phase reversals are also apparent as ripples in the OTFs shown in panels B – D.*

Appendix II: Visual acuity and stereoacuity with induced defocus plus spherical aberrations

A separate control experiment was conducted to determine the impact of blur induced by a combination of myopic defocus and positive spherical aberration with native and nullified phase on monocular visual acuity to validate the present study protocol by replicating the main experiment of Ravikumar et al and stereoacuity. Five observers from the main experiment participated in this experiment. Four levels of defocus: 0.45 µm, 0.90 µm, 1.35 µm and 1.80 µm (corresponding to 0.5 D, 1.0 D, 1.5 D and 2.0 D of defocus for 5 mm pupil diameter, respectively) plus 0.15 µm of positive spherical aberration was used to generate the blurred images. Stereoacuity was estimated only with the unilaterally-induced blur, as the main experiment showed greater impact of this condition over bilateral blur on stereoacuity. All other details of image generation and psychophysical estimation of visual acuity and stereoacuity were identical to the main experiment. Both visual acuity and stereoacuity worsened with induced blur, with the larger two magnitudes of blur showing a greater loss in performance and greater restoration of the performance loss, relative to the lower two magnitudes (Figure A2). The visual acuities obtained in this study for the 0.5 D and 1.0 D of blur were approximately in the same range as that reported by Ravikumar et al (2010). However, the acuities with 1.5 D and 2.0 D of blur were approximately 0.15 logMAR units worse than what was reported by Ravikumar et al (2010).

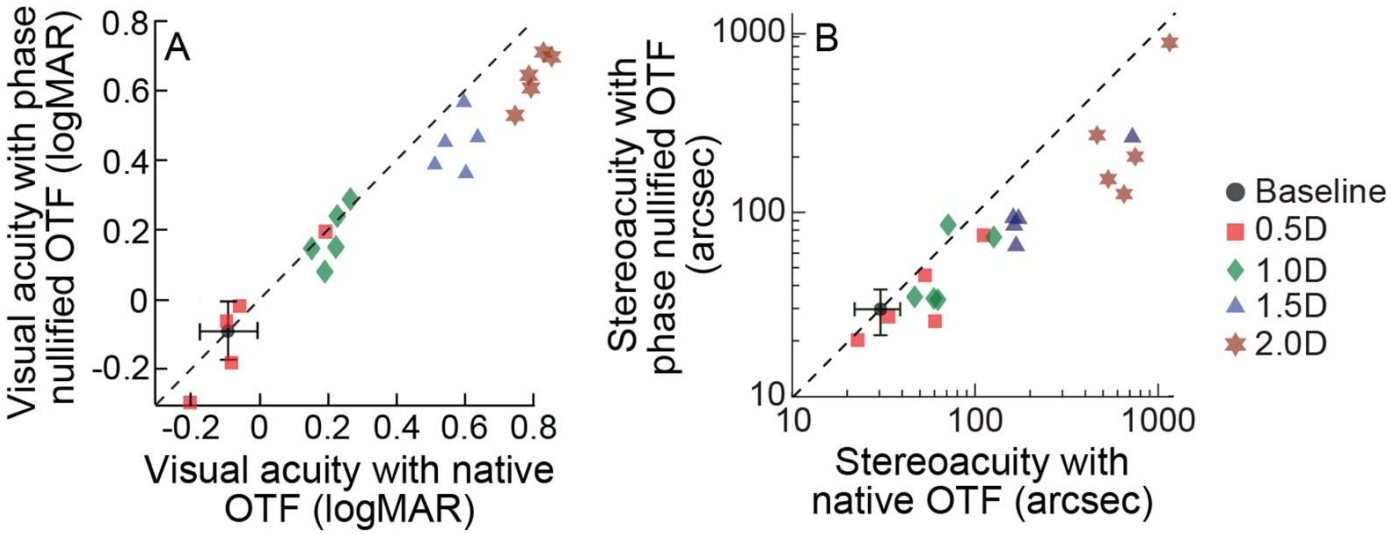

Figure A2: *Scatter diagram of logMAR visual acuity and stereoacuity obtained while viewing optotypes blurred using their native and nullified phase for the four keratoconus conditions tested in this study. Each symbol of a particular colour represents data from a single participant. The mean (±1SD) visual acuity obtained at baseline is also shown in this panel for comparison purposes.*

Optical phase nullification partially restores visual and stereo acuity lost to simulated blur from higher-order wavefront aberrations of keratoconic eyes

Bhagya Lakshmi Marella[1,2,3], Miriam Conway[3], Pravin K. Vaddavalli[4], Catherine Suttle[3], and Shrikant R. Bharadwaj[1,2]

[1]Brien Holden Institute of Optometry and Vision Sciences, L V Prasad Eye Institute, Road 2 Banjara Hills, Hyderabad – 500034 Telangana, India.

[2]Prof. Brien Holden Eye Research Centre, L V Prasad Eye Institute, Road 2 Banjara Hills, Hyderabad – 500034 Telangana, India.

[3]Centre for Applied Vision Research, City, University of London, Northampton Square, London EC1V 0HB, United Kingdom.

[4]Shantilal Sanghvi Cornea Institute, L V Prasad Eye Institute, Road no. 2, Banjara Hills, Hyderabad – 500034, Telangana, India.

Corresponding author: Shrikant R. Bharadwaj

Brien Holden Institute of Optometry and Vision Sciences, L V Prasad Eye Institute, Road no. 2, Banjara Hills, Hyderabad – 500034 Telangana, India.

bharadwaj@lvpei.org

Running title: Vision improvement with phase nullification in keratoconus

Number of figures in manuscript: 7

Number of figures in appendix: 2

Number of tables in manuscript: 1

Word count in abstract: 284

Word count in revised abstract: 250

Word count in original manuscript: 5435

Word count in revised manuscript: 6273

Highlights

- Keratoconic blur is characterized by exaggerated contrast demodulation and phase distortions.
- Phase nullification partially recovers the visual acuity and stereoacuity lost to this optical blurring.
- Stereoacuity improvement with phase nullification is more prominent for unilateral than bilateral blur.
- Discriminability of letters also improves following phase nullification of the blurred image.
- Alignment of local image features following phase nullification contributes to vision improvement in keratoconus.

Abstract

Contrast demodulation and phase distortions are exaggerated in retinal images blurred by the higher-order wavefront aberrations of keratoconic eyes. While the performance loss from the former parameter is well understood, little is known about the impact of the latter on visual functions in this disease condition. *The present study investigated the impact of phase distortions on the monocular logMAR visual acuity, letter discriminability and random-dot stereoacuity of seventeen visually healthy adults using images that were computationally blurred by four different higher-order wavefront aberration profiles of keratoconic eyes that showed significant distortions in the phase spectrum. Participants viewed these images through 2mm artificial pupils to negate their native ocular wavefront aberrations.* The results showed progressive losses in visual acuity and stereoacuity with increasing blur, a third of which could be recovered following phase nullification. Letter discriminability also improved following phase nullification, more so for smaller than larger optotypes. Stereoacuity loss and, consequently, its recovery following phase nullification was more prominent for profiles simulating unilateral asymmetric keratoconus than for profiles simulating bilateral symmetric keratoconus. These results agree with previous reports obtained from blur induced with lower-order aberrations and indicate that a similar trend may be observed for more complex patterns of blur like keratoconus. Overall, both contrast demodulation and misalignment of the local features of the blurred image may contribute to losses of spatial and depth vision in keratoconus. Phase nullification may partially mitigate these losses, thereby allowing the processing of finer spatial details and veridical disparity estimations for improved depth perception.

Keywords: Contrast; Correspondence matching; Ghosting; Higher-order aberrations; Retinal image quality, phase correction.

Keratoconus is an ectatic disorder of the cornea causing significant impairment in vision and vision-related quality of life (Fan, Kandel & Watson, 2024, Gothwal, Gujar, Sharma, Begum & Pesudovs, 2022, Pinto, Abe, Gomes, Barbisan, Martini, de Almeida Borges, Fernandes, Arieta & Alves, 2021, Santodomingo-Rubido, Carracedo, Suzaki, Villa-Collar, Vincent & Wolffsohn, 2022). This disease leads to elevated levels of wavefront error, which, when described by the Zernike polynomial, shows elevated levels of vertical coma (z_3^{-1}), horizontal coma (z_3^{1}), vertical trefoil (z_3^{-3}), spherical aberration (z_4^{0}), and secondary astigmatism (z_4^{2}) in the keratoconic eye, compared to a typical population (Devi, Kumar, Marella & Bharadwaj, 2022, Nilagiri, Metlapally, Schor & Bharadwaj, 2020, Pantanelli, MacRae, Jeong & Yoon, 2007). These Zernike components may all interact in complex ways to degrade the retinal image quality in keratoconus (Applegate, Sarver & Khemsara, 2002, Devi et al., 2022). This degraded retinal image, like any other defocused image, is characterized by significant contrast demodulation and phase alterations of the individual spatial frequency components (Artal, Santamaria & Bescos, 1988, Smith, 1982, Walsh & Charman, 1989, Yellott & Yellott, 2007). While the combined impact of contrast demodulation and phase alterations or the isolated impact of the former factor on the spatial and depth vision in keratoconus has been investigated earlier (Bell, Hastings, Nguyen, Applegate & Marsack, 2023, Marella, Conway, Suttle & Bharadwaj, 2021, Marella, Vaddavalli, Reddy, Conway, Suttle & Bharadwaj, 2023, Metlapally, Bharadwaj, Roorda, Nilagiri, Yu & Schor, 2019, Nilagiri, Metlapally, Kalaiselvan, Schor & Bharadwaj, 2018, Rozema, Hastings, Marsack, Koppen & Applegate, 2021), the latter's impact on visual functions is less well-understood. That the phase alterations may have a strong impact on vision in keratoconus is indicated by the "ghosting" / "doubling" of images often reported by patients during a routine eye examination. These effects qualitatively reduce with rigid contact lens wear that improve the eye's optical quality by replacing the distorted cornea with a uniform refracting surface (Devi, Kumar & Bharadwaj, 2023). However, the underlying optical/psychophysical basis for such perceptual experiences have not been systematically investigated in keratoconus thus far.

Given that the amplitude spectra of natural images often share a common 1/f distribution (Tadmor & Tolhurst, 1993), the global structure of an image is best described by its unique phase structure (Piotrowski & Campbell, 1982, Sarver & Applegate, 2004). Phase disruptions and the accompanying altered structure of an image created by optical aberrations certainly contribute to reduced visual acuity in humans (Akutsu, Bedell & Patel, 2000, Artal et al., 1988, Cheng, Bradley & Thibos, 2004, Ravikumar, Bradley & Thibos, 2010,

Yellott & Yellott, 2007). For instance, Ravikumar et al (2010) demonstrated the impact of phase alteration and its nullification by computationally blurring targets with specific combinations of monochromatic wavefront aberration terms and measuring visual acuity with the native and a nullified phase spectrum. Their results showed that the alignment of the local image features following phase nullification improved the edge contrast of the letter targets, partially restoring the visual acuity loss encountered with the native phase. Phase nullification also qualitatively decreased the ghosting/doubling of the targets (as evident from their simulations), even while these effects were not quantified in their study (Ravikumar et al., 2010). It remains unknown if these observations can be directly extrapolated to the visual experience of targets blurred using the pattern of retinal image blur generated in keratoconus.

When phase disruptions are dissimilar in the right and left eyes, the binocular perception of object location is affected and stereoacuity is impaired (Ding, Klein & Levi, 2013a, Ding, Klein & Levi, 2013b). These effects were demonstrated computationally for keratoconic blur by Metlapally et al (2019) who showed that retinal images blurred by dissimilar keratoconic point spread functions (PSFs) impaired the overall strength of the retinal disparity signal in the fused cyclopean image. Phase nullifying these PSF's decreased the false correspondence matches and produced a commensurate improvement in the strength of the retinal disparity signal (Metlapally et al., 2019). This improvement correlated with the participant's stereoacuity, even while the phase nullified stereoacuities were not directly tested in their study.

The present study addressed these gaps in the literature by investigating the impact of the phase distortions and their nullification on spatial and depth vision in keratoconus. Two specific hypotheses were tested. First, phase nullification of the keratoconic PSF will improve visual acuity and optotype discriminability through better alignment of the local image features, all relative to the native phase condition. Second, phase nullification of the keratoconic PSFs will enhance detection of the disparate monocular images of a random dot stereogram pair, resulting in improved stereoacuity, again relative to the native phase condition. The stereoacuity improvement will be greater for conditions simulating bilaterally asymmetric keratoconus than for conditions simulating bilaterally symmetric disease. This may be so, because, unlike the bilaterally symmetric disease conditions, monocular phase distortions will result in dissimilar contrast and dissimilar alterations in the local image structure of the two eyes. The former may be more deleterious to stereoacuity, as expected from the contrast paradox phenomenon of

stereopsis (Cormack, Stevenson & Landers, 1997, Stevenson & Cormack, 2000), while the latter may impact stereo processing by inducing mismatches in retinal correspondence (Ding et al., 2013a, Ding et al., 2013b, Metlapally et al., 2019). Nullifying the phase in the blurred eye may reduce the impact of both factors, resulting in greater improvement of stereoacuity, relative to the bilateral blur conditions. These hypotheses were tested by comparing the visual acuity, optotype discriminability, and random dot stereoacuity of otherwise visually healthy individuals who viewed images that were blurred by the native and phase nullified PSFs derived from the higher-order wavefront aberrations of keratoconic eyes.

2. Methods

2.1. Participants

Seventeen adults (23 to 31 years of age; 7 males), familiar with psychophysical measurement protocols but naïve to the present study aims, were recruited from the staff and student pool of L V Prasad Eye Institute (LVPEI), Hyderabad, India. The study protocol adhered to the tenets of the declaration of Helsinki and was approved by the Institutional Review Board of LVPEI and City, University London, London, UK. All participants were visually healthy, had best-corrected visual acuity better than 20/25 in both eyes and best-corrected stereoacuity of at least 40 arcsec, as estimated using routine clinical protocols. Ten individuals each participated in the visual acuity and stereoacuity experiments. Three individuals were common to both experiments. The participant's right eye was chosen for visual acuity testing (left eye remained occluded throughout). The participant's head was stabilized using a chin and forehead rest.

2.2. The wavefront aberration profiles for blurring the targets

Blurred targets were generated using the wavefront aberration profiles measured earlier in our laboratory in four patients with unilateral keratoconus through a mesopic pupil diameter of >5.0 mm for 555 nm light using the irx3™ wavefront aberrometer (Imagine Eyes®, Orsay, France) (Nilagiri et al., 2020). The wavefronts were then scaled down to a constant 5 mm pupil diameter using the technique described by Campbell (2003). Zernike coefficients of the three lower-order terms of defocus, and astigmatism ($z_2^2, z_2^0 \& z_2^{-2}$) were set to zero to determine the impact of only higher-order aberrations on visual functions before and after phase nullification. The coefficients of the 3rd to 5th order terms that were used for blurring the targets in this study were retained as is (Figure 1). The higher-order root mean squared (HORMS) deviation of these wavefront aberration profile were 0.52 µm, 0.93 µm, 1.21 µm and 1.39 µm

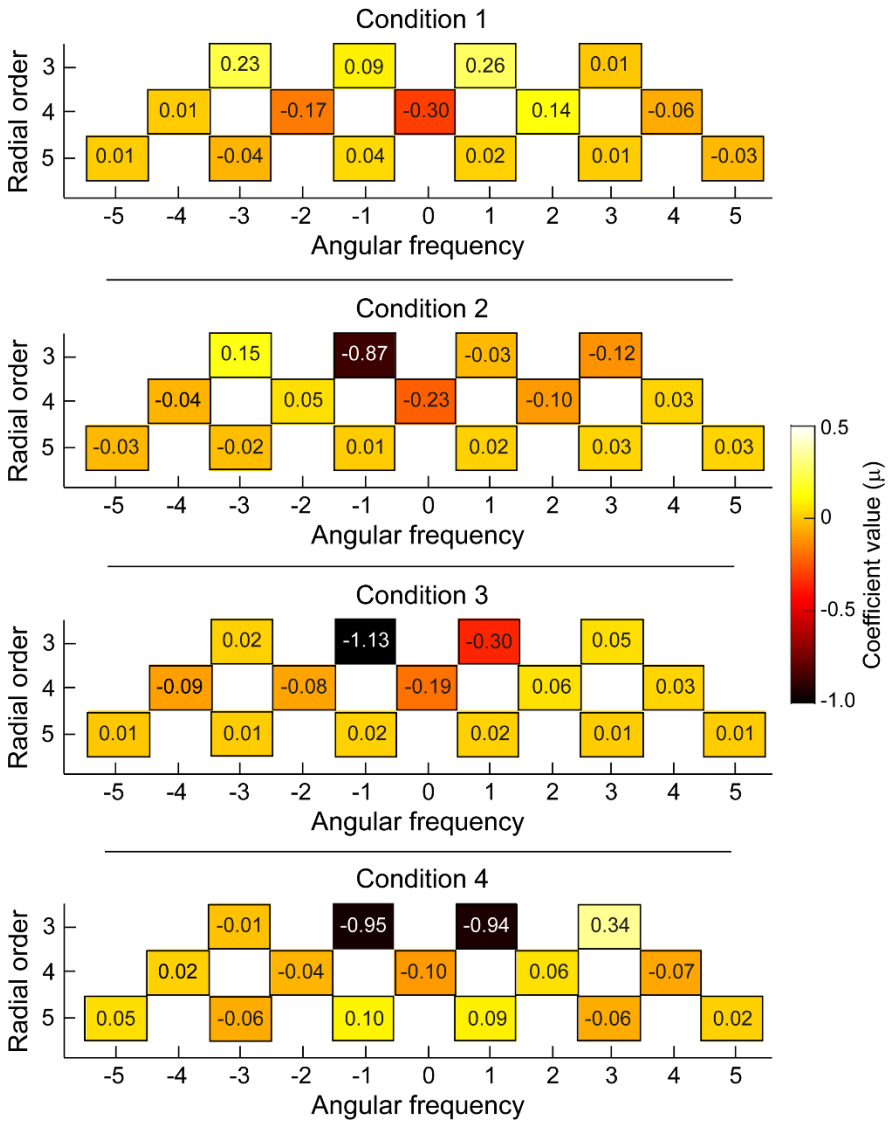

Figure 1: *Heatmaps of the coefficient values of the individual Zernike polynomial terms from the 3rd to the 5th radial order used in this study. Panels A – D show these values for Conditions 1 – 4, respectively. Zernike coefficients of the two lower-order terms of defocus, and astigmatism were set to zero to mimic an eye fully-corrected for its sphero-cylindrical refractive error.*

for Conditions 1 – 4, respectively. Two of the patients whose wavefront profiles were chosen had mild disease severity (Maximum keratometry value: 48.9 D and 48.7 D; henceforth referred to as Conditions 1 and 2, respectively) and the remaining two had moderate disease severity (Maximum keratometry value: 51.3 D and 52.9 D; henceforth referred to as Conditions 3 and 4, respectively). These profiles were specifically chosen as they showed significant phase reversals in the optical transfer function (OTF) [Figures 2A, C, E and G; see Appendix I for 3D representations of the OTF) and that there was enough contrast in the phase reversed portions of these functions to improve visual performance [see, portions of the phase

nullified OTFs – essentially the modulation transfer function (MTF) – crossing the neural transfer function in Figures 2B, D, F and H, relative to the OTFs with native phase]. In general, phase nullification had greater impact in increasing the spatial frequency range for eyes with moderate keratoconus (i.e., Conditions 3 and 4) than for eyes with mild keratoconus (i.e., Conditions 1 and 2) (Figure 2). The shift in the intersection of the highest spatial frequency of the radially-averaged MTFs and the NTF following phase nullification is indicated for each condition in Figure 2.

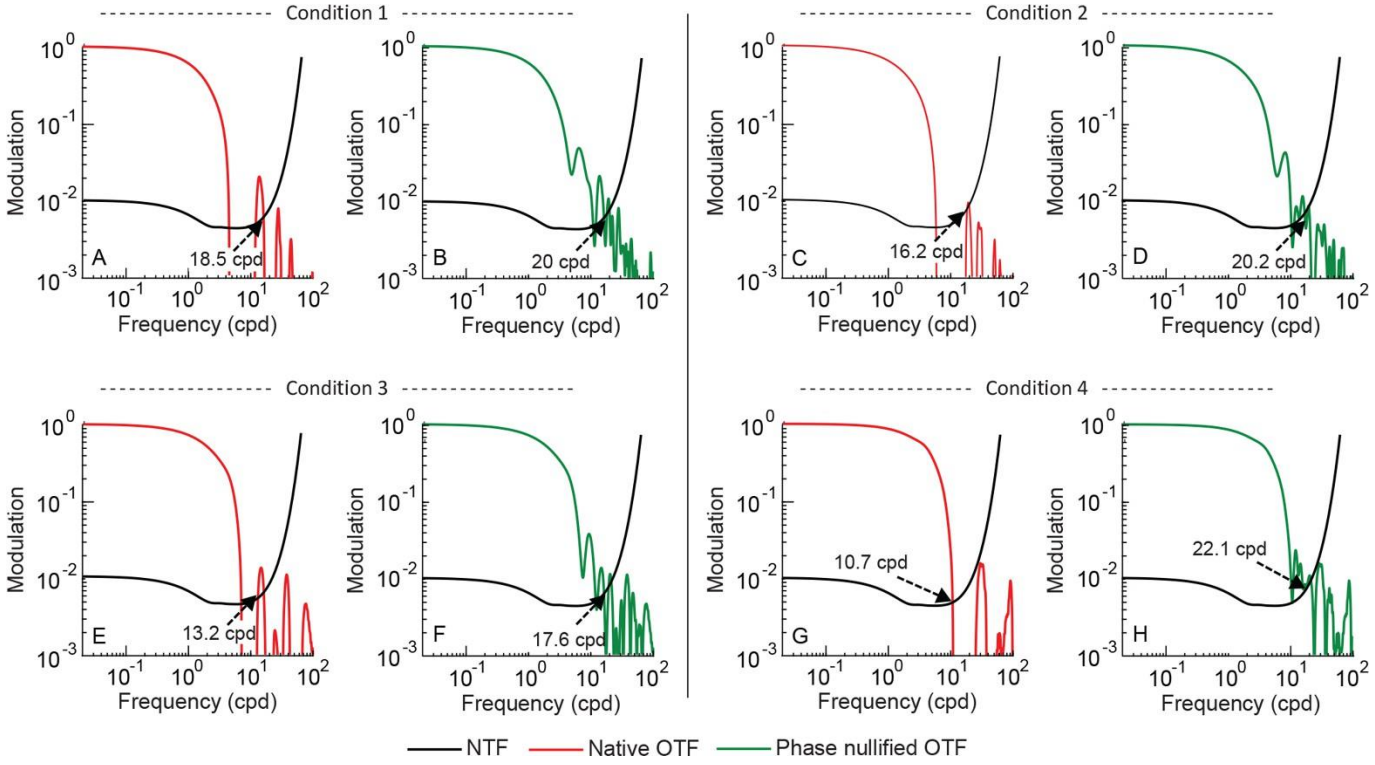

Figure 2: *The amplitude spectrum of the real part of the radially-averaged complex-valued optical transfer function (OTF) computed from the 3rd to 5th order monochromatic wavefront aberrations of the four keratoconic eyes chosen for this study (Conditions 1 – 4). Panels A, C, E and G show the OTF with native phase while panels B, D, F and H show the corresponding curves with phase nullification for Conditions 1 – 4. The portions of the OTF with contrast energy <10^{-3} indicate phase reversals for the corresponding spatial frequencies. The black trace in each panel shows the neural threshold function (NTF) obtained from Hastings et al (2020) for a 25-year-old human observer at 1100 Td of retinal illuminance. The spatial frequency cut-off at the point of last intersection between the OTF and NTF are indicated in each panel (Thibos, Hong, Bradley & Applegate, 2004).*

A separate control experiment was conducted to validate the present study protocol by replicating the main experiment of Ravikumar et al (2010) (see Appendix II for details). This experiment determined the impact of blur induced by a combination of myopic defocus and positive spherical aberration with native and nullified phase on visual acuity and stereoacuity. The blur levels induced in this experiment were equal

to those used by Ravikumar et al (2010) for estimating visual acuity. The visual acuity results of this control experiment were equivalent to the Ravikumar et al. study.

2.3. Generation of blurred optotypes and visual acuity assessment

The "source" method that allowed independent manipulation of the amplitude and phase spectrum of the image was employed in this study to generate the blurred optotypes (Chan, Smith & Jacobs, 1985, Smith, Jacobs & Chan, 1989). A database comprising of the grayscales images of all 10 Sloan optotypes between -0.50 logMAR unit (20/6.3 Snellen fraction) to +1.30 logMAR unit (20/399 Snellen fraction) was created in steps of 0.1 logMAR unit. All optotype sizes were calibrated for a 2-meter viewing distance and were 255 x 255 pixels in size, with a resolution of 92 dots per inch. These optotypes were blurred by convolving them with the PSFs derived from the wavefront aberrations profile described in the previous section using the techniques described by Thibos (2019) and implemented onto the Fourier Optics Calculator [presently called Indiana Retinal Image Simulator (IRIS); https://blogs.iu.edu/corl/iris/], an open-source software for retinal image simulations using standard Fourier optics techniques. The complex-valued OTF, obtained by Fourier transforming the keratoconic PSF, was then phase nullified by taking the absolute values of this OTF function using the syntax abs(OTF) in Matlab® (R2016b, MathWorks Inc, Natick, USA). This manipulation effectively returns the modulation transfer function (MTF) of the image, with phase information being set to zero. This absolute value of the OTF function with zero phase was inverse Fourier transformed to obtain the phase nullified PSF. These PSF's were then convolved with optotypes, as before, to get the phase nullified blurred images. This protocol was implemented using the Fourier Optics Calculator written in Matlab®.

Visual acuity was determined using a method of constant stimuli paradigm, custom-written in Matlab®. All measurements were obtained with each participant's sphero-cylindrical refractive correction placed in a trial lens frame at 10 mm vertex distance. Participants viewed the optotypes through a 2 mm diameter artificial aperture placed before the tested eye in the same trial frame to avoid any effect of inherent higher-order aberrations of the eye (Applegate, Donnelly, Marsack, Koenig & Pesudovs, 2007).[3] The

[3]Diffraction effects on the visual acuity could not controlled and it remained constant for both the native phase and phase nullified testing protocols.

psychometric function was constructed using 11 different-sized optotypes, presented 10 times each, resulting in a total of 110 presentations. For each presentation, the optotype and its size were randomly chosen from amongst the Sloan set (C, D, H, K, N, O, R, S, V and Z). The central value of the optotype was chosen based on pilot testing of the visual acuity for all four conditions tested in this study. Five sizes on either side of the central value with an interval of 0.1 logMAR unit was used for generating the psychometric function. The stimuli were presented from 2 meters on a gamma-corrected LCD monitor with 1680 x 1050-pixel resolution and 59Hz refresh rate using the Psychtoolbox-3 interface of Matlab (Brainard, 1997). A single optotype of the desired size with a bounding box was flashed for the duration of 300 msec to avoid eye movements from influencing the subjective response of the participant, as is the standard practice in psychophysical experiments of this nature (Pelli, Burns, Farell & Moore-Page, 2006). This duration is long-enough for the near-perfect identification of single optotypes in human adults (Bundesen & Harms 1999, Petersen & Andersen, 2012). Participants were asked to identify the letter from the English alphabet with a chance-level performance of 3.85%.[$] The resultant psychometric function was fit using a cumulative Gaussian distribution function, with the mean and standard deviation of the function optimized using the fminsearch function in Matlab, based on the maximum likelihood–based Nelder–Mead simplex algorithm. The logMAR value corresponding to 51.6% correct response was considered as the threshold visual acuity. The visual acuity was obtained nine times in each participant – baseline and once each for Conditions 1 – 4 with native and nullified phase spectra, all in random order.

2.4. The optotype discrimination task

A subset of five individuals that participated in the visual acuity experiment were recruited for the optotype discrimination task that involved identifying the 10 Sloan optotypes blurred using the PSF's from Condition 2 and 4 of the main experiment. Each blurred optotype was presented 10 times in random order, each for 300 msec duration, at the participant's visual acuity threshold value and two lines above this threshold value. The mean (± 1 SD) letter size at threshold value for the discrimination task was 0.45 ± 0.05 and 0.59 ± 0.05 logMAR units for Conditions 2 and 4, respectively, across participants. The examiner

[$]Some participants experienced in psychophysical assessment of visual acuity may tend to limit their choices to the 10 Sloan letters especially towards the end of the trials. This would change the chance-level performance to 10% from 3.85%. This small change in chance-level performance is unlikely to impact the threshold estimates obtained from the psychometric functions.

recorded the participant's response for each presentation and analysed the data using confusion matrices (Barhoom, Joshi & Schmidtmann, 2021, Candy, Mishoulam, Nosofsky & Dobson, 2011).

2.5. Generation of blurred stereograms and stereoacuity assessment

A database comprising of black and white random-dot stereogram pairs were generated using custom-written software in Matlab®. Each image of the stereogram pair was 500 x 500 pixels in size and subtended 17° × 17° at 50 cm viewing distance with 2 min of arc/pixel (Figure 3). The disparity stimulus in each stereogram pair was an isosceles triangle pattern with one of four possible apex orientations (right, left, up and down) (Figure 3). The stimuli were presented in crossed disparity ranging from 10 arcsec to 1000 arcsec in steps of 10 arcsec between 10 to 400 arcsec and in steps of 50 arcsec between 400 to 1000 arcsec. All disparities were generated for a constant interpupillary distance of 60 mm. Each image in the database had a different pattern of random dots to avoid participants using the spatial pattern of the stimulus to perform the psychophysical judgements. The convolution process used to generate the blurred stereograms with native and nullified phase was identical to that used for generating the blurred optotypes. Bilaterally symmetric keratoconus (i.e., similar severity of keratoconus in both eyes) was simulated by presenting the same pattern of blur to the individual images in a stereogram pair (Figures 3B and C). While optically normal individuals tend to show mirror symmetry of the wavefront aberrations in the two eyes (Castejon-Mochon, Lopez-Gil, Benito & Artal, 2002, Porter, Guirao, Cox & Williams, 2001, Thibos, Hong, Bradley & Cheng, 2002), such a pattern may not exist in keratoconic individuals owing to asymmetric disease progression in the two eyes. Hence, mirror symmetry in the Zernike coefficients of the two eyes was not introduced during the blurring of the stereogram image pairs in the bilateral blur conditions. Unilaterally asymmetric keratoconus (i.e., one eye was keratoconic while the fellow eye was normal) was simulated by presenting the blur pattern to the right eye while the left eye's pattern remained unmanipulated (Figures 3D and E). Bilaterally asymmetric keratoconus (i.e., both eyes with keratoconus but of different severities) were not tested due to the extensive nature of psychophysical testing involved.

Stereoacuity measurements were obtained from a viewing distance of 50 cm with the participant's sphero-cylindrical refractive correction placed in a trial lens frame at 10mm vertex distance. Subjects fused the stereogram pair through a stereoscope whose mirror angle could be adjusted to overcome the participant's horizontal heterophoria, if any. Participants viewed the stimuli through 2 mm diameter

artificial apertures that were mounted onto the back surface of the mirror stereoscope. The positions of the apertures and the mirror angle were carefully adjusted such that each image of the stereogram pair was dichoptically visible to the participant. Stereoacuity measurements started only after the subjects reported stable fusion. Stereoacuity was measured using a method of constant stimuli psychophysical procedure involving 11 different disparity values, each presented 10 times in random order. The experiment was carried out on the same LCD monitor used for acuity testing, with the stimuli displayed using the Psychtoolbox-3 interface of Matlab® (Brainard, 1997). The stimulus was flashed for a 300 msec

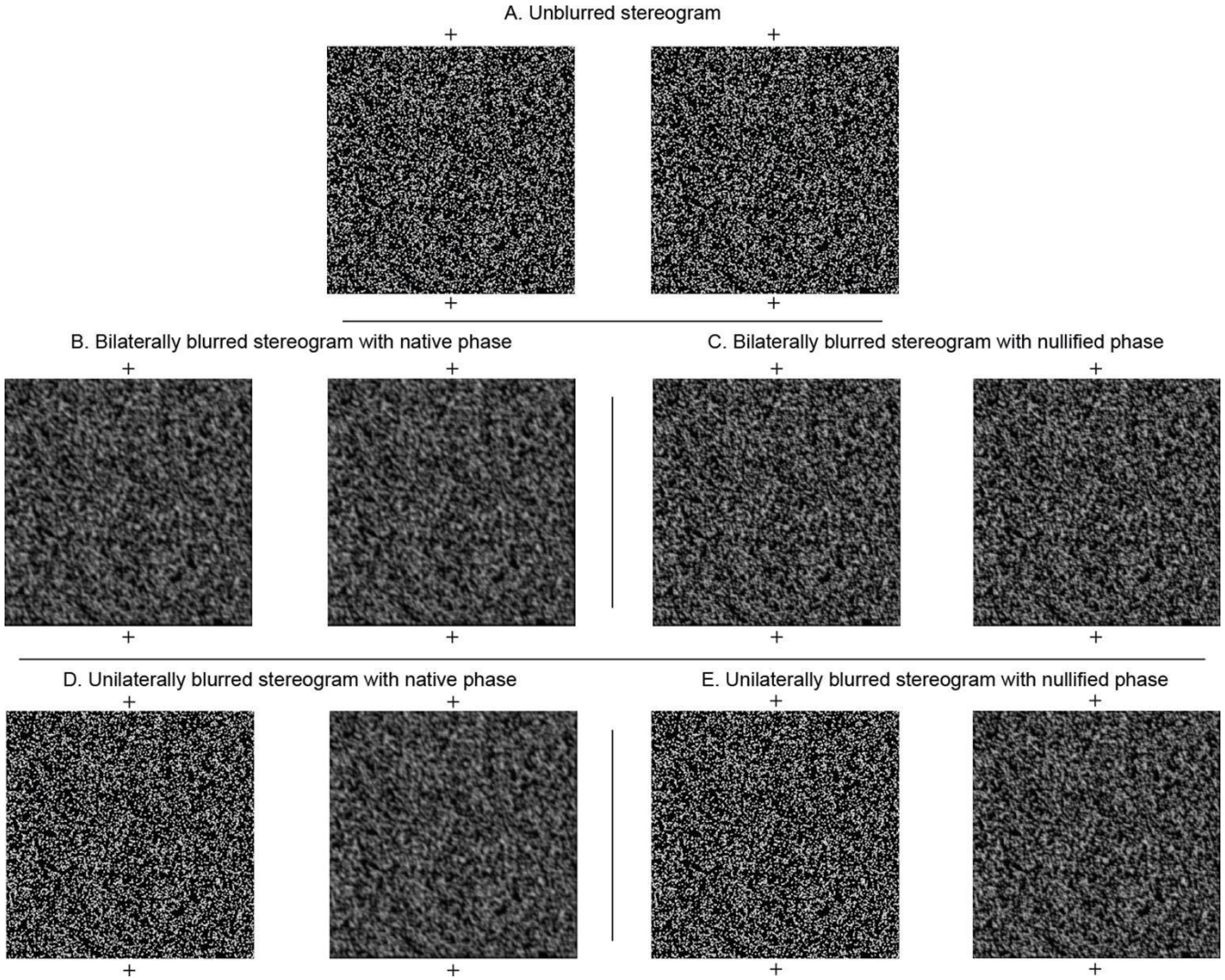

Figure 3: *Representative random-dot stereogram pairs used to estimate stereoacuity in this study. The unblurred stereogram pair shown in Panel A was blurred using the blur profile in Condition 3 (moderate keratoconus) of this study. Panels B and C show bilaterally blurred version of the stereogram pairs with native and nullified phase, respectively. Panels D and E show unilaterally blurred version of the same stereogram pairs. Each stereogram pair with 120 arcsec of crossed retinal disparity may be cross-fused to experience an isosceles triangle with its apex pointing downwards appearing in depth.*

duration and the participant made a four-alternate forced-choice judgement of the apex orientation of the triangle. The resultant psychometric function was fit using the same technique described for acuity judgments and the stereoacuity was estimated from the stimulus disparity value that produced a 62.5% correct response. Stereoacuities were obtained in 17 conditions in each participant – baseline and, four times each with native and nullified phase in the four bilateral- and four unilateral conditions.

It took several hours to complete the data collection across all 26 sessions (9 for visual acuity and 17 for stereoacuity) in a given participant. These sessions were grouped into several smaller blocks and executed on different days based on the participant's availability and fatigue. The visual acuity and stereoacuity measurements were obtained in no specific order on separate sessions in each participant.

2.6. Data analysis

Data were analysed using Microsoft Excel® (Microsoft Corporation, Redmond, USA), IBM SPSS statistics v20.0® (SPSS, Chicago, IL, USA) and Matlab R2016b. Kolmogorov-Smirnov test indicated that all data (except the stereoacuity at Condition 3) were normally distributed and, therefore, parametric tests were used for all statistical analyses. Separate two-factor repeated measures analysis of variances (RM-ANOVAs) were conducted to determine the impact of induced blur magnitude and phase nullification on visual acuity and the impact of bilaterally and unilaterally induced blur and phase nullification on stereoacuity. Separate one-factor RM-ANOVAs were conducted to determine the impact of blur magnitude and phase nullification on visual acuity and stereoacuity, from their respective baseline values (i.e., without any induced blur). The Mauchly's test of sphericity for equal variances among the differences between all possible pairs of blur magnitudes remained unviolated for visual acuity ($p = 0.11$) but was violated for the stereoacuity conditions ($\varepsilon \leq 0.45$, for both; $p = 0.001$). The within-subject effects of the RM-ANOVAs are therefore reported as for visual acuity and following the Greenhouse-Geisser correction for the stereoacuity measurements. Post-hoc Bonferroni test with adjustment for multiple comparisons was performed for all pairwise comparisons. $P < 0.05$ was considered statistically significant and the effect size was estimated using the partial η^2 values.

3. Results

3.1. Visual acuity with native and phase nullified blur

The mean (± 1SD) cohort level visual acuity at baseline was -0.02 ± 0.07 logMAR units. Figure 4 shows representative psychometric functions for visual acuity assessment from one participant across the four induced blur conditions tested in this study with native (solid curves) and nullified (dashed curves) phase. The psychometric functions expectedly shifted towards larger optotype sizes with an increase in induced blur magnitude (Figures 4A – D). Phase nullification resulted in a leftward shift in the psychometric function for all four wavefront aberration patterns, signalling a partial restoration in visual acuity relative to the native phase (Figures 4A – D). The two-factor RM-ANOVA showed significant main effects of blur magnitude [$F(3, 27) = 122.52$; $p < 0.001$; partial $\eta^2 = 0.98$] and phase profile [$F(1, 9) = 336.93$; $p < 0.001$; partial $\eta^2 = 0.97$] on visual acuity (Table 1, Figure 4E). Pairwise comparisons revealed the visual acuities differed significantly between all levels of induced blur ($p \leq 0.01$, for all). The interaction effect between the two main factors was also significant [$F(3, 27) = 4.60$; $p < 0.04$; partial $\eta^2 = 0.66$], indicating that the improvement in visual acuity with phase nullification was not uniform across all magnitudes of induced blur (Figure 4E). Condition 1, with the lowest magnitude of induced blur, resulted in the least visual acuity improvement with phase nullification (0.08 logMAR units) while the other three conditions, with increasing magnitudes of induced blur, resulted in larger but similar acuity improvements following phase nullification (Condition 2: 0.16 logMAR units; Condition 3: 0.15 logMAR units; Condition 4: 0.17 logMAR units). A separate one-way RM-ANOVA analysis with appropriate post hoc comparison revealed that the baseline visual acuity was significantly different from all the four levels of induced blur with native ($F = 267.69$; $p < 0.001$) and nullified phase profiles ($F = 94.56$; $p < 0.001$) (Figure 4E).

Table 1: *Mean (± 1SD) monocular visual and stereo acuity obtained across all four induced blur conditions with native and nullified phase. Stereoacuity obtained with bilaterally and unilaterally induced blur are shown in this table.*

	Visual acuity (logMAR)		Stereoacuity (arcsec)			
			Bilateral		Unilateral	
	Native	Nullified	Native	Nullified	Native	Nullified
Condition 1	0.25 (0.21 - 0.28)	0.17 (0.13 - 0.21)	68.30 (42.87 - 93.74)	60.58 (29.16 - 92.00)	63.76 (49.87 - 77.66)	45.2 (34.46 - 55.94)
Condition 2	0.44 (0.41 - 0.48)	0.29 (0.25 - 0.32)	69.78 (47.44 - 92.12)	62.67 (32.75 - 92.59)	93.27 (65.33 - 121.22)	53.89 (41.59 - 66.18)
Condition 3	0.53 (0.51 - 0.55)	0.38 (0.33 - 0.43)	120.71 (73.03 - 168.39)	98.32 (20.52 - 176.13)	152.97 (119.37 - 186.56)	86.54 (57.98 - 115.09)
Condition 4	0.59 (0.56 - 0.63)	0.42 (0.39 - 0.46)	85.52 (57.29 - 113.75)	63.43 (35.54 - 91.32)	197.81 (102.89 - 292.74)	85.25 (51.93 - 118.57)

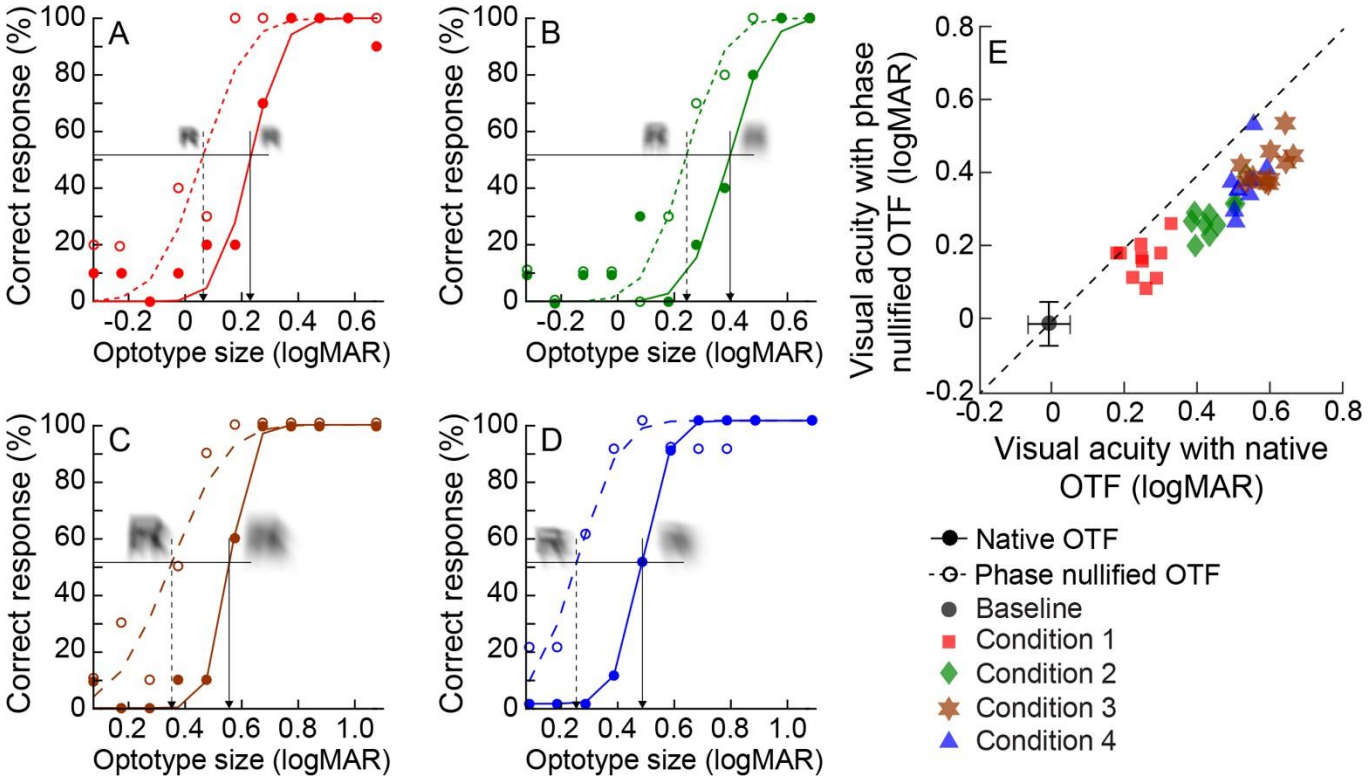

Figure 4: *Psychometric functions of visual acuity obtained from a representative participant for the four induced blur conditions tested in this study (Condition 1, Condition2, Condition 3 & Condition 4, respectively) (Panels A – D). The filled symbols and solid psychometric function show data obtained for the native phase condition while the open symbols and dashed psychometric function show data obtained for the phase nullified condition. Panel E shows the logMAR visual acuity obtained while viewing optotypes blurred using their native and nullified phase for the four keratoconus conditions tested in this study. Each symbol of a particular colour represents data from a single participant. The mean (±1SD) visual acuity obtained at baseline is also shown in this panel for comparison purposes.*

3.2. Optotype discrimination with native and phase nullified blur

Figure 5 shows bubble plots of the mean percentage correct identification of the presented optotype across the five subjects for targets blurred with the native and nullified phase of one mild (Condition 2; panels A and B) and one moderate (Condition 4; panels C and D) keratoconic eye used in this study. The mean percentage correct identification of the presented optotype across the five subjects that participated in this experiment is shown here. Three patterns were evident from the confusion matrices. First, the optotype discrimination for the native phase targets was far from ideal for both blurring conditions (Figure 5A and C). Some optotypes (e.g., C, D, O, R and V) were more prone to confusion than others (e.g., H, N, S and Z), with no uniform pattern of misjudgement across the confused optotypes. Second, phase nullification minimized this confusion for both blurring conditions, with the confusion matrix showing near 100% correct response for all 10 Sloan optotypes (compare red with green confusion matrices in Figure 5). Third, the

bubble plot obtained for native phase in Condition 4 with the larger optotypes obtained with showed relatively better discrimination that those in Condition 2 with the smaller optotypes. Consequently, the improvement in the confusion matrix following phase nullification was also smaller for Condition 4 than Condition 2 (Figures 5B and D). The visual impact of the two blurring conditions and the phase nullification on optotype discrimination may be observed from the simulated optotypes shown along the abscissa in each panel.

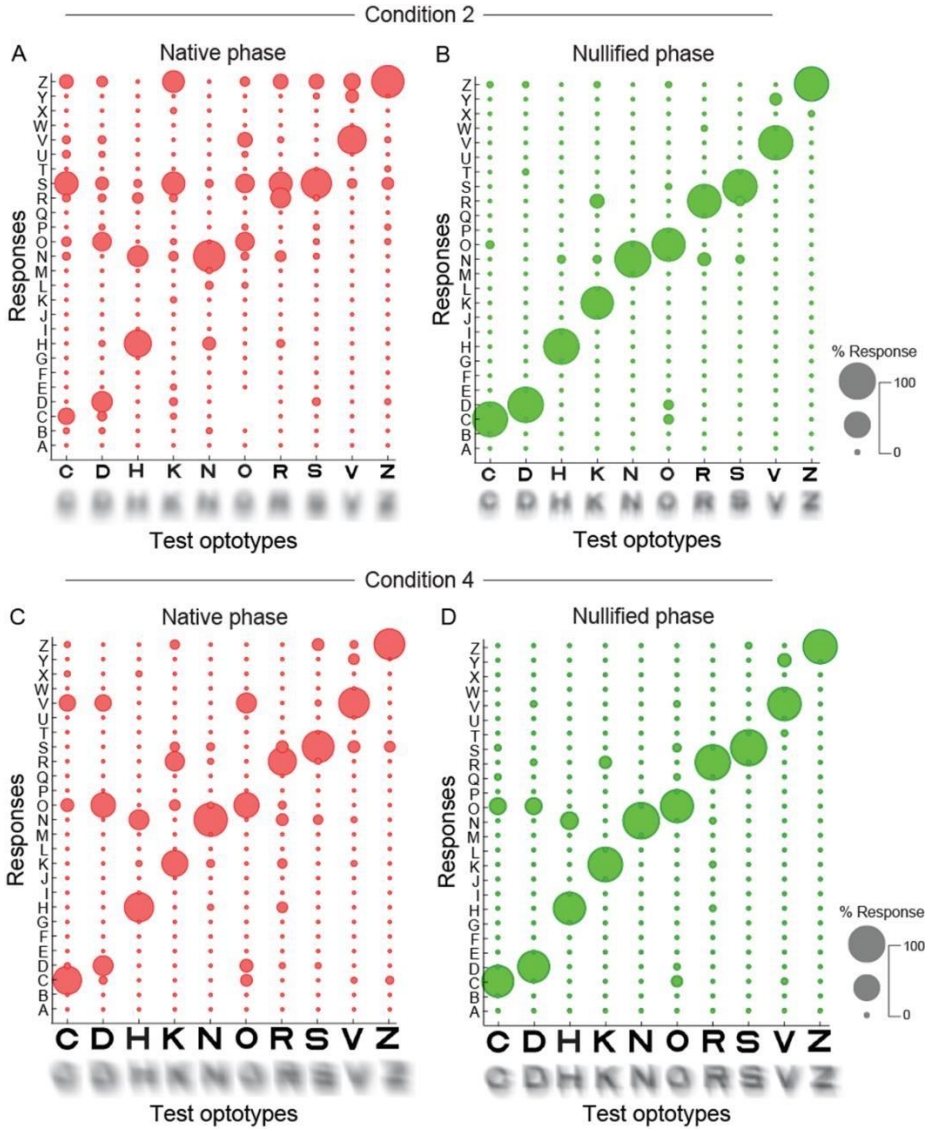

Figure 5: *Bubble plots showing the outcomes of the optotype discrimination task performed in this study using native and phase nullified blur of one mild (Condition 2; panels A and B) and one moderate (Condition 4; panels C and D) keratoconic eye. Bubble size represents the mean percentage of times the presented optotype (x-axis scale) was identified as a given English alphabet (y-axis scale). The scaling of bubble size to the percentage identification of the alphabet is shown in the figure inset. Optotypes simulated with the pattern of blur corresponding to the native and phase nullified viewing in Conditions 2 and 4 are shown along the abscissa in each panel.*

3.3. Stereoacuity with native and phase nullified blur

The mean (± 1SD) cohort level stereoacuity at baseline was 48.86 ± 20.13 arcsec. Table 1 and Figures 6 and 7 show representative psychometric functions for estimating stereoacuity and cohort level stereoacuity data for bilaterally-induced blur (Figure 6) and unilaterally-induced blur (Figure 7) with native and nullified phase in the four keratoconic conditions tested in this study. The impact of induced blur, and consequently, the phase nullification, on stereoacuity was smaller in the bilateral than unilateral induced-blur conditions (compare the partial η^2 values for the main effects of blur magnitude and phase nullification in the ANOVA analyses below). The representative psychometric functions showed a smaller and a non-uniform shift in the stereoacuity across the four bilaterally induced blur conditions (Figure 6A – D). The restoration of stereoacuity following phase nullification was also uniform across these conditions (Figure 6A – D). The two-factor RM-ANOVA showed no statistically significant main effect of blur magnitude [$F(1.28, 11.48) = 3.98$; $p = 0.063$; partial $\eta^2 = 0.31$], a marginal significance of phase nullification [$F(1, 9) = 5.17$; $p = 0.049$; partial $\eta^2 = 0.37$] and no significance of interaction between the two main effects [$F(1.19, 10.68) = 0.73$; $p = 0.44$; partial $\eta^2 = 0.08$] on stereoacuity with bilaterally induced blur (Table 1, Figure 6E).

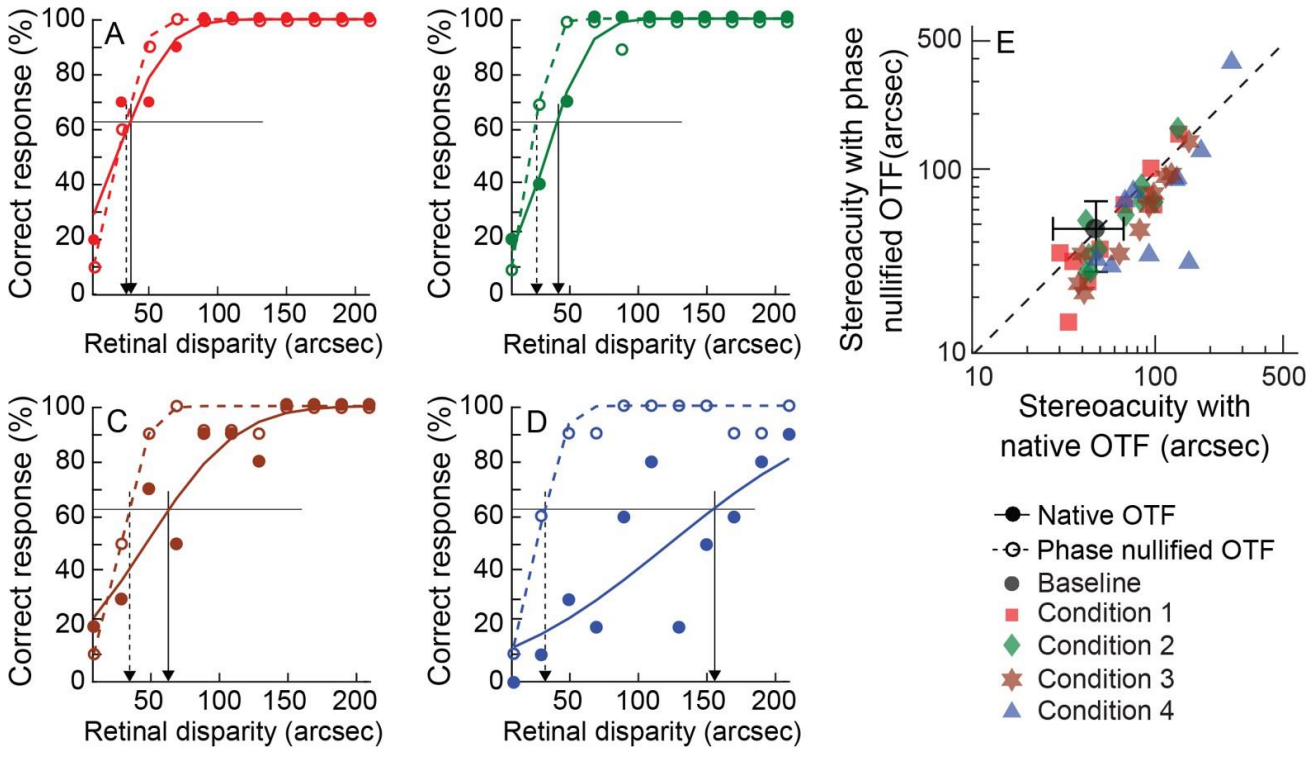

Figure 6: *Psychometric functions of stereoacuity obtained from a representative participant for the four bilaterally induced blur conditions tested in this study (Panels A – D). All other details are the same as Figure 4.*

In contrast, the psychometric functions for the unilaterally blurred conditions for the same participant in Figure 7A – D showed a progressive worsening of stereoacuity across Conditions 2, 3 and 4, while the stereoacuity in Conditions 1 and 2 were similar to each other. Phase nullification showed a larger restoration of stereoacuity for Conditions 3 and 4, relative to Conditions 1 and 2 (Figure 7A – D). The two-factor RM-ANOVA showed significant main effects of both blur magnitude [$F(1.34, 12.09) = 12.72$; $p = 0.002$; partial $\eta^2 = 0.59$] and phase nullification [$F(1,9) = 28.39$; $p < 0.001$; partial $\eta^2 = 0.76$] on stereoacuity with unilaterally induced blur (Table 1, Figure 7E). Pairwise comparisons indicated that the stereoacuity in each unilaterally induced blur condition was significantly different from the other three conditions ($p \leq 0.023$, for all) (Table 1). Although the interaction between the two main effects was not significant [$F(1.15, 10.3) = 4.20$; $p = 0.06$; partial $\eta^2 = 0.32$], the mean data showed a systematic increase in the improvement of stereoacuity following phase nullification, across blur magnitudes (Improvement in stereoacuity following phase nullification: 23.56 arcsec for Condition 1; 39.38 arcsec for Condition 2; 66.43 arcsec for Condition 3; 112.56 arcsec for Condition 4) (Table 1).

The results of the one-factor ANOVA analysis of the baseline stereoacuity to the stereoacuity with induced

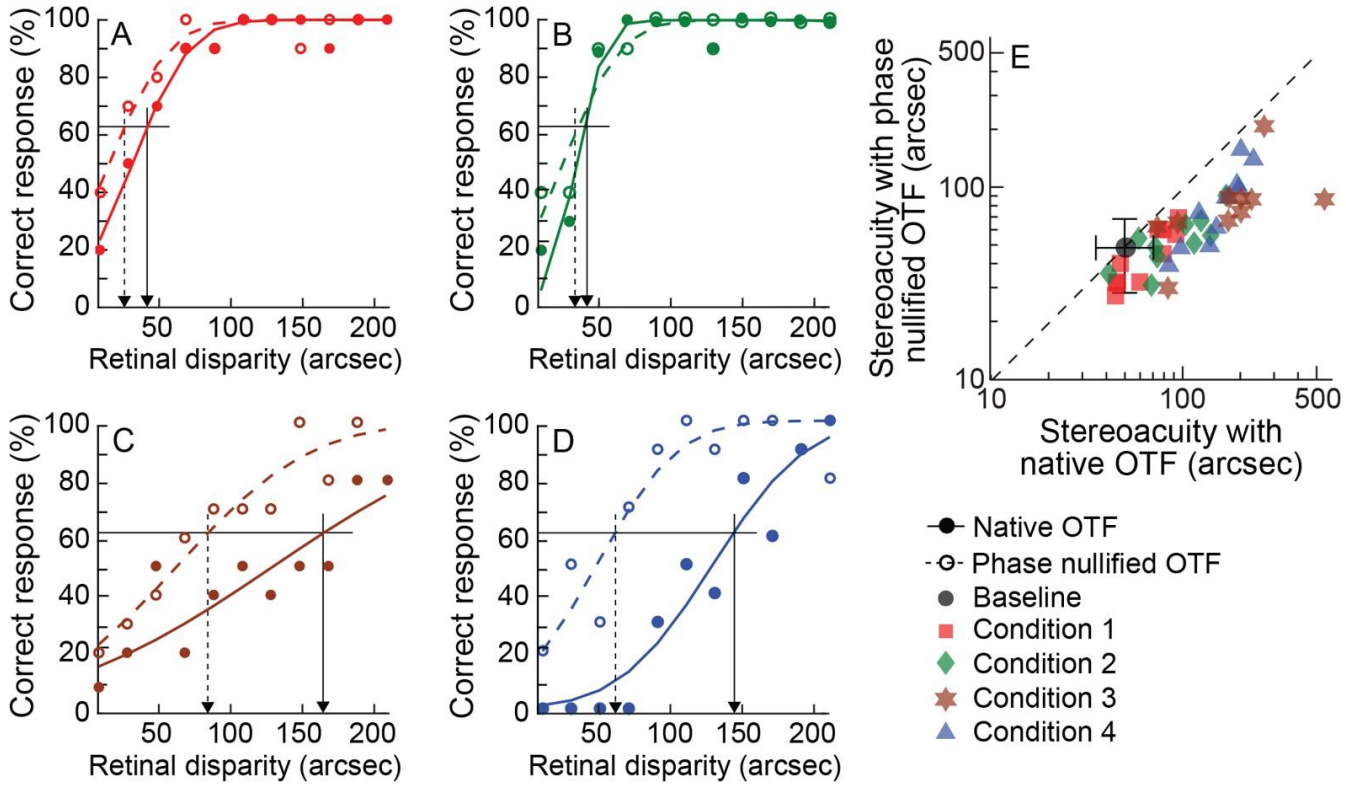

Figure 7: *Similar to Figure 6, but for the four unilaterally induced blur conditions.*

phase profiles and phase nullified conditions. A separate one-factor RM-ANOVA indicated that the baseline stereoacuity was significantly better than those with bilateral ($F = 4.18$; $P = 0.006$) and unilateral ($F = 8.87$; $p<0.001$) blur with native phase. Only the stereoacuity in Condition 3 of the bilateral blur was significantly worse than the baseline condition ($p = 0.004$) while Conditions 3 and 4 of unilateral blur were significantly worse than the baseline condition ($p \leq 0.01$, for both). Stereoacuity in the phase nullified conditions were not significantly different from the baseline level for bilateral and unilateral blur ($p \geq 0.09$).

4. Discussion

4.1. Summary of results and implications for vision loss in keratoconus

The present results confirm that visual and stereo acuity losses encountered for images blurred by keratoconic higher-order wavefront aberrations may be partially restored following phase nullification (Figures 3, 6 and 7). The impact of phase nullification on stereoacuity is more pronounced for targets simulating unilaterally asymmetric keratoconus with interocular differences in retinal image quality (Figure 7), relative to those simulating bilaterally symmetric disease (Figure 6). Phase nullification also improves character recognition, more so for those with smaller than larger angular subtense (Figure 5).

These results show that the combination of phase alterations and contrast demodulation of the component spatial frequencies arising in the blurred image contribute to spatial and depth vision losses in keratoconus. While contrast and phase are two independent characteristics of an image, alterations in the latter characteristic for local features in the image may influence the global contrast of complex images with broadband spatial frequency content, like the optotypes and random-dot patterns used in this study (Field & Brady, 1997, Haun & Peli, 2013, Peli, 1990). In fact, standard definitions of contrast, such as the Michaelson's contrast, may fail under such circumstances, as shown in the aforementioned literature. Phase nullification realigns the relative phases at which different spatial frequencies are combined, leading to improved edge contrast of the image feature (see the simulated optotypes before and after phase nullification in Figures 4 and 5), even while the overall contrast energy in the entire image may remain unchanged. The improved edge contrast may lead to an improved visual resolution and discrimination between optotypes, as seen in Figures 4 and 5, respectively, of this study. Perceptually, the phase realignment may also minimize the ghosting and doubling of targets (see simulated optotypes before and after phase nullification in Figures 4 and 5), improving object recognition and higher-level

functions like face perception (Ravikumar et al., 2010). All these factors combined may significantly improve the overall quality of vision and vision-related quality of life of the keratoconic patient (Fan et al., 2024, Gothwal et al., 2022, Pinto et al., 2021, Santodomingo-Rubido et al., 2022). Rigid contact lens designs that are routinely prescribed as a correction modality in keratoconus reduce both the contrast demodulation and the phase distortions simultaneously by virtue of their ability to replace the distorted cornea with a more uniform refracting surface (Devi et al., 2023, Kumar, Bandela & Bharadwaj, 2020). Similar outcomes are achieved under experimental conditions involving adaptive optics correction of the keratoconic eye's wavefront aberrations (Barbot, Park, Ng, Zhang, Huxlin, Tadin & Yoon, 2021, Sabesan, Ahmad & Yoon, 2007, Sabesan & Yoon, 2009). As a future possibility, the theoretical simulations of Yellott and Yellott (2007) propose phase nullifications as a means of restoring recognition of blurred images at near viewing distances in a presbyopic eye. The practical feasibility of this strategy, however, remains to be explored. Whether such corrections will directly benefit patients with chronic optical degradations like keratoconus also depends on how much of the patient's habitual visual experience is shaped by neural recalibration to prolonged blurred/distorted vision during the critical periods of visual development (Barbot et al., 2021, Ng, Sabesan, Barbot, Banks & Yoon, 2022, Sabesan, Barbot & Yoon, 2017, Sabesan & Yoon, 2009). All these issues need further investigation.

4.2. Changes in visual acuity before and after phase nullification

The present study extends the findings of Ravikumar et al (2010) to an optically complex situation like keratoconus wherein the retinal image quality is determined by complex interactions between several Zernike components in the higher-order wavefront aberration profile (Devi et al., 2023). The spatial frequency where the radially-averaged OTF intersected with the neural threshold function following phase nullification all increased to about 20 cpd in Conditions 1 – 4 tested in this study, even while these intersection points progressively declined with increasing magnitudes of blur with the native OTF (Figure 2). This translated into increases in the cut-off spatial frequency by 8.1% (18.5 cpd to 20 cpd = 8.1% increase), 24.7%, 33.3% and 106.5% following phase nullification in these four conditions (Figure 2). The empirical results, however, showed a uniform magnitude of improvement in visual acuity following phase nullification – 28.8% to 34% across Conditions 1 – 4 (Table 1, Figure 4E). This result may simply reflect how this study represents visual acuity changes in a logarithmic scale – the same percentage of improvement with phase nullification for a given blur condition may represent a larger quantum of change for

Conditions 3 and 4 with poorer logMAR acuities than for Conditions 1 and 2 with relative better logMAR acuities. Two alternate possibilities exist. First, the empirical measures of acuity loss restoration may not be veridically captured by the analysis involving the intersection of the radially-averaged OTF and the neural threshold function. After all, optotype recognition is a more complex task involving several cognitive processes and is only broadly correlated with acuity measures involving resolution of sinewave gratings (Mayer, Fulton & Rodier, 1984). Second, the Zernike coefficients present in a keratoconic wavefront aberration profile produce a radially asymmetric point spread function (Appendix I). Such radial asymmetries may significantly influence the recognition of Sloan optotypes used in this study, even while they were ignored by radially-averaging the OTF in the theoretical calculations described above (Figure 2). Perhaps, the intersection between the OTF and the neural threshold function should be computed for every orientation of the OTF, and the range of intersection values should be compared with the empirical estimates of acuity loss restoration obtained in this study. That this was not performed remains a limitation of the study.

4.3. Changes in stereoacuity before and after phase nullification

In the present study, the stereoacuity was determined as the smallest retinal disparity that allowed the participant to discern the orientation of an isosceles triangle from within a field of randomly distributed black and white dots (Figure 3). Optical blur challenges the computation of retinal disparity in two ways. First, the contrast loss associated with blur degrades stereoacuity, more so when the contrast attenuation is dissimilar in the two eyes compared to when they are bilaterally similar [the contrast paradox in stereopsis (Cormack et al., 1997, Cormack, Stevenson & Schor, 1991, Kumar, Campbell, Vaddavalli, Hull & Bharadwaj, 2023, Stevenson & Cormack, 2000)]. Second, the alterations in the spatial position of the local features in the monocular retinal image arising from dissimilar phase distortions in the two eyes impair correspondence matching, leading to false matches and non-veridical depth estimates (Ding et al., 2013a, Metlapally et al., 2019). Deterioration of stereo performance in the unilateral blur conditions is likely to arise from both the contrast paradox and non-veridical depth estimates from correspondence mismatches of the two differently blurred retinal images (Table 1, Figures 3, and 7). Phase nullification may minimize the positional mismatches between the two eyes in the unilateral-induced blur conditions, thus improving the strength of the retinal disparity signal available for stereo processing. Additionally, the reduction in positional mismatches following phase nullification decreases the interocular contrast

difference of the local image features, further supporting an improvement in stereoacuity. Stereoacuity losses with bilaterally symmetric blur may be attributed only to the overall attenuation of contrast arising from the blurred image in the two eyes (Table 1, Figures 3 and 6). The phase distortions may not impact stereoacuity in this condition as the positional shifts in the local features will be equal in both retinal images, thus leaving the correspondence matching process unimpaired. The modest improvement of stereoacuity in these conditions may be attributed only to the overall improvement of contrast of the locally realigned features following phase nullification. That the stereoacuity improvements following phase nullification were more pronounced for the unilateral- than bilateral-blur conditions indicate that the positional mismatches play a more dominant role in limiting stereo processing than the contrast attenuation of high spatial frequencies in keratoconus. This is not surprising considering that resolution of features in the stereo domain is mediated through low spatial frequencies, unlike the corresponding measures in the luminance domain – stereo spatial resolution is approximately a factor of ten lower than luminance spatial resolution (~30 cpd) (Banks, Gepshtein & Landy, 2004). Thus, the bulk of stereo processing may all happen in the region of the OTF that remains more or less unimpaired by the keratoconic blur (Figure 3). This may also explain why Vlaskamp et al. found no benefit to stereoacuity by correcting the higher-order monochromatic aberrations of individuals with otherwise normal optics (Vlaskamp, Yoon & Banks, 2011). The small magnitude of wavefront aberrations in normal eyes may not have induced significant phase distortions and, therefore, positional mismatches between the monocular images to impact stereoacuity to begin with; nullifying them may thus add no further benefit to stereo processing.

4.4. Study limitations

This study had three limitations from a clinical standpoint. First, the impact of phase nullification on spatial and depth vision have been demonstrated only for images blurred by the higher-order wavefront aberrations of the eye. In reality, even with the best-possible spherocylindrical correction, the keratoconic eye is seldom free of lower-order defocus and astigmatism. This is so because refining the sphero-cylindrical correction of the eye is a challenge in keratoconus owing to their large optical depth of focus (Nilagiri et al., 2020), poor repeatability of the objective and subjective refraction endpoints (Davis, Schechtman, Begley, Shin & Zadnik, 1998, Raasch, Schechtman, Davis, Zadnik & Study, 2001) and the possibility of the habitual correction of the patient not matching with the endpoint of subjective refraction

obtained through the earlier means. What this residual defocus and astigmatism for a keratoconic eye is and how this interaction will pan out is hard to predict (Applegate et al., 2002, Cheng, Bradley, Ravikumar & Thibos, 2010). Hence, the study took a more simplistic approach of removing all lower-order wavefront aberrations from the optical simulations and investigate only the impact of blur from higher-order aberrations on visual performance. A second limitation was the study's inability to test the stereoacuity impact of phase nullification on conditions that simulated bilateral asymmetric keratoconus. While testing these conditions was certainly considered during the study design, it was dropped for operational reasons of time spent in the experiment and the availability of participants for prolonged testing. Lack of this data does limit direct extrapolation of the results to the stereoscopic experience of patients with dissimilar severities of keratoconus in the two eyes. However, for the reasons described above, it may be hypothesized that phase nullification may improve stereoacuity in bilateral asymmetric keratoconus, perhaps, to a greater extent than what was observed here for the unilateral conditions (Figure 7). A third limitation of the study revolves around the extrapolation of the present results to the entire heterogeneity of keratoconus disease presentation (Santodomingo-Rubido et al., 2022). That only four wavefront aberration patterns were chosen in this study clearly indicates that such an extrapolation is superfluous, at best. Instead, the results should be viewed as a proof of concept for how phase nullification may augment vision in highly-aberrated and optically compromised eyes such as those with keratoconus.

5. Conclusions

Nullifying the phase disruptions caused by the monochromatic higher-order wavefront aberrations present in keratoconic eyes produces significant improvements in visual acuity, character recognition and stereoacuity. The effect is more pronounced for stereoacuity when the phase nullification is applied for unilateral than bilateral blur. These effects may be explained by the improved positional registry and the associated reduction in interocular contrast difference between the monocular image features aid veridical calculation of stereopsis. These results form the basis for the improvement in visual performance of keratoconic patients with optical interventions such as rigid contact lens or experimental adaptive optics corrections.

Acknowledgments

The authors thank the study participants, Dr L. S. Varadharajan for the visual acuity measurement software, Prof Larry Thibos and Prof. Arthur Bradley for assistance with the computational simulations described in this study, the terminology of "phase nullification" to faithfully represent the optical manipulation performed in the study and for a critical review of the manuscript. Financial support for the study came through intramural funds from the Hyderabad Eye Research Foundation, L V Prasad Eye Institute and a Fulbright-Nehru Academic and Professional Excellence Fellowship to SRB during the writing phase of the study.

References

Akutsu, H., Bedell, H.E., & Patel, S.S. (2000). Recognition thresholds for letters with simulated dioptric blur. Optom Vis Sci, 77 (10), 524-530.

Applegate, R.A., Donnelly, W.J., 3rd, Marsack, J.D., Koenig, D.E., & Pesudovs, K. (2007). Three-dimensional relationship between high-order root-mean-square wavefront error, pupil diameter, and aging. J Opt Soc Am A Opt Image Sci Vis, 24 (3), 578-587.

Applegate, R.A., Sarver, E.J., & Khemsara, V. (2002). Are all aberrations equal? J Refract Surg, 18 (5), S556-562.

Artal, P., Santamaria, J., & Bescos, J. (1988). Phase-transfer function of the human eye and its influence on point-spread function and wave aberration. J Opt Soc Am A, 5 (10), 1791-1795.

Banks, M.S., Gepshtein, S., & Landy, M.S. (2004). Why is spatial stereoresolution so low? J Neurosci, 24 (9), 2077-2089.

Barbot, A., Park, W.J., Ng, C.J., Zhang, R.Y., Huxlin, K.R., Tadin, D., & Yoon, G. (2021). Functional reallocation of sensory processing resources caused by long-term neural adaptation to altered optics. Elife, 10

Barhoom, H., Joshi, M.R., & Schmidtmann, G. (2021). The effect of response biases on resolution thresholds of Sloan letters in central and paracentral vision. Vision Res, 187, 110-119.

Bell, E.L.S., Hastings, G.D., Nguyen, L.C., Applegate, R.A., & Marsack, J.D. (2023). Utilising a visual image quality metric to optimise spectacle prescriptions for eyes with keratoconus. Ophthalmic Physiol Opt, 43 (5), 1007-1015.

Brainard, D.H. (1997). The Psychophysics Toolbox. Spat Vis, 10 (4), 433-436.

Bundesen, C., & Harms , L. (1999). Single-letter recognition as a function of exposure duration. Psychological Research, 62, 275–279.

Campbell, C.E. (2003). Matrix method to find a new set of Zernike coefficients from an original set when the aperture radius is changed. J Opt Soc Am A Opt Image Sci Vis, 20 (2), 209-217.

Candy, T.R., Mishoulam, S.R., Nosofsky, R.M., & Dobson, V. (2011). Adult discrimination performance for pediatric acuity test optotypes. Invest Ophthalmol Vis Sci, 52 (7), 4307-4313.

Castejon-Mochon, J.F., Lopez-Gil, N., Benito, A., & Artal, P. (2002). Ocular wave-front aberration statistics in a normal young population. Vision Res, 42 (13), 1611-1617.

Chan, C., Smith, G., & Jacobs, R.J. (1985). Simulating refractive errors: source and observer methods. Am J Optom Physiol Opt, 62 (3), 207-216.

Cheng, X., Bradley, A., Ravikumar, S., & Thibos, L.N. (2010). Visual impact of Zernike and Seidel forms of monochromatic aberrations. Optom Vis Sci, 87 (5), 300-312.

Cheng, X., Bradley, A., & Thibos, L.N. (2004). Predicting subjective judgment of best focus with objective image quality metrics. J Vis, 4 (4), 310-321.

Cormack, L.K., Stevenson, S.B., & Landers, D.D. (1997). Interactions of spatial frequency and unequal monocular contrasts in stereopsis. Perception, 26 (9), 1121-1136.

596 Cormack, L.K., Stevenson, S.B., & Schor, C.M. (1991). Interocular correlation, luminance contrast and cyclopean
597 processing. Vision Res, 31 (12), 2195-2207.
598 Davis, L.J., Schechtman, K.B., Begley, C.G., Shin, J.A., & Zadnik, K. (1998). Repeatability of refraction and corrected
599 visual acuity in keratoconus. The CLEK Study Group. Collaborative Longitudinal Evaluation of Keratoconus.
600 Optom Vis Sci, 75 (12), 887-896.
601 Devi, P., Kumar, P., & Bharadwaj, S.R. (2023). Computational analysis of retinal image quality with different contact
602 lens designs in keratoconus. Cont Lens Anterior Eye, 46 (2), 101794.
603 Devi, P., Kumar, P., Marella, B.L., & Bharadwaj, S.R. (2022). Impact of Degraded Optics on Monocular and Binocular
604 Vision: Lessons from Recent Advances in Highly-Aberrated Eyes. Semin Ophthalmol, 37 (7-8), 869-886.
605 Ding, J., Klein, S.A., & Levi, D.M. (2013a). Binocular combination in abnormal binocular vision. J Vis, 13 (2), 14.
606 Ding, J., Klein, S.A., & Levi, D.M. (2013b). Binocular combination of phase and contrast explained by a gain-control
607 and gain-enhancement model. J Vis, 13 (2), 13.
608 Fan, L., Kandel, H., & Watson, S.L. (2024). Impacts of keratoconus on quality of life: a qualitative study. Eye (Lond),
609 Field, D.J., & Brady, N. (1997). Visual sensitivity, blur and the sources of variability in the amplitude spectra of natural
610 scenes. Vision Res, 37 (23), 3367-3383.
611 Gothwal, V.K., Gujar, R., Sharma, S., Begum, N., & Pesudovs, K. (2022). Factors affecting quality of life in
612 keratoconus. Ophthalmic Physiol Opt, 42 (5), 986-997.
613 Hastings, G.D., Marsack, J.D., Thibos, L.N., & Applegate, R.A. (2020). Combining optical and neural components in
614 physiological visual image quality metrics as functions of luminance and age. J Vis, 20 (7), 20.
615 Haun, A.M., & Peli, E. (2013). Perceived contrast in complex images. J Vis, 13 (13), 3.
616 Kumar, P., Bandela, P.K., & Bharadwaj, S.R. (2020). Do visual performance and optical quality vary across different
617 contact lens correction modalities in keratoconus? Cont Lens Anterior Eye, 43 (6), 568-576.
618 Kumar, P., Campbell, P., Vaddavalli, P.K., Hull, C.C., & Bharadwaj, S.R. (2023). Structure-Function Relationship in
619 Keratoconus: Spatial and Depth Vision. Transl Vis Sci Technol, 12 (12), 21.
620 Marella, B.L., Conway, M.L., Suttle, C., & Bharadwaj, S.R. (2021). Contrast Rivalry Paradigm Reveals Suppression of
621 Monocular Input in Keratoconus. Invest Ophthalmol Vis Sci, 62 (2), 15.
622 Marella, B.L., Vaddavalli, P.K., Reddy, J.C., Conway, M.L., Suttle, C.M., & Bharadwaj, S.R. (2023). Interocular Contrast
623 Balancing Partially Improves Stereoacuity in Keratoconus. Optom Vis Sci, 100 (4), 239-247.
624 Mayer, D.L., Fulton, A.B., & Rodier, D. (1984). Grating and recognition acuities of pediatric patients. Ophthalmology,
625 91 (8), 947-953.
626 Metlapally, S., Bharadwaj, S.R., Roorda, A., Nilagiri, V.K., Yu, T.T., & Schor, C.M. (2019). Binocular cross-correlation
627 analyses of the effects of high-order aberrations on the stereoacuity of eyes with keratoconus. J Vis, 19 (6), 12.
628 Ng, C.J., Sabesan, R., Barbot, A., Banks, M.S., & Yoon, G. (2022). Suprathreshold Contrast Perception Is Altered by
629 Long-term Adaptation to Habitual Optical Blur. Invest Ophthalmol Vis Sci, 63 (11), 6.
630 Nilagiri, V.K., Metlapally, S., Kalaiselvan, P., Schor, C.M., & Bharadwaj, S.R. (2018). LogMAR and Stereoacuity in
631 Keratoconus Corrected with Spectacles and Rigid Gas-permeable Contact Lenses. Optom Vis Sci, 95 (4), 391-
632 398.
633 Nilagiri, V.K., Metlapally, S., Schor, C.M., & Bharadwaj, S.R. (2020). A computational analysis of retinal image quality
634 in eyes with keratoconus. Sci Rep, 10 (1), 1321.
635 Pantanelli, S., MacRae, S., Jeong, T.M., & Yoon, G. (2007). Characterizing the wave aberration in eyes with
636 keratoconus or penetrating keratoplasty using a high-dynamic range wavefront sensor. Ophthalmology, 114
637 (11), 2013-2021.
638 Peli, E. (1990). Contrast in complex images. J Opt Soc Am A, 7 (10), 2032-2040.
639 Pelli, D.G., Burns, C.W., Farell, B., & Moore-Page, D.C. (2006). Feature detection and letter identification. Vision Res,
640 46 (28), 4646-4674.
641 Petersen, A., & Andersen, T.S. (2012). The effect of exposure duration on visual character identification in single,
642 whole, and partial report. J Exp Psychol Hum Percept Perform, 38 (2), 498-514.

Pinto, R.D.P., Abe, R.Y., Gomes, F.C., Barbisan, P.R.T., Martini, A.F., de Almeida Borges, D., Fernandes, A.G., Arieta, C.E.L., & Alves, M. (2021). Quality of life in keratoconus: evaluation with Keratoconus Outcomes Research Questionnaire (KORQ). Sci Rep, 11 (1), 12970.

Piotrowski, L.N., & Campbell, F.W. (1982). A demonstration of the visual importance and flexibility of spatial-frequency amplitude and phase. Perception, 11 (3), 337-346.

Porter, J., Guirao, A., Cox, I.G., & Williams, D.R. (2001). Monochromatic aberrations of the human eye in a large population. J Opt Soc Am A Opt Image Sci Vis, 18 (8), 1793-1803.

Raasch, T.W., Schechtman, K.B., Davis, L.J., Zadnik, K., & Study, C.S.G.C.L.E.o.K. (2001). Repeatability of subjective refraction in myopic and keratoconic subjects: results of vector analysis. Ophthalmic Physiol Opt, 21 (5), 376-383.

Ravikumar, S., Bradley, A., & Thibos, L. (2010). Phase changes induced by optical aberrations degrade letter and face acuity. J Vis, 10 (14), 18.

Rozema, J.J., Hastings, G.D., Marsack, J., Koppen, C., & Applegate, R.A. (2021). Modeling refractive correction strategies in keratoconus. J Vis, 21 (10), 18.

Sabesan, R., Ahmad, K., & Yoon, G. (2007). Correcting highly aberrated eyes using large-stroke adaptive optics. J Refract Surg, 23 (9), 947-952.

Sabesan, R., Barbot, A., & Yoon, G. (2017). Enhanced neural function in highly aberrated eyes following perceptual learning with adaptive optics. Vision Res, 132, 78-84.

Sabesan, R., & Yoon, G. (2009). Visual performance after correcting higher order aberrations in keratoconic eyes. J Vis, 9 (5), 6 1-10.

Santodomingo-Rubido, J., Carracedo, G., Suzaki, A., Villa-Collar, C., Vincent, S.J., & Wolffsohn, J.S. (2022). Keratoconus: An updated review. Cont Lens Anterior Eye, 45 (3), 101559.

Sarver, E.J., & Applegate, R.A. (2004). The importance of the phase transfer function to visual function and visual quality metrics. J Refract Surg, 20 (5), S504-507.

Smith, G. (1982). Ocular defocus, spurious resolution and contrast reversal. Ophthalmic Physiol Opt, 2 (1), 5-23.

Smith, G., Jacobs, R.J., & Chan, C.D. (1989). Effect of defocus on visual acuity as measured by source and observer methods. Optom Vis Sci, 66 (7), 430-435.

Stevenson, S.B., & Cormack, L.K. (2000). A contrast paradox in stereopsis, motion detection, and vernier acuity. Vision Res, 40 (21), 2881-2884.

Tadmor, Y., & Tolhurst, D.J. (1993). Both the phase and the amplitude spectrum may determine the appearance of natural images. Vision Res, 33 (1), 141-145.

Thibos, L.N. (2019). Calculation of the geometrical point-spread function from wavefront aberrations. Ophthalmic Physiol Opt, 39 (4), 232-244.

Thibos, L.N., Hong, X., Bradley, A., & Applegate, R.A. (2004). Accuracy and precision of objective refraction from wavefront aberrations. J Vis, 4 (4), 329-351.

Thibos, L.N., Hong, X., Bradley, A., & Cheng, X. (2002). Statistical variation of aberration structure and image quality in a normal population of healthy eyes. J Opt Soc Am A Opt Image Sci Vis, 19 (12), 2329-2348.

Vlaskamp, B.N., Yoon, G., & Banks, M.S. (2011). Human stereopsis is not limited by the optics of the well-focused eye. J Neurosci, 31 (27), 9814-9818.

Walsh, G., & Charman, W.N. (1989). The effect of defocus on the contrast and phase of the retinal image of a sinusoidal grating. Ophthalmic Physiol Opt, 9 (4), 398-404.

Yellott, J.I., & Yellott, J.W. (2007). Correcting spurious resolution in defocused images. Proceedings of SPIE - The International Society for Optical Engineering, 6492.

Appendices

Appendix I: 3D representation of the optical transfer function

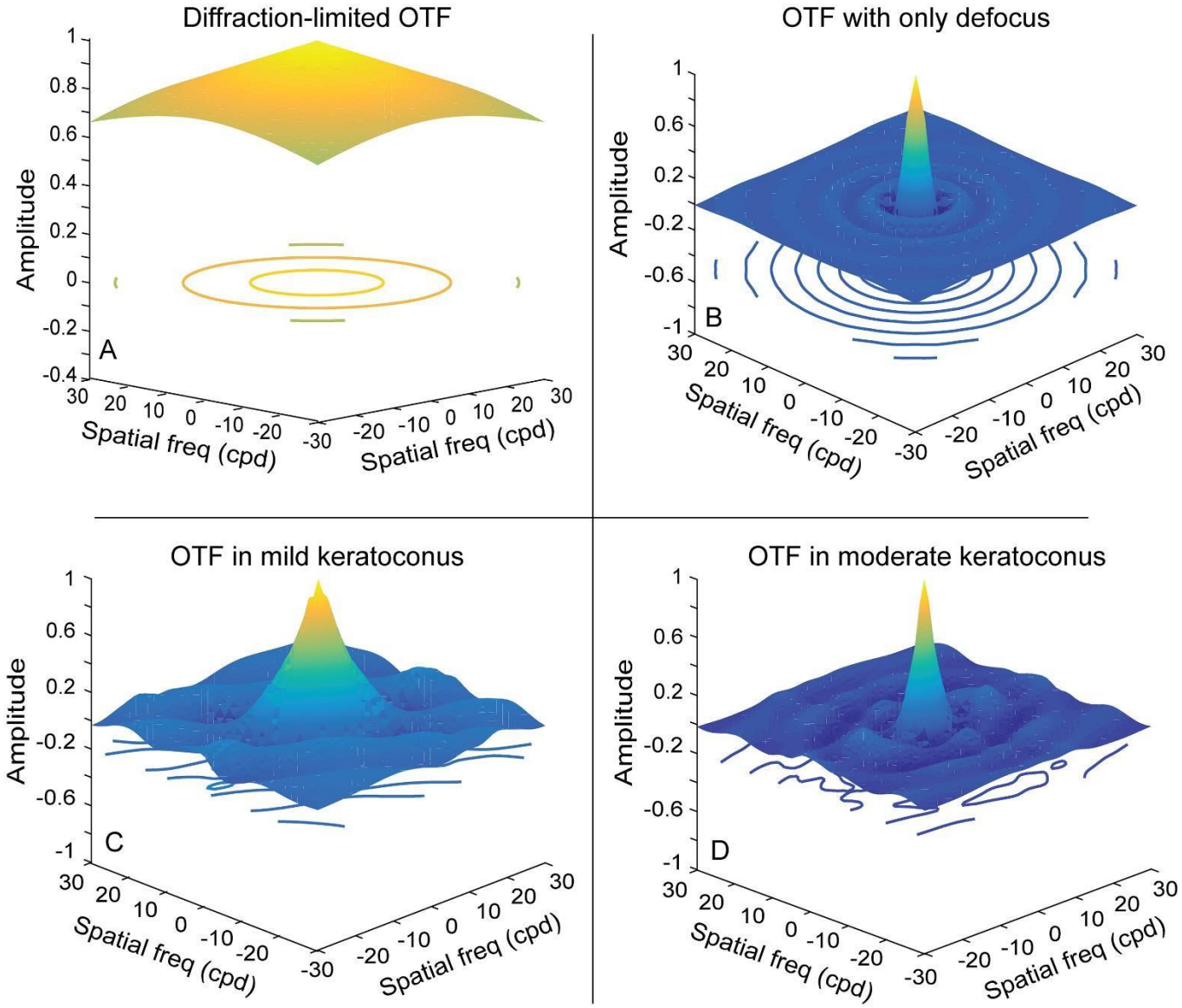

Figure A1: *3D surf plots of the real-part of the complex-valued optical transfer function (OTF) constructed from the monochromatic wavefront aberrations of a diffraction-limited eye (panel A), an eye with only 1D myopic defocus (panel B), an eye with mild keratoconus (panel C) and an eye with moderate keratoconus (D), all for 5 mm pupil diameter. The OTF's for the two keratoconic eyes are the same used for generating the blurred optotypes and stereograms. They are constructed using only their 3rd to 5th order wavefront aberrations. The ripples in the OTF are indicative of the phase reversals. In contrast to the OTF with only defocus, those from keratoconic eyes show also prominent differences in contrast demodulation across orientations, reflecting the impact of the radially-asymmetric Zernike polynomials in the keratoconic wavefront profiles. Prominent phase reversals are also apparent as ripples in the OTFs shown in panels B – D.*

Appendix II: Visual acuity and stereoacuity with induced defocus plus spherical aberrations

A separate control experiment was conducted to determine the impact of blur induced by a combination of myopic defocus and positive spherical aberration with native and nullified phase on monocular visual acuity to validate the present study protocol by replicating the main experiment of Ravikumar et al and stereoacuity. Five observers from the main experiment participated in this experiment. Four levels of defocus: 0.45 µm, 0.90 µm, 1.35 µm and 1.80 µm (corresponding to 0.5 D, 1.0 D, 1.5 D and 2.0 D of defocus for 5 mm pupil diameter, respectively) plus 0.15 µm of positive spherical aberration was used to generate the blurred images. Stereoacuity was estimated only with the unilaterally-induced blur, as the main experiment showed greater impact of this condition over bilateral blur on stereoacuity. All other details of image generation and psychophysical estimation of visual acuity and stereoacuity were identical to the main experiment. Both visual acuity and stereoacuity worsened with induced blur, with the larger two magnitudes of blur showing a greater loss in performance and greater restoration of the performance loss, relative to the lower two magnitudes (Figure A2). The visual acuities obtained in this study for the 0.5 D and 1.0 D of blur were approximately in the same range as that reported by Ravikumar et al (2010). However, the acuities with 1.5 D and 2.0 D of blur were approximately 0.15 logMAR units worse than what was reported by Ravikumar et al (2010).

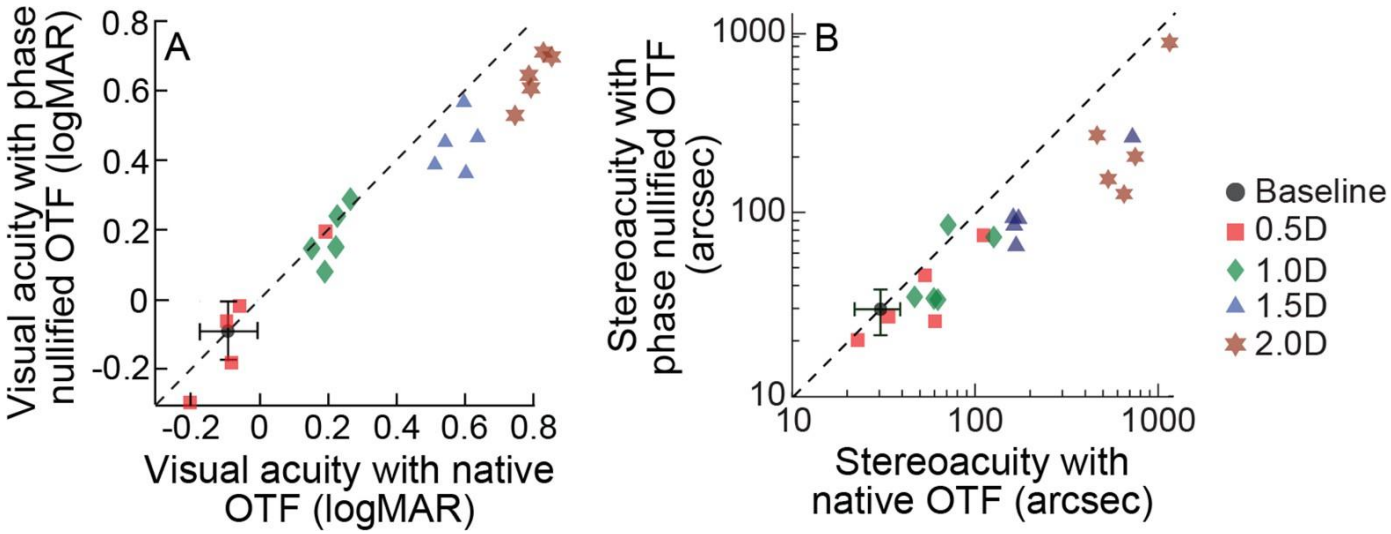

Figure A2: *Scatter diagram of logMAR visual acuity and stereoacuity obtained while viewing optotypes blurred using their native and nullified phase for the four keratoconus conditions tested in this study. Each symbol of a particular colour represents data from a single participant. The mean (±1SD) visual acuity obtained at baseline is also shown in this panel for comparison purposes.*